



# **Isolation, Characterization and Biomimetic Oxidation of Selected Marine Natural Products and their Analogues**

A thesis Submitted in the Fulfilment of the Requirements for the Degree of

**Master of Science (Pharmacy)**

of

RHODES UNIVERISTY

By

Tafadzwa Mutsvairo

February 2015

# Acknowledgements

I would like to take the time to acknowledge everyone who has been instrumental to the success of my research, who have contributed in a big or small way but nevertheless their support is greatly appreciated.

- To my supervisor Professor D.R Beukes, thank you very much boss for the support and constant encouragement especially during the difficult times. I truly would never have managed without you.
- To my co-supervisor Dr E Antunes, I am truly grateful for all of the support, for taking care of us both you and boss on our Cape Town trips which helped tremendously, I will never forget it truly touched my heart.
- Professor J Bolton, at the department of Botany at the University of Cape Town for the identification of marine algae samples.
- Dr M Stander and Mr L Mokwena for the mass spectrometry at the Central Analytical Facilities, University of Stellenbosch.
- Mr D Morley for the technical assistance, the support and encouragement and organizing all our academic trips to Cape Town.
- Dr C Oltmann, my tutor , your advice was very invaluable to me.
- Dr R Tandlich for looking after us throughout the course of 2014.
- Mrs T Kent for the assistance especially when sending samples.
- Mama Prudence for always ensuring a clean laboratory for us to work in.
- To my G5 lab colleagues with special mention to Chikomborero Chakaingesu and Archibald Svogie for the good laugh and support it does mean a lot to me
- To my G3 labmates: Jameel, Mohammed and Maynard I could never have asked for any better labmates and friends. Thank you so much.
- To Maynard, I am truly grateful that you have been a mentor to me from my fourth year right to the end. I thank you for being so selfless in assisting me in every way you are a great friend.
- To my friends; Emilia Chibanguza, Sandra Mashava, Trish Gumpo, Shumie Pswarai, Edith Mshoperi, Kudzai Kuipa, Simba Mtambanengwe, you guys are all amazing thank you for being a stress relief and always encouraging me.

- To my siblings Taku and Fari love you guys so much thanks for being there. Fari thank you for setting a good example for me to follow, thank you for everything
- To my best friend Kudzai Mtambanengwe, thank you so much for putting up with me, for always encouraging me in difficult times, for being a shoulder to cry on, you are one in a million.
- And to my amazing parents Munyaradzi and Charity Mutsvairo, I owe everything that I am and who I have become to you. Thank you for being the voice of reason, for always supporting me, urging me to follow my dreams and nudging me in the right direction. I love you mum and dad.

*For you Mum and Dad,*

## Table of Contents

Acknowledgements.....	ii
Table of Contents.....	v
List of Figures.....	vii
List of Schemes.....	xii
List of Tables.....	xii
List of Abbreviations.....	xiii
Abstract.....	xv

### Chapter 1

<b>General introduction to marine natural products.....</b>	<b>1</b>
1.1 Natural products.....	1
1.1.1 Marine natural products.....	1
1.1.1.1 Phaeophyta (Brown algae).....	2
1.1.1.2 Chlorophyta (Green Algae).....	4
1.1.1.3 Rhodophyta (Red Algae).....	6
1.1.2 Clinically successful drugs from natural products.....	7
1.2 Research aims and objectives.....	9
1.3 Thesis outline.....	9
1.4 References.....	10

### Chapter 2

<b>Literature review.....</b>	<b>13</b>
2.1 The drug discovery and development process.....	13
2.2 Overview of drug metabolism.....	15
2.2.1 The cytochrome P450 monooxygenases.....	18
2.3 Importance of drug metabolism in drug discovery and medicinal chemistry.....	20
2.3.1 <i>In vivo</i> drug metabolism models.....	20
2.3.2 <i>In vitro</i> drug metabolism models.....	20
2.3.2.1 Hepatic tissue slices and isolated hepatocytes.....	21
2.3.2.2 Isolated and expressed enzymes.....	22

2.3.2.4 <i>In silico</i> prediction for drug metabolism.....	22
2.3.2.5 Biomimics of Cytochrome P450 enzymes.....	23
2.3.2.5.1 Terminal oxidant.....	23
2.3.2.5.2 Metalloporphyrin catalysts.....	24
2.4 Natural products as potential drug molecules.....	28
2.5 References:.....	30

## Chapter 3

<b>Natural products from <i>Brassicophycus brassicaeformis</i> and related species.....</b>	<b>36</b>
3.1. General introduction .....	36
3.1.1. Secondary metabolites from genus <i>Bifurcaria</i> .....	38
3.1.2 Biosynthetic pathways for secondary metabolites from genus <i>Bifurcaria</i> .....	40
3.1.3 Biological activity of secondary metabolites from the genus <i>Bifurcaria</i> .....	43
3.1.4 Chapter aims and objectives.....	45
3.2 Results and Discussion .....	46
3.2.1 Isolation of secondary metabolites from <i>Brassicophycus brassicaeformis</i> .....	46
3.2.2 Structure elucidation of secondary metabolites from <i>B. brassicaeformis</i> .....	50
3.2.2.1 Structure elucidation of compound <b>3.9</b> .....	50
3.2.2.2 The structure elucidation of compound <b>3.16</b> .....	53
3.2.2.3 The structure elucidation of compound <b>3.17</b> and <b>3.18</b> .....	55
3.3 Experimental.....	66
3.3.1 General experimental .....	66
3.3.2 Plant material .....	67
3.3.3 Isolation of secondary metabolites from <i>B. brassicaeformis</i> .....	67
3.3.3.1 Isolated secondary metabolites ( <b>3.9</b> , <b>3.16</b> , <b>3.17</b> , <b>3.18</b> ).....	68
3.4 References.....	73

## Chapter 4

<b>Biomimetic oxidation and its application to selected natural products and their analogues.....</b>	<b>77</b>
4.1 General introduction .....	77
4.1.1 Models for biomimetic oxidation.....	81
4.1.2 Success of the biomimetic models in mimicking <i>in vivo</i> drug metabolism.....	82
4.1.3 Natural products selected for biomimetic studies .....	86

4.1.4 Chapter aims and objectives.....	89
4.2 Results and Discussion .....	90
4.2.1 Biomimetic oxidation models .....	90
4.2.1.1 Biomimetic oxidation of phenylbutazone .....	91
4.2.1.2 Biomimetic oxidation of acetanilide .....	97
4.2.1.3 Biomimetic oxidation of natural products .....	102
4.3 Experimental .....	114
4.3.1 General experimental .....	114
4.3.2 Isolation of sargahydroquinonic acid .....	115
4.3.3 Determination of the hydrogen peroxide content.....	115
4.3.4 Biomimetic oxidation model (Catalyst-H <sub>2</sub> O <sub>2</sub> ) .....	115
4.3.5 Biomimetic oxidation model (Catalyst-PhIO(Ac) <sub>2</sub> ).....	116
4.3.6 Isolated oxidation products .....	117
4.4 References.....	119

## Chapter 5

<b>Conclusions.....</b>	<b>125</b>
-------------------------	------------

## Appendices

Appendix 1.....	127
Appendix 2.....	131
Appendix 3.....	133
Appendix 4.....	135

<b>Supplementary Data.....</b>	<b>CD</b>
--------------------------------	-----------

## List of Figures

<b>Figure 1.1</b> Cytotoxic metabolites isolated from <i>Sargassum tortile</i> .....	<b>4</b>
<b>Figure 1.2</b> Biologically active halogenated metabolites from Rhodophyta.....	<b>7</b>

<b>Figure 2.1</b> Summary of drug discovery and development process.....	14
<b>Figure 2.2</b> Bioactivation of chloramphenicol succinate <i>in vivo</i> .....	15
<b>Figure 2.3</b> Metabolism of paracetamol in the human body .....	16
<b>Figure 2.4</b> Summary of drug metabolism .....	17
<b>Figure 2.5</b> Protoporphyrin IX core of cytochrome P450 monooxygenase enzyme.....	18
<b>Figure 2.6</b> The catalytic cycle occurring in a cytochrome P450 isoenzyme active centre .....	19
<b>Figure 2.7</b> Homolytic and heterolytic cleavage with alkylhydroxides and hydrogen peroxide in biomimetic catalysis.....	24
<b>Figure 2.8</b> General porphyrin structure.....	25
<b>Figure 2.9</b> Iron tetraphenylporphyrin (FeTPP)Cl .....	25
<b>Figure 2.10</b> First generation metalloporphyrin <i>meso</i> -tetraphenylporphyrin (TPP) .....	26
<b>Figure 2.11</b> Second generation metalloporphyrin <i>meso</i> -tetrakis(2,6-dichlorophenyl)porphyrin dianion (TDCPP).....	27
<b>Figure 2.12</b> Third generation metalloporphyrin <i>meso</i> -tetrakis(4-N-methylpyridinyl)porphyrin tetracation (TMPyP).....	28
<b>Figure 3.1</b> Acyclic diterpenes isolated from <i>Bifurcaria bifurcata</i> .....	38
<b>Figure 3.2</b> C <sub>16</sub> scaffold for diterpene metabolites for genus <i>Bifurcaria</i> .....	40
<b>Figure 3.3</b> A general biosynthetic scheme for geranylgeraniol derived secondary metabolites .....	42
<b>Figure 3.4</b> Biogenetic formation of bifurcarenone (3.8).....	43
<b>Figure 3.5</b> Photograph of <i>Brassicophycus brassicaeformis</i> .....	45
<b>Figure 3.6</b> <sup>1</sup> H-NMR (600MHz, CDCl <sub>3</sub> ) spectrum of the crude <i>B. brassicaeformis</i> extract ...	46
<b>Figure 3.7</b> <sup>1</sup> H-NMR (600 MHz, CDCl <sub>3</sub> ) spectra of the crude and fractions <b>A-I</b> .....	48
<b>Figure 3.8</b> <sup>1</sup> H-NMR (600 MHz, CDCl <sub>3</sub> ) spectrum of fraction <b>C</b> .....	48



<b>Figure 3.9</b> $^1\text{H-NMR}$ (600 MHz, $\text{CDCl}_3$ ) spectrum of fraction <b>E</b> .....	49
<b>Figure 3.10</b> $^1\text{H-NMR}$ (600 MHz, $\text{CDCl}_3$ ) spectrum of fraction <b>G</b> .....	49
<b>Figure 3.11</b> $^1\text{H-NMR}$ spectrum (600 MHz, $\text{CDCl}_3$ ) of compound <b>3.9</b> .....	51
<b>Figure 3.12</b> $^{13}\text{C-NMR}$ (150MHz, $\text{CDCl}_3$ ) spectrum of compound <b>3.9</b> .....	51
<b>Figure 3.13</b> Key HMBC correlations observed for compound <b>3.9</b> .....	53
<b>Figure 3.14</b> $^1\text{H-NMR}$ spectrum (600 MHz, $\text{CDCl}_3$ ) of compound <b>3.16</b> .....	54
<b>Figure 3.15</b> $^{13}\text{C-NMR}$ spectrum (150 MHz, $\text{CDCl}_3$ ) of compound <b>3.16</b> .....	55
<b>Figure 3.16</b> $^1\text{H-NMR}$ spectra (600 MHz, $\text{CDCl}_3$ ) of crude fraction <b>G</b> and purified compounds <b>3.17</b> and <b>3.18</b> .....	56
<b>Figure 3.17</b> $^{13}\text{C-NMR}$ (150 MHz, $\text{CDCl}_3$ ) spectra of <b>3.17</b> and <b>3.18</b> .....	57
<b>Figure 3.18</b> Key $^1\text{H-}^1\text{H}$ COSY and HMBC correlations observed for the galactosylglycerol unit in compounds <b>3.17</b> and <b>3.18</b> .....	59
<b>Figure 3.19</b> GC-MS data for FAME analysis of <b>3.17</b> .....	61
<b>Figure 3.20</b> GC-MS data for FAME analysis of <b>3.18</b> .....	63
<b>Figure 4.1</b> The most common metalloporphyrins used in biomimetic oxidation studies .....	85
<b>Figure 4.2</b> $^1\text{H-NMR}$ (400MHz, $\text{CDCl}_3$ ) spectrum of phenylbutazone ( <b>4.1</b> ) and reaction product of phenylbutazone containing compound <b>4.26</b> .....	91
<b>Figure 4.3</b> $^{13}\text{C-NMR}$ (100 MHz, $\text{CDCl}_3$ ) spectrum of compound <b>4.26</b> .....	92
<b>Figure 4.4</b> Key HMBC correlations for compound <b>4.26</b> .....	94
<b>Figure 4.5</b> $^1\text{H-NMR}$ (400 MHz, $\text{CDCl}_3$ ) spectra comparing control 1, control 2 and starting material (catalyst- $\text{H}_2\text{O}_2$ model) .....	96
<b>Figure 4.6</b> $^1\text{H-NMR}$ (400 MHz, $\text{CDCl}_3$ ) spectra comparing control 1, control 2 and starting material (catalyst- $\text{PhIO}(\text{Ac})_2$ model) .....	97
<b>Figure 4.7</b> TLC assessment of reaction of acetanilide using catalyst- $\text{H}_2\text{O}_2$ biomimetic oxidation model .....	98

<b>Figure 4.8</b> <sup>1</sup> H-NMR (400 MHz, CDCl <sub>3</sub> ) spectra of the starting material ( <b>4.4</b> ) and crude reaction mixture .....	99
<b>Figure 4.9</b> HSQC spectrum of crude oxidation product of acetanilide biomimetic oxidation reaction highlighting some correlations .....	100
<b>Figure 4.10</b> <sup>1</sup> H-NMR (400 MHz, CDCl <sub>3</sub> ) spectrum of sargahydroquinic acid ( <b>4.20</b> ) and sargaquinic acid ( <b>4.30</b> ) .....	102
<b>Figure 4.11</b> <sup>13</sup> C-NMR (100 MHz, CDCl <sub>3</sub> ) spectrum of sargahydroquinic acid ( <b>4.20</b> ) and sargaquinic acid ( <b>4.30</b> ) .....	103
<b>Figure 4.12</b> <sup>1</sup> H-NMR (400 MHz, CDCl <sub>3</sub> ) spectrum of the control reactions of <b>4.20</b> , SHQA and SQA highlighting region δ 6.40-6.60 .....	105
<b>Figure 4.13</b> <sup>1</sup> H-NMR (400 MHz, CDCl <sub>3</sub> ) spectrum of lapachol crude reaction mixture and starting material ( <b>4.21</b> ) .....	107
<b>Figure 4.14</b> <sup>1</sup> H-NMR (400 MHz, CDCl <sub>3</sub> ) region δ 5.25- 7.50 with signals for <b>4.31</b> .....	108
<b>Figure 4.15</b> Mestrenova <sup>®</sup> <sup>1</sup> H-NMR (400.00 MHz, CDCl <sub>3</sub> ) spectrum prediction of compound <b>4.31</b> highlighting the distinguishing doublet signals .....	109
<b>Figure 4.16</b> <sup>1</sup> H-NMR (400 MHz, CDCl <sub>3</sub> ) region δ 2.90- 5.10 with signals for <b>4.32</b> .....	110
<b>Figure 4.17</b> <sup>1</sup> H-NMR (400 MHz, CDCl <sub>3</sub> ) region δ 2.50- 4.50 with signals for <b>4.33</b> .....	111
<b>Figure 4.18</b> Edited HSQC spectrum of crude reaction mixture of lapachol biomimetic oxidation illustrating key correlations in compound <b>4.33</b> .....	111

## List of Schemes

<b>Scheme 3.1</b> Isolation of secondary metabolites <b>3.9</b> and <b>3.16-3.18</b> from <i>B.brassicaeformis</i> ...	47
<b>Scheme 3.2</b> FAME analysis of monogalactosylglycerol lipids .....	60
<b>Scheme 4.1</b> Phase I metabolites of phenylbutazone ( <b>4.1</b> ) .....	78

<b>Scheme 4.2</b> Phase I metabolism of ibuprofen ( <b>4.2</b> ).....	79
<b>Scheme 4.3</b> Phase I metabolism of indomethacin ( <b>4.3</b> ).....	80
<b>Scheme 4.4</b> Phase I metabolism of acetanilide ( <b>4.4</b> ).....	81
<b>Scheme 4.5</b> Biomimetic oxidation of nicotine .....	83
<b>Scheme 4.6</b> Biomimetic biotransformation of androst-4-en-3,17-dione ( <b>4.16</b> ) .....	84
<b>Scheme 4.7</b> Proposed oxidation of acetanilide using the biomimetic model catalyst-H <sub>2</sub> O <sub>2</sub> ...	98
<b>Scheme 4.8</b> Proposed mechanism for sargahydroquinonic acid oxidation catalyzed by metalloporphyrin catalyst.....	106
<b>Scheme 4.9</b> Proposed reaction mechanism for the formation of <b>4.33</b> in a biomimetic oxidation model.....	112

## List of Tables

<b>Table 1.1</b> Examples of clinically significant natural products from Chlorophyta.....	5
<b>Table 3.1</b> Summary of differences between <i>B. brassicaeformis</i> , <i>B. bifurcata</i> , <i>B.</i> <i>galapagensis</i> .....	37
<b>Table 3.2</b> Classification of diterpene metabolites isolated from genus <i>Bifurcaria</i> .....	41
<b>Table 3.3</b> Comparison of observed and literature <sup>1</sup> H-NMR (600 MHz, CDCl <sub>3</sub> ) and <sup>13</sup> C-NMR (150 MHz, CDCl <sub>3</sub> ) and observed <sup>1</sup> H- <sup>1</sup> H- COSY and HMBC correlations of fucosterol ( <b>3.9</b> ).....	52
<b>Table 3.4</b> <sup>1</sup> H-NMR (600 MHz, CDCl <sub>3</sub> ) and <sup>13</sup> C-NMR (150 MHz, CDCl <sub>3</sub> ) assignments for galactosylglycerol moieties of <b>3.17</b> and <b>3.18</b> .....	58

<b>Table 3.5</b> HRESIMS and LC-MS data for compound <b>3.17</b> and <b>3.18</b> .....	64
<b>Table 4.1</b> Summary of natural products.....	88
<b>Table 4.2</b> Metalloporphyrins used in biomimetic oxidation models.....	90
<b>Table 4.3</b> Comparison of 4.1 and 4.26 <sup>1</sup> H-NMR (400 MHz, CDCl <sub>3</sub> ) and <sup>13</sup> C-NMR (100 MHz, CDCl <sub>3</sub> ) and 2D NMR ( <sup>1</sup> H- <sup>1</sup> H-COSY and HMBC spectroscopic data for compound <b>4.26</b> .....	93
<b>Table 4.4</b> Percentage conversion of phenylbutazone to <b>4.26</b> with biomimetic oxidation model catalyst-H <sub>2</sub> O <sub>2</sub> .....	95
<b>Table 4.5</b> Percentage conversion of phenylbutazone to <b>4.26</b> with biomimetic oxidation model catalyst-PhIO(Ac) <sub>2</sub> .....	95
<b>Table 4.6</b> NMR spectroscopic data , <sup>1</sup> H-NMR (400 MHz, CDCl <sub>3</sub> ) and <sup>13</sup> C-NMR (100 MHz, CDCl <sub>3</sub> ) comparing compounds <b>4.20</b> and <b>4.30</b> .....	104
<b>Table 4.7</b> Summary of natural product biomimetic oxidation reactions.....	113
<b>Table 4.8</b> TLC solvent systems used in biomimetic oxidation models.....	117

## List of Abbreviations

°C	Degrees Celsius
br. d	Broad doublet
br. s	Broad singlet
CDCl <sub>3</sub>	Deuterated chloroform
cDNA	Complementary DNA
COSY	<sup>1</sup> H- <sup>1</sup> H Homonuclear Correlation Spectroscopy
CYP	Cytochrome
d	Doublet
dd	Double doublet
DCM	Dichloromethane
DEPT	Distortionless Enhancement by Polarization Transfer
EtOAc	Ethyl acetate
FAME	Fatty Acid Methyl Ester
Fe	Iron
Fr	Fraction
GC	Gas Chromatography
GC-MS	Gas Chromatography-Mass Spectrometry
HMBC	Heteronuclear Multiple Bond Correlation
HPLC	High Performance Liquid Chromatography
HRESIMS	High Resolution Electron Spray Ionization Mass Spectrometry
HSQC	Heteronuclear Single Quantum Coherence
Hz	Hertz
<i>J</i>	Spin-spin coupling constant (Hz)
LC-MS	Liquid chromatography-mass spectrometry
m	Multiplet
m/z	Mass to charge ratio
MeOH	Methanol
MIC	Minimum Inhibitory Concentration
Mn	Manganese
multi	Multiplicity

NADPH	Nicotinamide adenine dinucleotide phosphate
NADP <sup>+</sup>	Reduced nicotinimide adenine dinucleotide phosphate
MHz	Megahertz
NMR	Nuclear Magnetic Resonance
s	Singlet
t	Triplet
TLC	Thin Layer Chromatography
UV	Ultra Violet
$\delta$	Chemical shift (ppm)

## Abstract

Marine brown algae produce a variety of terpenes with a wide range of biological activities. However, very few phytochemical studies of brown algae have been conducted in South Africa. Therefore, in our continued search for biologically active natural products, we examined the South African brown alga *Brassicophycus brassicaeformis*. The dichloromethane-methanol extract of *B.brassicaeformis* was fractionated by silica gel column chromatography followed by normal phase HPLC to give pure four pure compounds which were identified by spectroscopic methods as; fucosterol, fucoxanthin and two monogalactosyldiacylglycerol lipids.

Many potential drug molecules such as natural products have failed to reach the market due to poor pharmacokinetic and metabolic profiles despite having potent biological activity. Therefore the importance of early drug metabolism studies in the drug development process is clear. A biomimetic oxidation model was used for *in vitro* drug metabolism studies to predict any possible metabolites that could be produced by these natural products.

Two biomimetic oxidation models catalyzed by two water soluble metalloporphyrins as biomimics of cytochrome P450, in the presence of two terminal oxidants either hydrogen peroxide or iodobenzene diacetate were successfully developed. The models were applied to a range of natural products. The oxidation of the quinone natural products, sargahydroquinone acid, and lapachol was most easily achieved by metalloporphyrins employed in this study.

# Chapter 1

## General introduction to marine natural products

### 1.1 Natural products

Marine natural products are secondary metabolites which are produced by living organisms, plants microorganisms, invertebrates, etc. in the marine environment. These secondary metabolites differ from the primary metabolites in that the latter metabolites are simple molecules produced for the provision nutrients, energy and upkeep of organism cells, whereas secondary metabolites provide an evolutionary advantage to an organism critical to its survival (Chemler and Koffas, 2008). Secondary metabolites are produced by organisms to act as herbivore deterrents, as chemical defence agents against predators and in some organisms, offer a reproductive advantage by acting as chemical attractants (Donia and Hamann, 2003; Haefner, 2003).

#### 1.1.1 Marine natural products

The marine environment has an immensely rich biodiversity, providing a wide variety of unique and novel natural products, prompting a renaissance in the marine natural products research in the search for new potential drugs (Fattorusso *et al.*, 2012; Glaser and Mayer, 2009). Of interest to this work are the marine natural products derived from marine macroalgae also known as seaweeds (i.e. Chlorophyta, Rhodophyta and Phaeophyta). Marine macroalgae are a group of heterogeneous plants with a history of fossils which occupy the littoral zones of the sea (El Gamal, 2010). Seaweeds are considered to be a food delicacy in East Asian countries such as Japan and China. In these countries, seaweeds were used to treat iodine deficiencies and other conditions such hypocholesterolaemia and hypoglycaemia (El Gamal, 2010). This history therefore promises a plethora of biological activities brought about by the natural product metabolites present in the seaweeds.

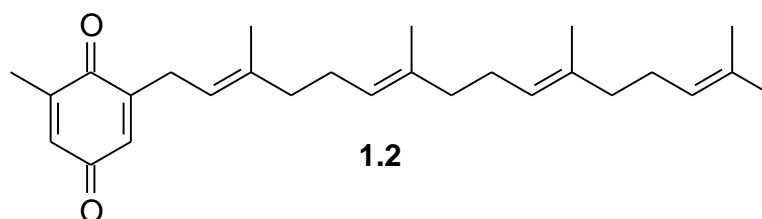
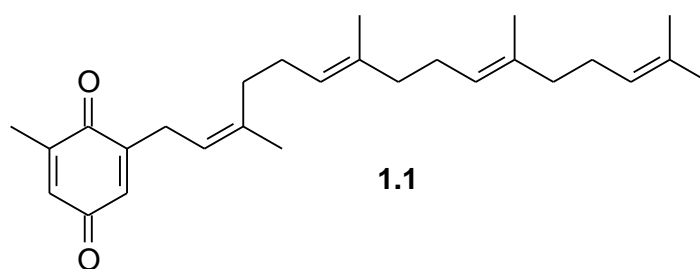


### 1.1.1.1 Phaeophyta (Brown algae)

Almost 1700 species of brown algae have been described in the literature by researchers with more than 1500 compounds already isolated from this group of marine algae. About two-thirds of the natural products from brown algae have been isolated from species belonging to the families Dictyotaceae and Sargassaceae (Muñoz *et al.*, 2012). Brown seaweeds have long been shown to possess an array of biological activities which include: anti-inflammatory, antioxidant, cytotoxic activities (Wijesinghe and Jeon, 2011). In the following section, selected natural products exhibiting these activities will be briefly reviewed.

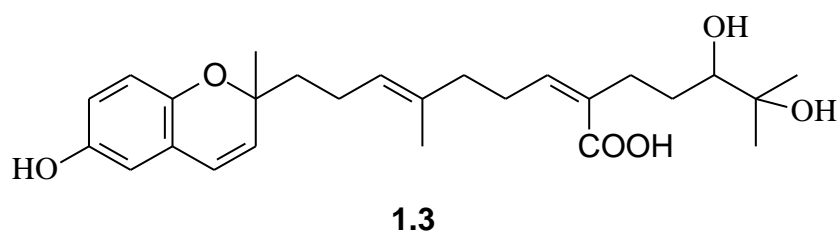
#### Anti-inflammatory activity

Inflammation is a process whereby the inflammatory mediators such as histamine and leukotrienes are produced as highly reactive species in response to cell and tissue damage or harmful stimuli. It has been associated with several disease states which include cancer and autoimmune conditions (Tziveleka *et al.*, 2005). The natural products (*Z*)-sargaquinone (**1.1**) and its analogue (*E*)-sargaquinone (**1.2**) isolated from the brown alga *Taonia atomaria* have demonstrated *in vitro* anti-inflammatory activity by inhibition of leukotriene biosynthesis. These two metabolites have also been isolated from *Styopodium zonale* and *Cystoseira jabukae* (El Gamal, 2010; Tziveleka *et al.*, 2005).



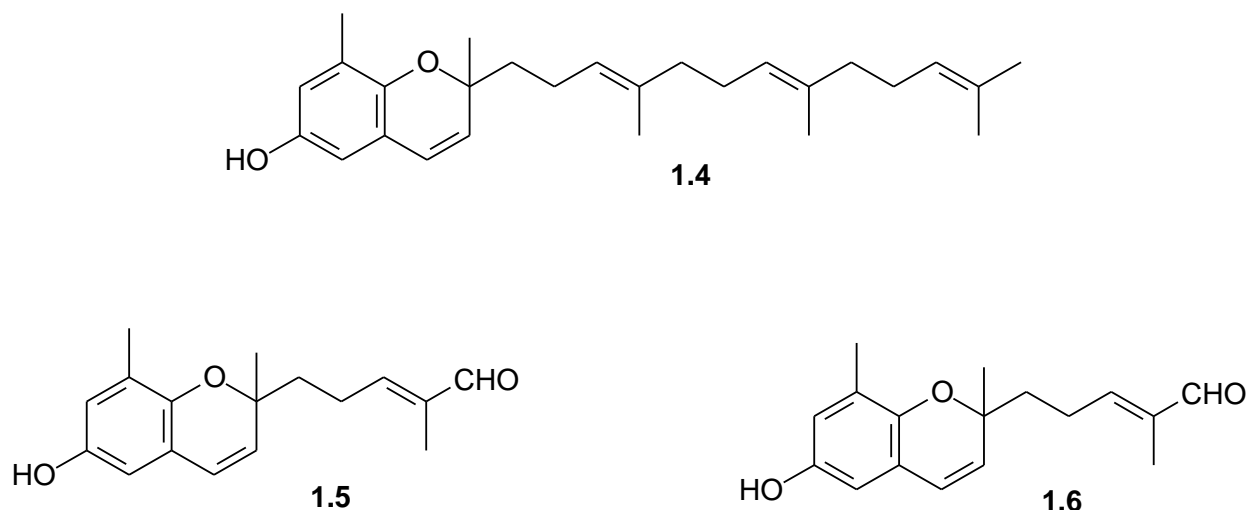
### Antioxidant activity

Free radicals, such as nitric oxide (NO), when produced in large amounts are responsible for the pathogenesis of several pathological conditions such as tissue damage and carcinogenesis. Antioxidants are therefore essential in counteracting the activity of free radicals (Lopes *et al.*, 2014). A novel antioxidant natural product, sargathunbergol (**1.3**) isolated from *Sargassum thunbergii* is structurally related to vitamin E. The antioxidant activity of **1.3** was determined by the ability of the natural product to scavenge the free radical DPPH (1,1-diphenyl-2-picrylhydrazyl) by comparison to known antioxidants  $\alpha$ -tocopherol and butylated hydroxytoluene (BHT). Sargathunbergol was found to exhibit better antioxidant activity than BHT, but less so than  $\alpha$ -tocopherol (Lopes *et al.*, 2014).



### Cytotoxic activity

Diterpenoid secondary metabolites isolated from brown alga have been shown to possess potent cytotoxic activities against a wide range of human cancer cell lines. Meroterpenoids isolated from *Sargassum tortile* such as sargaol (**1.4**) and its derivatives sargasal-I (**1.5**) and sargasal-II (**1.6**) were shown to exhibit cytotoxic activity against cultured P-388 lymphatic leukemia cells with sargasal-I and sargasal-II showing most significant activity (Numata *et al.*, 1992).

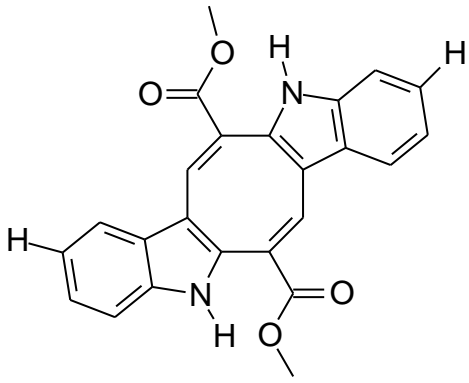
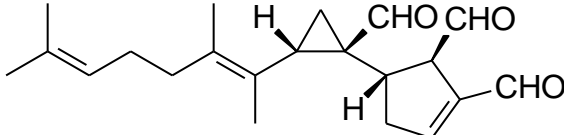
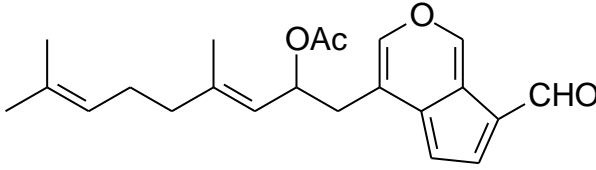


**Figure 1.1** Cytotoxic metabolites isolated from *Sargassum tortile*

### 1.1.1.2 Chlorophyta (Green Algae)

Green algae are so named due to the presence of chlorophyll a and b, which gives the seaweed their characteristic colour (El Gamal, 2010). Fewer novel natural products have been isolated from green algae compared to the brown and red algae, but those isolated have also been shown to exhibit biological activities such as anti-inflammatory, cytotoxic and antiviral activities (Blunt *et al.*, 2007; El Gamal, 2010). Table 1.1 below summarizes the natural products isolated from Chlorophyta, together with their biological activities.

**Table 1.1** Examples of clinically significant natural products from Chlorophyta

Biological Activity	Example of Natural Product	Algae	Reference
Anti-tuberculosis activity	 <p>Natural product Caulerpin, with activity against <i>Mycobacterium tuberculosis</i> strain H37Rv</p>	<i>Caulerpa</i> sp.	Chay <i>et al.</i> , 2014
Cytotoxic activity	 <p>Halimedatrial, a natural product with cytotoxic and antimicrobial activities</p>	<i>Halimida lamouroux</i>	El Gamal, 2010
Antiviral	 <p>Halitunal, a marine natural product with <i>in vitro</i> antiviral activity against murine coronavirus A59</p>	<i>Halimeda tuna</i>	El Gamal, 2010; Koehn <i>et al.</i> , 1991

### 1.1.1.3 Rhodophyta (Red Algae)

Red algae are a source of a vast number of biologically significant natural products which are mostly of terpene and halogenated polyphenol origin. The rich source of halogenated secondary metabolites is attributed to the presence of haloperoxidases. This group of algae is so named due to their colour owing to the presence of the pigments phycoerythrin and phycocyanin which dominate over the other pigments such as chlorophyll a and b and  $\beta$ -carotene (El Gamal, 2010; Blunt *et al.*, 2007).

Brominated sesquiterpenes, which have been typically isolated from the *Laurencia* species, are the most common type of secondary metabolite found in red algae (de Carvalho and Roque, 2004). In fact, the secondary metabolites isolated from *Laurencia* species have been found to have the highest degree of halogenation compared to the other Rhodophyta species. The plethora of halogenated secondary metabolites include diterpenes, triterpenes, sesquiterpenes and C-15 acetogenins which exhibit a variety of biological activities (Cabrita *et al.*, 2010). The biological activities include cytotoxic, antibacterial, antiviral and even anti-inflammatory activities (Cabrita *et al.*, 2010).

Many species of *Laurencia* have afforded elatol (**1.7**) (Figure 1.2), a potent antibacterial and anti-herbivory agent against the black sea urchin (Cabrita *et al.*, 2010). Elatol has demonstrated antibacterial activity against *Salmonella*, *Staphylococcus epidermis* and *Klebsiella pneumonia* (El Gamal, 2010). Other remarkable secondary metabolites isolated from Rhodophyta include the five halogenated monoterpenes isolated from the South African red algae, *Plocamium cornutum*, a species rich in polyhalogenated metabolites. Three compounds (**1.8**, **1.9**, **1.10**) (Figure 1.2) isolated from *Plocamium cornutum* showed significant activity against *Plasmodium falciparum*, the malaria causing parasite, where the activity has been attributed to the chloromethyl moiety of the compounds. However, the activities of **1.8** ( $IC_{50}$ = 17 $\mu$ M), **1.9** ( $IC_{50}$ = 27 $\mu$ M) and **1.10** ( $IC_{50}$ = 16 $\mu$ M) against the *Plasmodium* parasite were still found to be less than that of chloroquine ( $IC_{50}$ = 9.3 nM) (Afolayan *et al.*, 2009; Cabrita *et al.*, 2010). Another marine red alga, *Portiera hornemanni* produces a unique compound halomon (**1.11**), shown to possess potent anticancer activity against several human cancer cell lines (Fuller *et al.*, 1992; Davies-Coleman and Beukes, 2004).

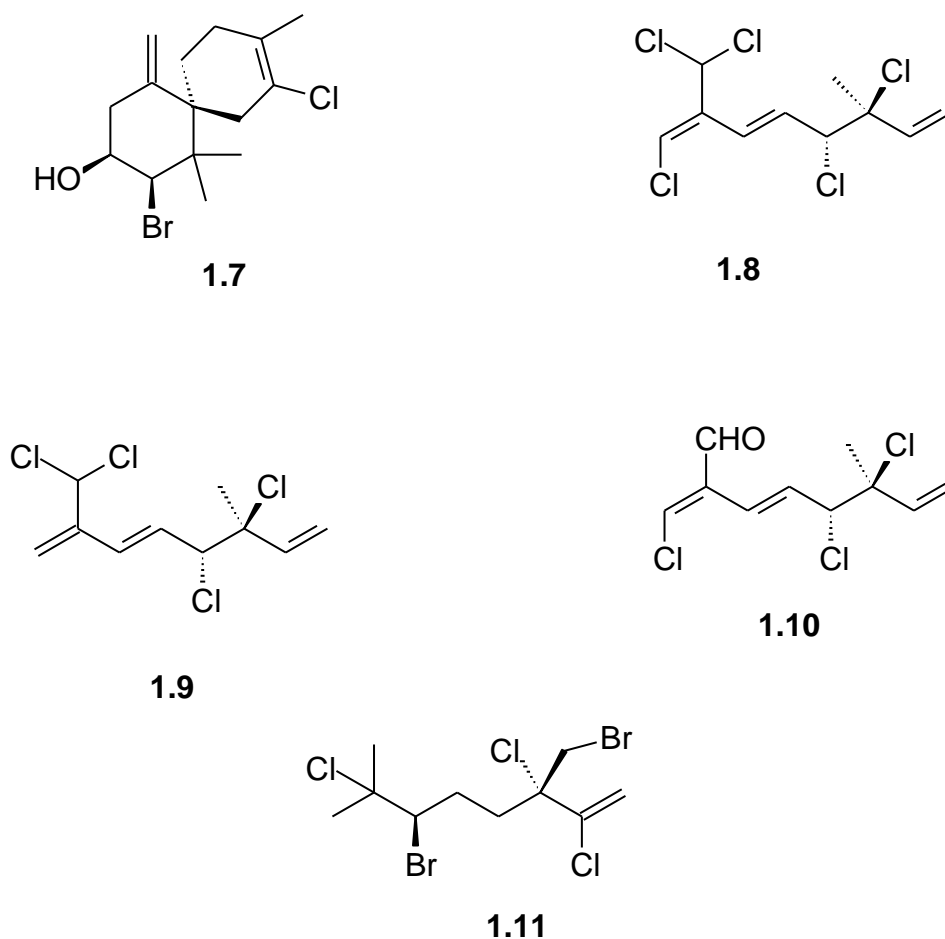


**Figure 1.2** Biologically active halogenated metabolites from Rhodophyta

### 1.1.2 Clinically successful drugs from natural products

The marine environment has provided numerous compounds with prodigious structural, chemical diversity entwined with a wealth of biological activities; with some metabolites exhibiting a novel mechanism of action. These novel chemical entities and biological activities therefore form the basis for further exploration for the natural product and medicinal chemistry scientist (Liu, 2012). In the period of 1998-2008 the global marine pharmaceutical pipeline included a total of 592 marine natural products with antitumor and

cytotoxic activities, thus illustrating the potential of marine natural products have in drug development (Liu, 2012). For example, the first marine natural product to be marketed in the United States was ziconotide. It was isolated from the tropical marine snail *Cornus magus* as a treatment for chronic pain. It was marketed as Prialt<sup>®</sup> and used in the management of chronic pain in spinal cord injury (Laser and Mayer, 2009; Liu, 2012). Carraguard<sup>®</sup> is another example of a bioactive compound derived from carrageenans from seaweed. It is a polysaccharide-type metabolite marketed as a vaginal microbicide in preventing sexually transmitted diseases such as human papilloma virus (HPV) (Marais *et al.*, 2011). Propylene glycol alginate sodium sulfate (PSS) is the first marine natural product marketed as an antiangiocardopathy agent in China in treating heart and brain diseases. PSS is a secondary metabolite derived from seaweed polysaccharides (Li *et al.*, 2013).

## Conclusion

Marine natural products are a source of new chemical entities which provide basis for the exploration of new drug targets and mechanisms of action. The chemical and biological diversity pointed out by the marine organisms gives the natural products and medicinal chemists a key to combat pathologies that have developed resistance (such as microbial infections) and those that have presented challenges in treatment such as cancer. Marine natural products therefore present a unique opportunity to provide a wide variety of new drug molecules as well as an aid in understanding several disease states.

## 1.2 Research aims and objectives

Many natural products isolated from the marine environment particularly from marine macroalgae have a wealth of biological activities including cytotoxicity, antimicrobial, antiviral and anti-inflammatory activities. As a result, it would be worthwhile exploring the potential metabolites that can be obtained from such natural products. The metabolism of xenobiotics in humans plays a major role in the development of new drugs. Drug metabolism impacts on pharmacokinetics and potential toxicity of new chemical entities. It may therefore be useful to explore the metabolism of lead compounds early in the drug discovery and development process. The overall aim of the current research was therefore, to discover biologically active natural products and to develop a general methodology for the biomimetic metabolism of biologically active natural products.

The objectives of the research were:

- To isolate and characterize natural products from marine brown alga *Brassicophycus brassicaeformis*
- To create an easily reproducible biomimetic oxidation model for use within a laboratory setting using known non-steroidal anti-inflammatory drugs as an *in vitro* drug metabolism study
- To apply the biomimetic oxidation models to selected natural products

## 1.3 Thesis outline

This thesis contains five comprehensive chapters. The first chapter contains a general introduction to marine natural products while chapter two gives a detailed literature review for drug metabolism and its place in drug discovery and development. Chapter three describes the natural products isolated from *Brassicophycus brassicaeformis*. In the fourth chapter, the development of biomimetic oxidation models was accomplished and applied to selected natural products with known biological activities. Finally chapter five provides a conclusion to the research carried out and evaluation of research outcomes.



## 1.4 References

- Afolayan A.F., Mann M.G.A., Lategan C.A., Smith P.J., Bolton J.J., Beukes D.R. (2009). Antiplasmodial halogenated monoterpenes from marine alga *Plocamium cornutum*. *Phytochemistry* 70: 597-600
- Blunt J.W., Copp B.R., Hu W., Munro M.H.G., Northcote P.T., Prinsep M.R. (2007). Marine natural products. *Natural Product Reports* 24: 31-86
- Cabrita M.T., Vale C., Rauter A.P. (2010). Halogenated compounds from marine algae. *Marine Drugs* 8: 2301-2317
- Chay C.I.C., Cansino R.G., Pinzón C.I.E., Torres-Ochoa R.O., Martínez R. (2014). Synthesis and anti-tuberculosis activity of marine natural product caulerpin and its analogues. *Marine Drugs* 12: 1757-1772
- Chemler J.A., Koffas M.A.G. (2008). Metabolic engineering for plant natural product biosynthesis in microbes. *Current Opinion in Biotechnology* 19: 597-605
- Davies-Coleman M.T., Beukes D.R. (2004). Ten years of marine natural products research at Rhodes University. *South African Journal of Science* 100: 539- 544
- De Carvalho L.R., Roque N.F. (2004). Correlations between primary and secondary metabolites in Ceramiales (Rhodophyta). *Biochemical Systematics and Ecology* 32: 337-342
- Donia M., Hamann M.T. (2003). Marine natural products and their applications as anti-infective agents. *The Lancet Infectious Diseases* 3: 338-348
- El Gamal A.A. (2010). Biological importance of marine algae. *Saudi Pharmaceutical Journal* 18: 1-25
- Fattorusso E., Gerwick W.H., Tagliatela-Scafati O. (2012). Part 1: Natural product trends in different groups of marine life. (Fattorusso E., Gerwick W.H., Tagliatela-Scafati O Ed.) Dordrecht: Springer, Netherlands: 1- 295

Fuller R.W., Cardellina J.H., Kato Y., Brinen L.S., Clardy J., Snader K.M., Boyd M.R. (1992). A pentahalogenated monoterpene from red alga *Portiera hornemannii* produces a novel cytotoxicity profile against a diverse panel of human tumor cell lines. *Journal of Medicinal Chemistry* 35: 3007-3011

Glaser K.B., Mayer A.M.S. (2009). A renaissance in marine pharmacology: from preclinical curiosity to clinical reality. *Biochemical Pharmacology* 78: 440-448

Haefner B. (2003). Drugs from the deep: marine natural products as drug candidates. *Drug Discovery Today* 8: 536-544

Koehn F.E., Gunasekera S.P., Niel D.N., Cross S.S. (1991). Halitunal, an unusual diterpene aldehyde from the marine alga *Halimeda tuna*. *Tetrahedron Letters* 32: 169-172

Li P., Li C., Xue Y., Li H., Liu H., He X., Yu G., Guan H. (2013). An HPLC method for microanalysis and pharmacokinetics of marine sulfated polysaccharide PSS-loaded poly lactic-*co*-glycolic acid (PLGA) nanoparticles in rat plasma. *Marine Drugs* 11: 1113-1125

Liu Y. (2012). Renaissance of marine natural product drug discovery and development. *Journal of Marine Science Research and Development* 2: 1-2

Lopes G., Daletos G., Proksch P., Andrade P.B., Valentão P. (2014). Anti-inflammatory potential of monogalactosyl diacylglycerols and a monoacylglycerol from the edible seaweed *Fucus spiralis* Linnaeus. *Marine Drugs* 12: 1406-1418

Marais D., Gawarecki D., Allan B., Ahmed K., Altini L., Cassim N., Gopolang F., Hoffman M., Ramjee G., Williamson A. (2011). The effectiveness of Carraguard, a vaginal microbicide, in protecting women against high-risk human papillomavirus infection. *Antiviral Therapy* 16: 1219-1226

Muñoz J., Culioli G., Köck M. (2012). Linear diterpenes from the marine brown alga *Bifurcaria bifurcata*: a chemical perspective. *Phytochemical Reviews* 12: 407-424

Numata A., Kanbara S., Takahashi C., Fujiki R., Yoneda M., Usami Y., Fujita E. (1992). A cytotoxic principle of brown alga *Sargassum tortile* and structures of chromenes. *Phytochemistry* 31: 1209-1213

Tziveleka L., Abatis D., Paulus K., Bauer R., Vaglas C., Roussis V. (2005). Marine polyprenylated hydroquinones, quinones and chromenols with inhibitory effects on leukotriene formation. *Chemistry and Biodiversity* 2: 901-909

Wijesinghe W.A.J.P., Jeon Y. (2011). Biological activities and potential cosmeceutical applications of bioactive components from brown seaweeds: a review 10: 431-443

# Chapter 2

## Literature review

### 2.1 The drug discovery and development process

Drug discovery and development is a process initiated in the search for new chemical entities to combat diseases. A need arises for development of new drugs especially when resistance to existing drugs occurs, prompting the need to search for new drug targets. Drug development is a long process taking 10-15 years from drug discovery to drug marketing. The process is very expensive, costing pharmaceutical companies as much as one billion US dollars. Taking all these factors into consideration, there is consequently a low turnover for new drug molecules entering the market (Hughes *et al.*, 2011).

The drug development process starts with the identification of a drug target which could be: proteins, DNA, RNA or even the biochemical pathways essential to the etiology of a disease. A good drug target should be 'druggable', meaning that it should elicit a measurable biological response upon attachment of the potential drug to the target (Hughes *et al.*, 2011). After identifying a drug target, lead discovery is the next step involving screening and isolation of a potential new drug. Lead discovery involves high throughput screening, combinatorial screening and assay development, and isolation from nature amongst other processes (Hughes *et al.*, 2011; Nicolau, 2014). Medicinal chemistry studies are the next step in the drug development process. These studies provide structure-activity information and facilitate development of a library of compounds via chemical synthesis using the lead compound as a template (Hughes *et al.*, 2011; Nicolau, 2014). The next stage in the drug development process is the *in vitro* and *in vivo* animal studies which provide activity and safety data as well as the pharmacokinetic profile of a drug molecule: *viz.* absorption,

distribution, metabolism and excretion (Gunaratna, 2000; Lin and Lu, 1997). This provides insight into the safety and efficacy of a potential drug, ultimately assisting in prioritizing lead compounds. The final stage in the drug development process is the submission of an Investigational New Drug (IND) application to facilitate human clinical trials (Hughes et al., 2011). Figure 2.1 gives a summary of the drug discovery and development process.

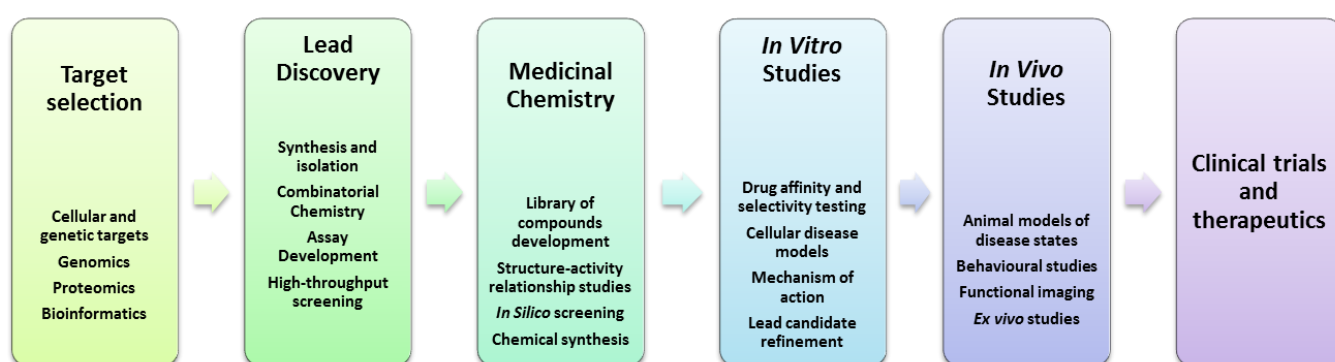


**Figure 2.1** Summary of drug discovery and development process<sup>1</sup>

Drug metabolism studies are a crucial component of the drug discovery and development process and provide the safety and efficacy data of any new potential drug molecule. As a result, early metabolism studies are important in determining these parameters, giving new insight into the success or failure of a potential drug early in the drug development process. For this reason, an important part of this research project is centred on early metabolism studies on biologically active natural products.

<sup>1</sup> Accessed (06/01/2015), Adapted from: [http://drugdiscovery.com/upimages/1373879800\\_drug-discovery-1.jpg](http://drugdiscovery.com/upimages/1373879800_drug-discovery-1.jpg)

## 2.2 Overview of drug metabolism

Drug metabolism is a process which occurs mainly in the liver, in which lipophilic drug molecules are converted to water-soluble products that can be excreted from the body. It also takes part in the bioconversion of inactive drug molecules to therapeutically active molecules; the basis of prodrug design (Gunaratna, 2000; Cutler and Block, 2004). Chloramphenicol is an antibacterial agent with poor water solubility which affects the parenteral route of administration. As a result, a succinate ester of chloramphenicol with no antibacterial activity was developed which undergoes *in vivo* ester hydrolysis to release the active chloramphenicol. Figure 2.2 below shows the prodrug activation of chloramphenicol succinate (Smith and Clark, 2004).

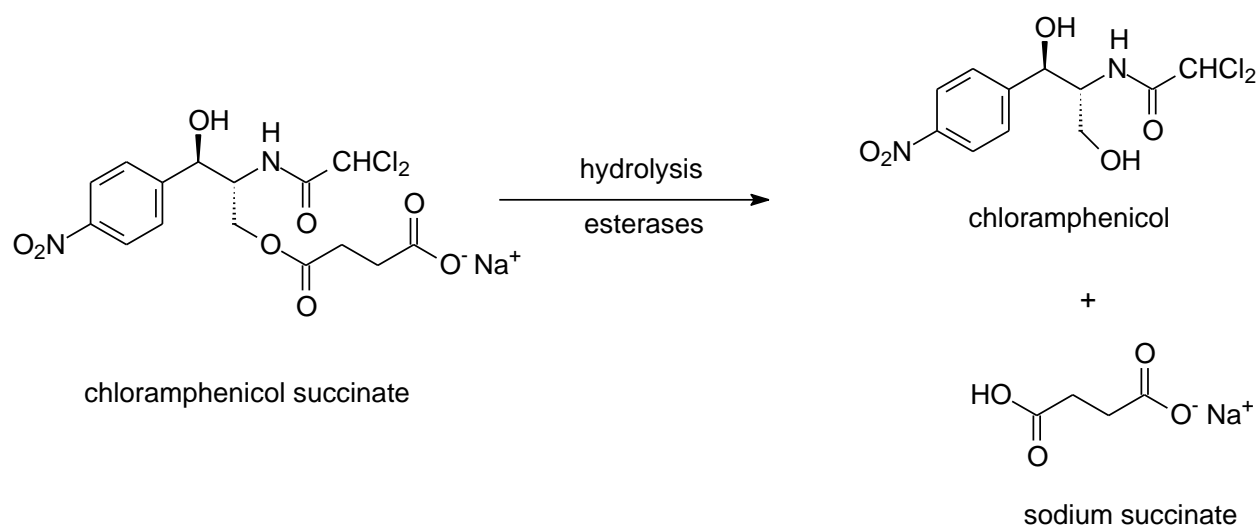


**Figure 2.2** Bioactivation of chloramphenicol succinate *in vivo* (Adapted from Smith and Clark, 2004)

Drug metabolism also involves bioinactivation of active drug molecules to inactive metabolites excreted from the body or it may facilitate the conversion of drug molecules to toxic metabolites resulting in toxicity and side effects. The metabolism of paracetamol illustrated in Figure 2.3 gives an example of bioinactivation.

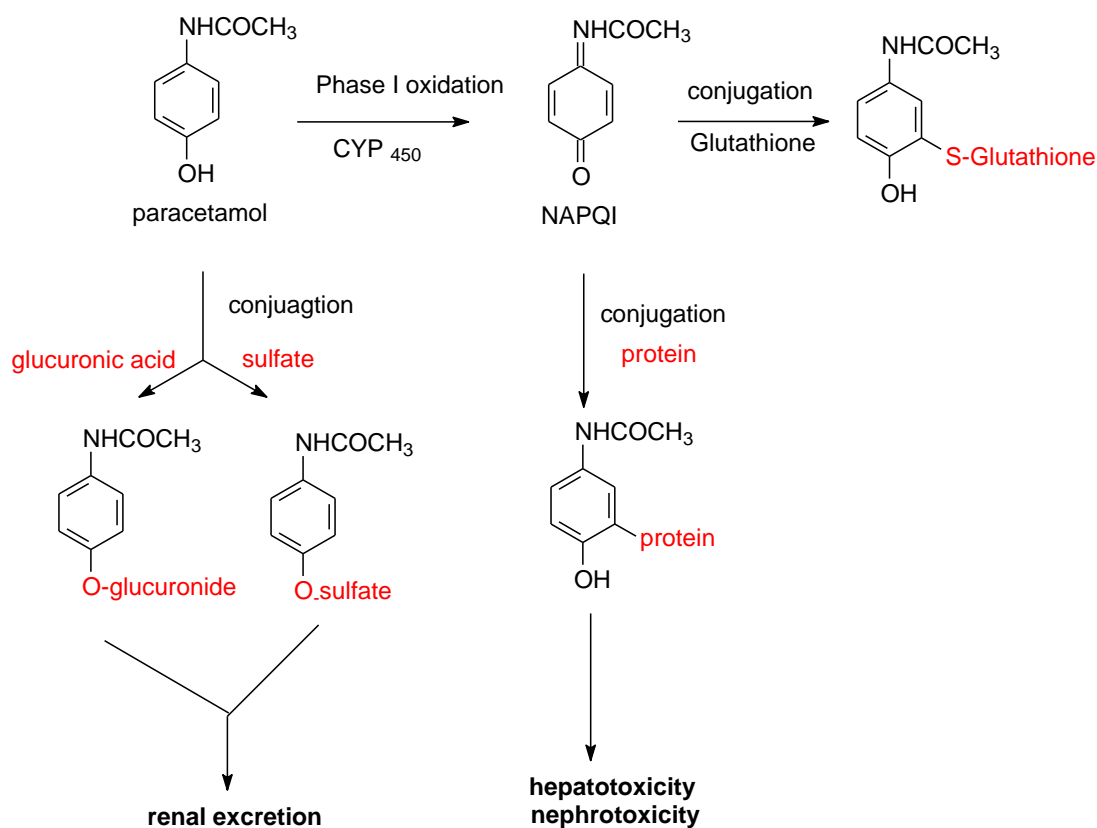


**Figure 2.3** Metabolism of paracetamol in the human body (Adapted from Dybing *et al.*, 1984; Xie *et al.*, 2014)

Metabolism is achieved by phase I and phase II metabolism. Phase I metabolism catalyzed by cytochrome P450 enzymes which involves functionalization of a drug molecule, rendering it more polar. The functionalization reactions include oxidation, ester and amide hydrolysis, as well as hydroxylation reactions (Kumar and Surapaneni, 2001). Phase II metabolism therefore involves derivatization reactions whereby conjugation of parent drug molecules, or phase I metabolites with conjugates such as sulfates, glucuronic acid and glutathione occurs to ensure excretion from the human body (Kumar and Surapaneni, 2001; Cutler and Block, 2004).

Paracetamol has been used as an example to illustrate phase I and phase II metabolic reactions that occur in the body as well as the possible metabolic fate of a drug upon administration (Figure 2.3). Paracetamol is mainly metabolized via phase II metabolic processes by conjugation with glucuronic acid and sulfate to enable renal excretion of inactive metabolites (Cutler and Block, 2004; Xie *et al.*, 2014). The drug is also oxidized to

its quinone derivative, N-acetyl-p-benzoquinone imine (NAPQI), via phase I metabolism. NAPQI is a hepatotoxic and nephrotoxic metabolite which accumulates in paracetamol overdose causing liver damage. Glutathione conjugation of NAPQI, on the other hand, occurs via phase II metabolism to form a non-toxic secondary metabolite which is then excreted from the body (Dybing *et al.*, 1984; Xie *et al.*, 2014).

Drug metabolism is one of the pharmacokinetic processes which a drug undergoes following administration. When a drug is administered, it is absorbed, distributed and metabolized before being excreted from the body. Each of these processes is important in ensuring an effective therapy (Ionescu and Cairn, 2006). Figure 2.4 summarizes drug metabolism in the human body.

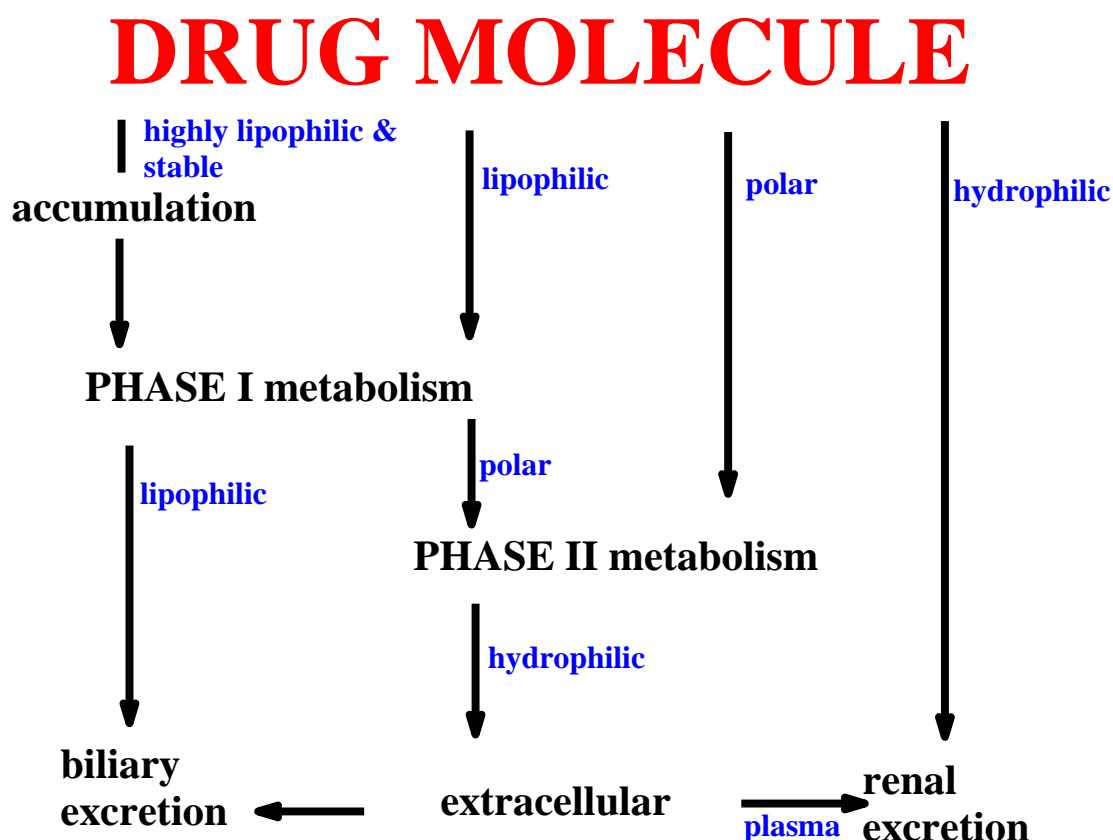


**Figure 2.4** Summary of drug metabolism<sup>2</sup>

<sup>2</sup> (Adapted from; Accessed 29/01/2015), Available at: [http://3.bp.blogspot.com/-dH0RnpwIwcQ/UF4jpf\\_s8dI/AAAAAAAAAFs/w5bkdVYZVUk/s1600/clinical%20pharmacology-%20drug%20&%20body%20interactions%20part%20I%20&2.117.tiff](http://3.bp.blogspot.com/-dH0RnpwIwcQ/UF4jpf_s8dI/AAAAAAAAAFs/w5bkdVYZVUk/s1600/clinical%20pharmacology-%20drug%20&%20body%20interactions%20part%20I%20&2.117.tiff) )



### 2.2.1 The cytochrome P450 monooxygenases

Cytochrome P450 isoenzymes are a group of enzymes which catalyze phase I metabolism *via* oxidation, reduction, epoxidation, hydroxylation and hydrogenation reactions (Stachulski, 2000; Cutler and Block, 2004). Functional groups added to lipophilic drug molecules to improve polarity include hydroxyl, carboxyl and amino functional groups which are added via oxidation, reduction and hydrolysis reactions (Cutler and Block, 2004). About 57 cytochrome P450 enzymes are found in the human body, but only a quarter of these are responsible for the metabolism of xenobiotics (Guengerich, 2006). Some of these include: CYP3A4, CYP2C9 and CYP1A2 which are amongst the major metabolizing enzymes in the human body where CYP3A4 metabolizes approximately half of the known drugs (Gunaratna, 2000).

Cytochrome P450 isoenzymes are heme containing monooxygenases with a protoporphyrin IX (Figure 2.5) core as the active site. The protoporphyrin centre has cysteine as a fifth ligand and a sixth coordination site where molecular oxygen is able to bind during catalytic reactions (Lohmann and Karst, 2008).

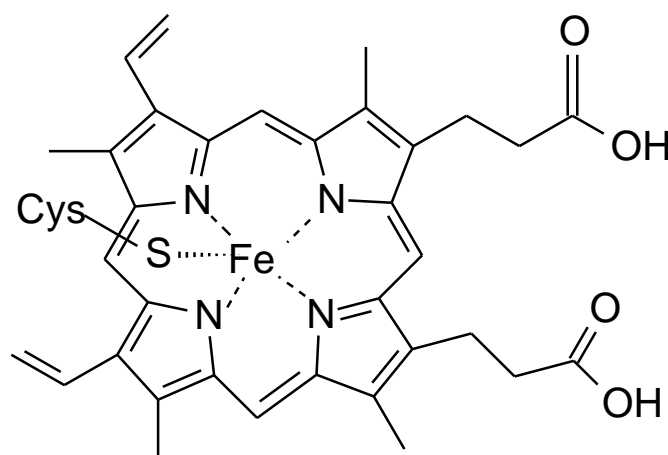
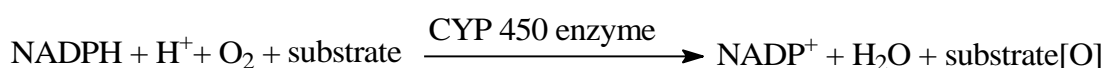


**Figure 2.5** Protoporphyrin IX core of cytochrome P450 monooxygenase enzyme

(Adapted from Lohmann and Karst, 2008)

The oxygenation of substrates by CYP 450 enzymes occurs in a catalytic cycle (Figure 2.6) with the end result being the transfer of an oxygen atom to the substrate (Gunaratna, 2000; Lohmann and Karst, 2008). In the ground state, the Fe (III) moiety of the protoporphyrin core IX has a water molecule bound to the sixth coordination site. The iron centre attains its activated state upon receiving electrons from NADPH to release the water molecule and Fe (IV) oxo-species which are the active oxidants (Lohmann and Karst, 2008; Gunaratna, 2000). The reaction is summarised below.



(Gunaratna, 2000; Lohmann and Karst, 2008)

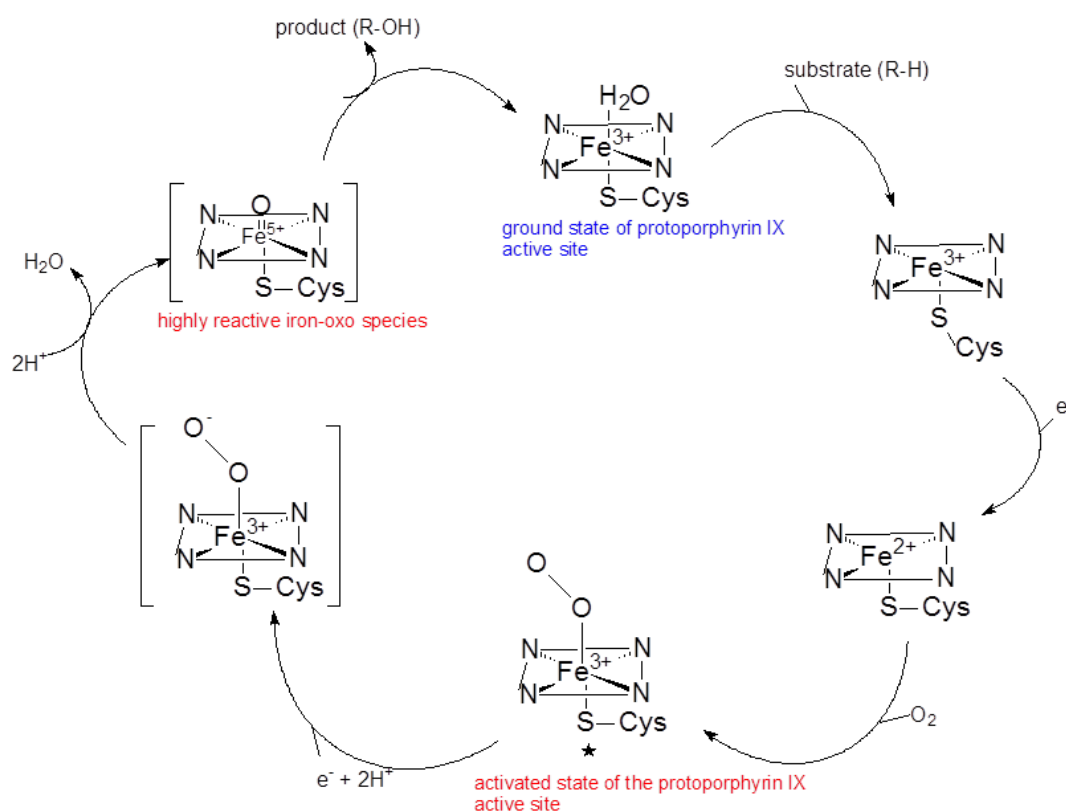


**Figure 2.6** The catalytic cycle occurring in a cytochrome P450 isoenzyme active centre<sup>3</sup>

<sup>3</sup> (Adapted from Fleming, 2001)

## 2.3 The importance of drug metabolism in drug discovery and medicinal chemistry

Current drug discovery and development guidelines require that *in vitro* and *in vivo* metabolism studies be conducted in the early stages of the process in order to guide drug development where potential metabolites are ascertained and issues of potential drug-drug interactions are addressed (Bai and Liu, 2005). There are a number of pre-clinical drug metabolism studies that have been employed to identify the expected drug metabolites. Some of these are discussed below.

### 2.3.1 *In vivo* drug metabolism models

Animal studies have been conducted as a model for *in vivo* metabolism studies of potential drug molecules in humans. In this case, animals such as rats and dogs provide important, relevant models which may be used to predict the formation of possible metabolites upon administration of the potential drug molecule to humans (Gunaratna, 2000; Tingle and Helsby, 2006). Animal models provide the physiological environment for drug metabolism, illustrating any potential biotransformations new chemical entities are liable to undergo (Tingle and Helsby, 2006). However, there are drawbacks associated with animal models. One issue is that they cannot always be translated to human drug metabolism as there are differences between enzyme expression in animals and humans. Another concern is differing substrate specificity (Chauret *et al.*, 1997; Tingle and Helsby, 2006; Vaclavikova *et al.*, 2004). Furthermore, animal studies require ethical clearance since ethical issues arise with these models and, as such, the studies are expensive to conduct (Bernadou and Meunier, 2004). On the other hand, animal models are useful in predicting pharmacokinetic profiles for drug molecules that remain unchanged upon excretion, i.e. drug molecules that are cleared renally (Tingle and Helsby, 2006).

### 2.3.2 *In vitro* drug metabolism models

The big question with animal studies is whether the results can be translated to humans, after factoring in inter-species variation (Tingle and Helsby, 2006; Wrighton *et al.*, 1995). *In vitro* drug metabolism models have therefore been developed to counteract inter-species variation

which may occur with animal models (Wrighton *et al.*, 1995). These *in vitro* models include; hepatic tissue slices, isolated hepatic cells, expressed enzymes, isolated enzymes, *in silico* drug metabolism and biomimics of cytochrome P450 monooxygenases (Gunaratna, 2000). The liver has been targeted as the source of most *in vitro* metabolism studies because it is the site where most of the drug metabolism occurs (Tingle and Helsby, 2006).

### 2.3.2.1 Hepatic tissue slices and isolated hepatocytes

Hepatic tissue slices provide liver cells with intact cell structure and physiology including drug metabolizing enzymes, thus the integrity of hepatocytes is maintained. As a result, potential metabolic pathways of a drug molecule are preserved. These tissue slices are easy to produce in a rapid process which makes them readily available to conduct studies (Gunaratna, 2000; Wrighton *et al.*, 1995). The major disadvantage with hepatic tissue slices is that they quickly lose their viability and therefore they cannot be preserved to perform experiments at a later time. This issue, however, can be counteracted somewhat by cryopreservation of the tissue slices (Gunaratna, 2000).

Isolated hepatocytes, like tissue slices, are part of cellular systems that have been used in *in vitro* drug metabolism studies. They are obtained from tissue cultures or they are isolated from collagen perfusion techniques from fresh liver cells (Gunaratna, 2000; Wrighton *et al.*, 1995). Isolated hepatocytes, like tissue slices also preserve cell integrity thus affording study of the metabolic pathways of a drug. Many disadvantages arise from the use of isolated hepatocytes. The isolated cells lose their integrity upon cryopreservation due to the freezing and thawing process (Coundouris *et al.*, 1993; Wrighton *et al.*, 1995). Other studies have shown that culturing hepatocytes alters the expression of some drug metabolizing enzymes in the cells, consequently altering the biotransformation of the drug molecules by these cells (LeCluyse *et al.*, 2001; Wrighton *et al.*, 1995).

### 2.3.2.2 Isolated and expressed enzymes

Isolated enzymes include cytochrome P450 enzymes and other enzymes such as the peroxidases which make up the hepatic microsomal system. These are purified and concentrated enzymes which can be obtained from human hepatocytes. They provide a purified natural system to enable studies of drug biotransformation (Bernadou *et al.*, 1991). Isolated enzymes are the most popular and purest *in vitro* metabolism models available to scientists because they are easily prepared and stored without any loss of viability of enzymes. These systems usually provide possible phase I metabolism data, however since there is no cellular environment fostering the drug metabolism, data may differ from the actual metabolism that may occur under physiological conditions (Bernadou *et al.*, 1991; Gunaratna, 2000).

Expressed enzymes are specific cytochrome P450 enzymes which are commercially available and have been expressed *via* biotechnological methods. In this case, cDNA specific to a particular P450 enzyme is cloned and expressed (Gunaratna, 2000; Tingle and Helsby, 2006). Enzymes are then purified and concentrated for *in vitro* pharmacokinetic studies. Expressed enzymes, like isolated enzymes, do not offer a physiological cell environment for metabolism as that provided by tissue slices and isolated hepatocytes. Furthermore, they lack post translational folding of the enzyme which occurs in the human body-suggesting differences with the human cytochrome P450 enzymes (Gunaratna, 2000; Tingle and Helsby, 2006).

### 2.3.2.3 *In silico* prediction of drug metabolism

*In silico* drug metabolism prediction is a form of high throughput screening which can be applied to facilitate the drug discovery and development (Zhang *et al.*, 2011). It is a computer generated system which predicts potential drug metabolites, the specific CYP450 enzyme isoform responsible for the metabolism and the prediction of pharmacokinetic properties of a new chemical entity (Dimelow *et al.*, 2012; Ntie-Kang *et al.*, 2013; Zhang *et al.*, 2011). These technologies are gaining ground in drug discovery and development as they eliminate compounds with the potential to have an undesirable pharmacokinetic profiles and toxic side effects early in the process (Ntie-Kang *et al.*, 2013). The advantages of *in silico* drug

metabolism processes are that it reduces the cost of drug development while screening a large number of potential drugs.

#### 2.3.2.4 Biomimics of cytochrome P450 enzymes

Biomimics of cytochrome P450 monooxygenase enzymes refers to molecules with the ability to mimic the activity of cytochrome P450 isoenzymes in a chemical system. Biomimics provide a simple chemical system which overcomes some of the disadvantages that arise with *in vivo* drug metabolism models and some of the *in vitro* models discussed above (Gotardo *et al.*, 2006). For the purpose of this research, the emphasis is on metalloporphyrins as biomimics of a cytochrome P450 metabolism system. Biomimics are mainly focused on oxidation reactions as the majority of the drug metabolism processes occurring in a human body involves oxidative processes. These systems include: a terminal oxidant, a biomimetic catalyst and a co-catalyst.

##### 2.3.2.4.1 Terminal oxidant

A biomimetic catalytic system acts to imitate the oxidative reactions catalyzed by CYP450 isoenzymes that occur naturally in the human body, where molecular oxygen is the source of oxygen. Likewise, in a synthetic metabolic system, an oxygen source is required. Therefore the terminal oxidants in biomimetic drug metabolism models are used. A wide variety of terminal oxidants have been used in these models in literature including: iodosylbenzene (PhIO), peroxides such as hydrogen peroxide ( $H_2O_2$ ), cumene hydroperoxide (CumOOH) and *tert*-butylhydroperoxide (tBuOOH), sodium hypochlorite (NaOCl) amongst others; all of which are single oxygen donors (Bernadou and Meunier, 2004). In nature, cytochrome P450 monooxygenases utilize a single oxygen molecule from molecular oxygen which is then coupled to oxidative reactions, whilst the second oxygen molecule is lost as water (Feiters *et al.*, 2000).

Alkylhydroperoxide oxidants such as *tert*-butyl-hydroperoxide as well as hydrogen peroxide have the main disadvantage of undergoing homolytic fission in the presence of a catalyst to result in degradation of the oxidant and formation of free radicals, whilst product yields are low. This has been observed with first generation, unsubstituted metalloporphyrins, which in the presence of alkylhydroperoxide or H<sub>2</sub>O<sub>2</sub>, have led to poor epoxidation of the alkene moiety while the oxidant rapidly decomposes (Mansuy *et al.*, 1989; Meunier, 1992). This has been counteracted by the addition of a strong ligand donor which is a nitrogen base such as pyridine or imidazole. The ligand donor acts to encourage heterolytic cleavage of the oxidant, facilitating formation of the reactive high-valent, oxo-species (Figure 2.7) (Meunier, 1992).

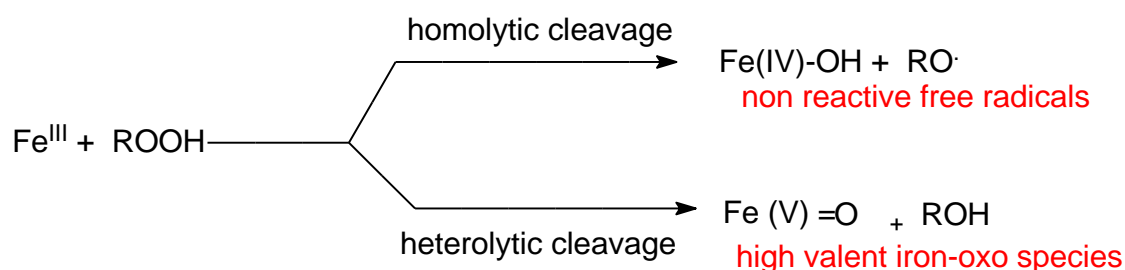


**Figure 2.7** Homolytic and heterolytic cleavage with alkylhydroperoxides and hydrogen peroxide in biomimetic catalysis (Adapted from Mansuy *et al.*, 1989)

#### 2.3.2.4.2 Metalloporphyrin catalysts

Porphyrins are aromatic, heterocyclic macrocycles consisting of four pyrrole rings where the nitrogen can coordinate with a transition metal to form the metalloporphyrin. The pyrrole rings are bridged by a methine moiety to form the macrocyclic structure (Nantes *et al.*, 2011). Figure 2.8 gives a general porphyrin structure. Transition metals that have been incorporated into metalloporphyrins include: iron (Fe), manganese (Mn), zinc (Zn) and ruthenium (Ru) amongst others (Che and Huang, 2009).

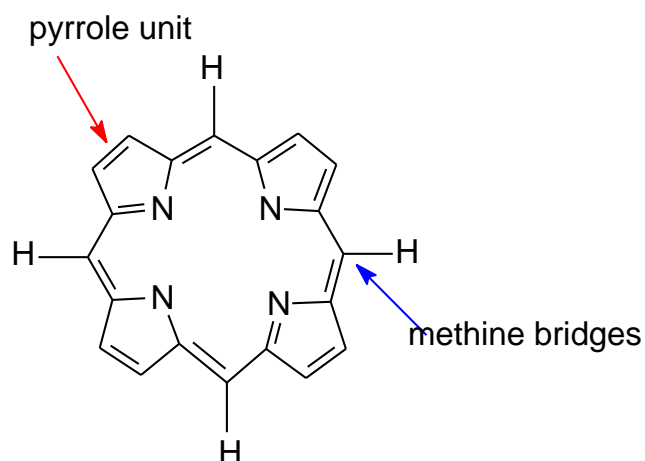


**Figure 2.8** General porphyrin structure

Metalloporphyrins have been extensively studied for more than 20 years as biological mimics of cytochrome P450 in an effort to understand the functional groups of drug molecules most susceptible to metabolism, as well as in understanding the *in vivo* metabolism processes (Gotardo *et al.*, 2006). The first system was described by Groves *et al.*, (1979) where iron tetraphenyl porphyrin (Figure 2.9) was used to catalyze the epoxidation and hydroxylation reactions of simple alkenes and alkanes using iodosylbenzene (PhIO) as the single oxygen donor. Metalloporphyrin chemistry has expanded over the years to such an extent that they have been grouped into first, second and third generation metalloporphyrins.

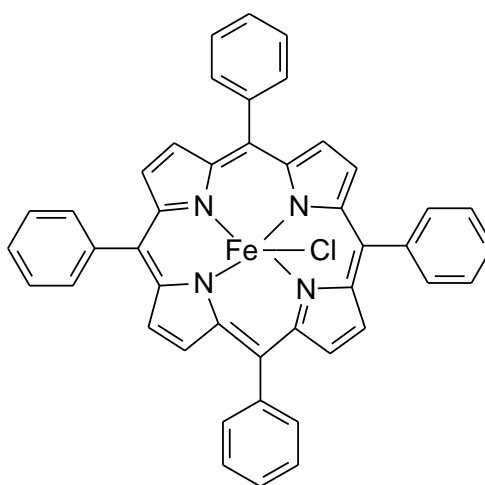


**Figure 2.9** Iron tetraphenylporphyrin (FeTPP)Cl



### First generation metalloporphyrins

The first generation metalloporphyrins (Figure 2.10) represent the first metalloporphyrins that were used. These are structurally simple, with no substituents on the  $\beta$ -pyrrole positions or the aryl positions. These first generation metalloporphyrins have been shown to be highly susceptible to oxidative degradation, limiting the number of catalytic cycles in the oxidation process (Bernadou and Meunier, 2004; Lohmann and Karst, 2008).

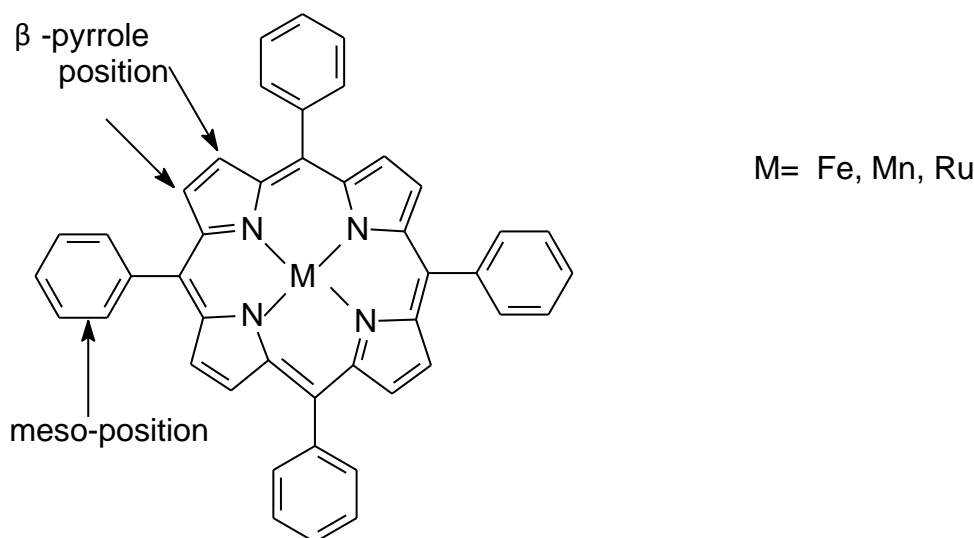


**Figure 2.10** First generation metalloporphyrin *meso*-tetraphenylporphyrin (TPP)

(Bernadou and Meunier, 2004)

### Second generation metalloporphyrins

In order to counteract the problem of oxidative degradation experienced by first generation metalloporphyrins, second generation metalloporphyrins were developed. Electron-withdrawing and sterically hindering substituents were added to the aryl groups of the *meso*-tetraarylporphyrins and the  $\beta$ -pyrrolic positions of the porphyrin ring (Figure 2.11) (Bernadou and Meunier, 2004; Lohmann and Karst, 2008). The addition of these substituents saw an increased catalytic efficiency for the metalloporphyrin, with increased reactivity for the high-valent oxo intermediates, with reduced catalytic degradation (Bernadou and Meunier, 2004; Lohmann and Karst, 2008).

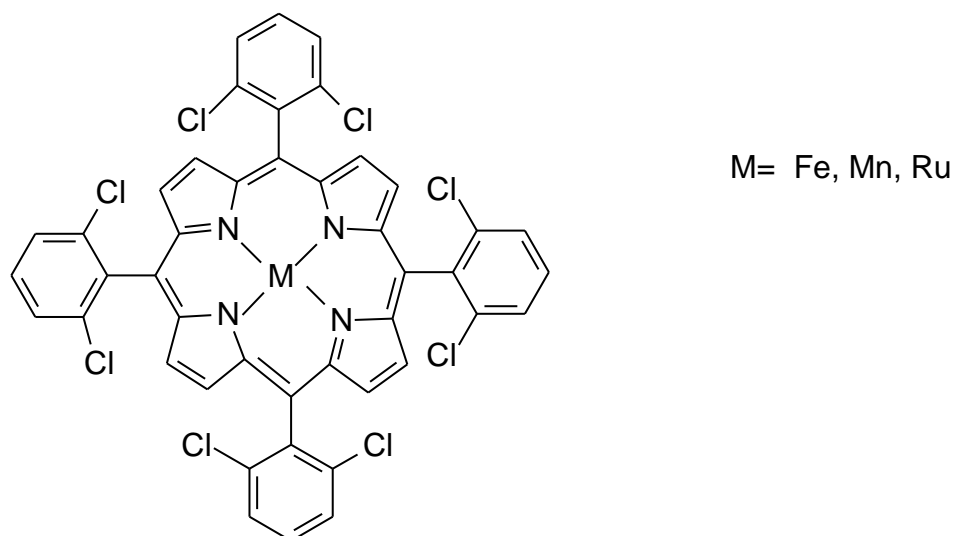


**Figure 2.11** Second generation metalloporphyrin *meso*-tetrakis(2,6-dichlorophenyl)porphyrin dianion (TDCPP) (Bernadou and Meunier, 2004)

### Third generation metalloporphyrins

Third generation metalloporphyrins bear substituents such as quaternary ammonium and sulfonic groups which render them more water soluble. These have been developed for catalysis within an aqueous medium which may better imitate the natural drug metabolism environment (Bernadou and Meunier, 2004; Lohmann and Karst, 2008). Figure 2.12 below gives a general structure for a third generation metalloporphyrin.

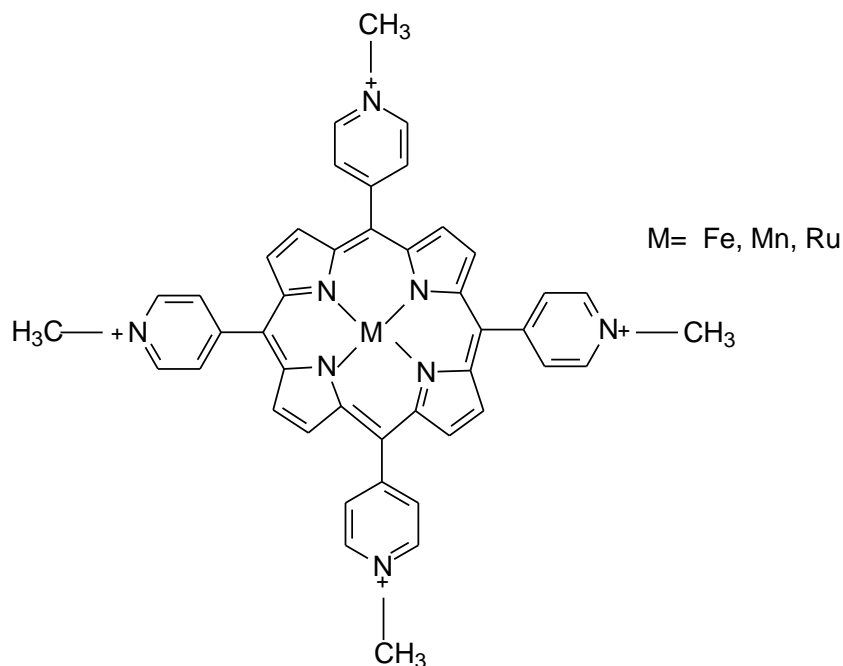


**Figure 2.12** Third generation metalloporphyrin *meso*-tetrakis(4-N-methylpyridinyl)porphyrin tetracation (TMPyP) (Bernadou and Meunier, 2004)

## 2.4 Natural products as potential drug molecules

Natural products present a source of new chemical entities with therapeutic potential against numerous diseases, thus they have the potential to be marketed as new drug molecules. When developing a new chemical entity, determination of absorption, distribution, metabolism and excretion parameters of a potential drug is important in establishing its therapeutic efficacy as part of the initial stages of drug discovery and development (Ansede and Thakker, 2004; Dos Santos *et al.*, 2005). Metabolism studies provide information on potential metabolites thus facilitating prodrug design as well as the determination of the safety and efficacy of the metabolites. Approximately 40% of new, potential chemical entities fail to proceed to market due to their poor metabolism and pharmacokinetic profiles (Ansede and Thakker, 2004). As a result, a natural product chemist should determine any potential metabolites of promising natural product molecules, therefore establishing safety and toxicity profiles in addition to the activity of metabolites against disease states, early in the drug development process. The

biomimetic oxidation profiles (in this case, a chemical *in vitro* drug metabolism system) of natural products with therapeutic potential, is the main focus of this research.

### **Conclusions**

Biomimetic oxidation models are associated with some disadvantages which include the absence of the protein environment which is present in the human body and as such, cannot reproduce the regioselectivity which takes place occurs with the cytochrome enzymes (Othman *et al.*, 2000) but however, they do present other unique advantages making them a viable *in vitro* drug metabolism model. Biomimetic drug metabolism models represent chemical *in vitro* drug metabolic studies which allow isolation of potential drug metabolites in sufficient amounts for characterization, therapeutic and toxicological assays, whilst avoiding the ethical issues and expense associated with animal studies, the variable potency seen with liver preparations, and the binding of metabolites to biological matrices as in *in vivo* drug metabolism models (Bernadou and Meuiner, 2004; Niehues *et al.*, 2012).

## 2.5 References:

- Ansede J.H., Thakker D.R. (2004). High-throughput screening for stability and inhibitory activity of compounds towards cytochrome P450-mediated metabolism. *Journal of Pharmaceutical Sciences* 93: 239-255
- Bai X., Liu C. (2005). Overview of major CYP450 isoforms and “Cocktail Approach”. *Asian Journal of Drug Metabolism and Pharmacokinetics* 5: 257-264
- Bernadou J., Bonnafous M., Labat G., Loiseau P., Meunier B. (1991). Biomimetic oxidation of acetaminophen and ellipticine derivatives with water-soluble metalloporphyrins associated to potassium monopersulfate. *Drug Metabolism and Disposition* 19: 360-365
- Bernadou J., Meunier B. (2004). Biomimetic catalysts in the oxidative activation of drugs. *Advanced Synthesis and Catalysis* 346: 171-184
- Chauret N., Gauthier A., Martin J., Nicoll-Griffith D.A. (1997). *In vitro* comparison of cytochrome P450-mediated metabolic activities in human, dog, cat, horse. *Drug Metabolism and Disposition* 25: 1130-1136
- Che C., Huang J. (2009). Metalloporphyrins-based oxidation systems: from biomimetic reactions to application in organic synthesis. *Chemical Communications* 27: 3996-4015
- Coundouris J.A., Grant M.H., Engeset J., Petrie J.C., Hawksworth G.M. (1993). Cryopreservation of human adult hepatocytes for use in drug metabolism and toxicity studies. *Xenobiotica* 23: 1399-1409
- Cutler S.J., Block J.H. (2004). Chapter 4 Metabolic Changes of Drugs and Related Organic Compounds. *Wilson and Gisvold’s Textbook of Organic and Pharmaceutical Chemistry* 11th Ed (Troy D.B Ed). Lippincott Williams and Wilkins, Philadelphia: 65-126
- Dimelow R.J., Metcalfe P.D., Thomas S. (2012). *In silico* models of drug metabolism and drug interactions. *Encyclopedia of Drug Metabolism and Interactions* VI: 1-55

Dos Santos M.D., Martins P.R., Dos Santos P.A., Bortocan R., Iamamoto Y., Lopes N.P. (2005). Oxidative metabolism of 5-*o*-caffeoylquinic acid (chlorogenic acid), a bioactive natural product by metalloporphyrin and rat liver mitochondria. *European Journal of Pharmaceutical Sciences* 26: 62-70

Dybing E., Holme J.A., Gordon W.P., S oderlund E.J., Dahlin D.C., Nelson S.D. (1984). Genotoxicity studies with paracetamol. *Mutation Research* 138: 21-32

Feiters M.C., Rowan A.E., Nolte R.J.M. (2000). From simple to supramolecular cytochrome P450 mimics. *Chemical Society Reviews* 29: 375-384

Fleming I. (2001). Cytochrome P450 enzymes in vascular homeostasis. *Circulation Research* 89:753-762

Gotardo M.C.A.F., De Moraes L.A.B., Assis M.D. (2006). Metalloporphyrins as biomimetic models for cytochrome-P450 in the oxidation of atrazine. *Journal of Agricultural and Food Chemistry* 54: 10011-10018

Groves J.T., Nemo T.E., Myers R.S. (1979). Hydroxylation and epoxidation of catalysed by iron-porphine complexes. Oxygen transfer from iodosylbenzene. *Journal of American Chemical Society* 101: 1032-1033

Guengerich, F.P. (2006). Cytochrome P450s and Other Enzymes in Drug Metabolism and Toxicity. *The AAPS Journal* 8: E101-E111

Gunaratna, C. (2000). Drug Metabolism and Pharmacokinetics in Drug Discovery: A primer for Bioanalytical Chemists, Part 1. *Current Separations* 19: 17-23

Hughes J.P., Rees S., Kalindjian S.B., Philpott K.L. (2011). Principles of early drug discovery. *British Journal of Pharmacology* 162: 1239-1249

Ionescu, C. and Cairns, M.R. (2006). Drug Metabolism in Concept. *Drug Metabolism: Current Concepts*. Berlin: Springer. 1-2.

Kumar G.N., Surapaneni S. (2001). Role of drug metabolism in drug discovery and development. *Medicinal Research Reviews* 21: 397-411

LeCluyse E.L. (2001). Human hepatocyte culture systems for the *in vitro* evaluation of cytochrome P450 expression and regulation. *European Journal of Pharmaceutical Sciences* 13: 343-368

Lin J.H., Lu A.Y.H. (1997). Role of pharmacokinetics and metabolism in drug discovery and development. *The American Society for Pharmacology and Experimental Therapeutics* 49: 404-449

Lohmann, W. and Karst, U. (2008). Biomimetic modeling of oxidative drug metabolism. *Analytical and Bioanalytical Chemistry* 391: 79-96

Mansuy D., Battioni P., Battioni J. (1989). Chemical model systems for drug-metabolizing cytochrome P-450-dependent monooxygenases. *European Journal of Biochemistry* 184: 267-285

Meunier B. (1992). Metalloporphyrins as versatile catalysts for oxidation reactions and oxidative DNA cleavage. *Chemical Reviews* 92: 1411-1456

Nantes I.L., Durán N., Pinto S.M.S., da Silva F.B., de Souza J.S., Isoda N., Luz R.A.S., de Oliveira T.G., Fernandes V.G. (2011). Modulation of the catalytic activity of porphyrins by lipid-and surfactant-containing nanostructures. *Journal of Brazilian Chemical Society* 22: 1621-1633

Nicolau K.C. (2014). Advancing the drug discovery and development process. *Angewandte Chemie International Edition* 53: 9128-9140

Niehues M., Barros V.P., da Silva E., Dias-Baruffi M., Assis M.D., Lopes N.P. (2012). Biomimetic *in vitro* oxidation of lapachol: a model to predict and analyse the *in vivo* phase I metabolism of bioactive compounds. *European Journal of Medicinal Chemistry* 54: 804-812

Ntie-Kang F., Lifongo L.L., Mbah J.A., Owono Owono L.C., Megnassan E., Mbaze L.M., Judson P.N., Sippl W., Efang S.M. (2013). *In silico* drug metabolism and pharmacokinetic profiles of natural products from medicinal plants in the Congo basin. *In silico Pharmacology* 1 (12): 1-12

Othman S., Mansuy-Mouries V., Bensoussan C., Battioni P., Mansuy D. (2000). Hydroxylation of diclofenac: an illustration of the complementary roles of biomimetic metalloporphyrin catalysts and yeasts expressing human cytochromes P450 in drug metabolism studies. *Comptes Rendus de l'Academie des Sciences Series IIC Chemistry* 3: 751-755

Smith F.T., Clark R. (2004). Chapter 5 Prodrugs and Drug Latentiation. Wilson and Gisvold's Textbook of Organic and Pharmaceutical Chemistry 11th Ed (Troy D.B Ed). Lippincott Williams and Wilkins, Philadelphia: 142-159

Stachulski A.V. (2000). Drug Metabolism: The Body's Defence against Chemical Attack. *Journal of Chemical Education* 77: 349-353

Tingle M.D., Helsby N.A. (2006). Can *in vitro* drug metabolism studies with human tissue replace *in vivo* animal studies?. *Environmental Toxicology and Pharmacology* 21: 184-190

Vaclavikova R., Soucek P., Svobodova L., Anzenbacher P., Simek P., Guengerich F.P., Gut I. (2004). Different *in vitro* metabolism of paclitaxel and docetaxel in humans, rats, pigs and minipigs. *Drug Metabolism and Disposition* 32: 666-674

Wrighton S.A., Ring B.J., Vandenbranden M. (1995). The use of *in vitro* metabolism techniques in the planning and interpretation of drug safety studies. *Toxicologic Pathology* 23: 199-208

Xie Y., McGill M.R., Dorko K., Kumer S.C., Schmitt T.M., Forster J., Jaeschke H. (2014). Mechanisms of acetaminophen-induced cell death in primary human hepatocytes. *Toxicology and Applied Pharmacology* 279: 266-274



Zhang T., Chen Q., Li L., Liu L.A., Wei D.Q. (2011). *In silico* prediction of cytochrome P450-mediated drug metabolism. *Combinatorial Chemistry and High Throughput Screening* 14:388-395

# Chapter 3

## Natural products from *Brassicophycus brassicaeformis* and related species

### Abstract

Brown algae of the family Sargassaceae are responsible for the production of the vast majority of biologically active brown algal secondary metabolites. Biological activities exhibited by these metabolites include cytotoxic, antimicrobial, and antifouling activities. In continuation of our search for new biologically active metabolites from South African marine algae, an examination of the organic extracts of the alga *Brassicophycus brassicaeformis* was conducted.

Two monogalactosyldiacylglycerol lipids 1-*O*-(5*Z*,8*Z*,11*Z*,14*Z*-eicosatetraenoyl)-2-*O*-(9*Z*,12*Z*,15*Z*-octadecatrienoyl)-3-*O*- $\beta$ -D-galactopyranosyl-*sn*-glycerol (**3.17**) and 1-*O*-(9*Z*-octadecenoyl)-2-*O*-(hexadecanoyl)-3-*O*- $\beta$ -D-galactopyranosyl-*sn*-glycerol (**3.18**) were isolated, as well as two known compounds fucosterol (**3.9**) and fucoxanthin (**3.16**).

This study represents the first phytochemical investigation of *Brassicophycus brassicaeformis*.

# Chapter 3

## Natural products from *Brassicophycus brassicaeformis* and related species

### 3.1. General introduction

*Brassicophycus brassicaeformis* is a brown marine algae belonging to the Family Sargassaceae, a combination of the families of Sargassaceae and Cystoseiraceae (Muñoz *et al.*, 2013). It was previously described as *Bifurcaria brassicaeformis* (Kützinger) (Culioli *et al.*, 2004) belonging to the genus *Bifurcaria* Stackhouse a small genus in the family Cystoseiraceae with three species: *Bifurcaria bifurcata* (Velley) R.Ross which is distributed on the Atlantic coasts from Morocco (south) to north west Ireland (north); *Bifurcaria brassicaeformis* which is distributed on the western (Stegenga *et al.*, 1997) and Indian ocean coasts of South Africa (Silva *et al.*, 1996) and *Bifurcaria galapagensis* (Piccone and Grünow) Womersley which distributed in the Galapagos (Culioli *et al.*, 2004; Valls and Piovetti, 1995b).

A study by Draisma *et al.*, (2010) showed the genus *Bifurcaria* as not being monophyletic with European *Bifurcaria bifurcata* (accepted name *Bifurcaria tuberculata*) and thus the authors suggested that *B. brassicaeformis* and *B. tuberculata* be classified as two separate genera. The three species of *Bifurcaria* were shown to possess chemotaxonomic differences which further support the difference between *B. bifurcata*, *B. galapagensis* and *B. brassicaeformis*. *B. bifurcata* is known to produce a wide array of acyclic diterpenes; *B. galapagensis* produces meroditerpenes as secondary metabolites whilst *B. brassicaeformis* does not produce diterpenes but is rich in sterols (Culioli *et al.*, 2004; Draisma *et al.*, 2010). Structural differences between *B. brassicaeformis* and the other two species, further supports the idea postulated by Draisma *et al.*, (2010). *B. bifurcaria* and *B. galapagensis* are

monoecious and the algae branches tri-radiate. Both species have conceptacles that are scattered with where *B. bifurcata* does not retain the eggs to the receptacles (Draisma *et al.*, 2010). *B. brassicaeformis*, however, is dioecious with flat receptacles which expel eggs that remain part of the stalks of the algae. It branches bilaterally with conceptacles marginalised on flat receptacles (Draisma *et al.*, 2010). With all these differences, Draisma *et al.*, (2010) therefore proposed that *B. brassicaeformis* be classified in a genus of its own viz. *Brassicophycus* Draisma, Ballesteros, F.Rousseau and T. Thibaut, a monotypic genus fourth sargassacean and fifth fucalean endemic to South Africa.

**Table 3.1** Summary of the differences between *B. brassicaeformis*, *B. bifurcata*, *B. galapagensis*

	<i>B. brassicaeformis</i>	<i>B. bifurcata</i>	<i>B. galapagensis</i>
<b>Distribution</b>	South Africa	Europe (west)	Galapagos
<b>Secondary metabolites</b>	No diterpenoids Sterols	Acyclic diterpenes	Cyclic meroditerpenes
<b>Sexual reproduction structures</b>	Dioecious Extruded eggs remain part of algae stalk	Monoecious Eggs not retained to receptacles	Monoecious
<b>Branching of algae</b>	Bilaterally	Tri-radiate	Tri-radiate

(Daoudi *et al.*, 2001; Culioli *et al.*, 2004; Draisma *et al.*, 2010)

### 3.1.1. Secondary metabolites from Genus *Bifurcaria*

Acyclic diterpenes isolated from *B. bifurcata* (Figure 3.1, structures **3.1-3.7**) are geranylgeraniol (**3.1**) derived diterpenes and this precursor has been previously isolated from two *Cystoseira brachycarpa* and *C. balearica* species as well as the genus *Bifurcaria* (Culioli *et al.*, 1999a). Isolation of geranylgeraniol from *B. bifurcata* shows a close relationship between these species and the Mediterranean Cystoseiraceae species i.e. *C. brachycarpa* and *C. balearica*, the last of the *Cystoseira* species which produces linear diterpenes (Culioli *et al.*, 1999b; Muñoz, 2013).

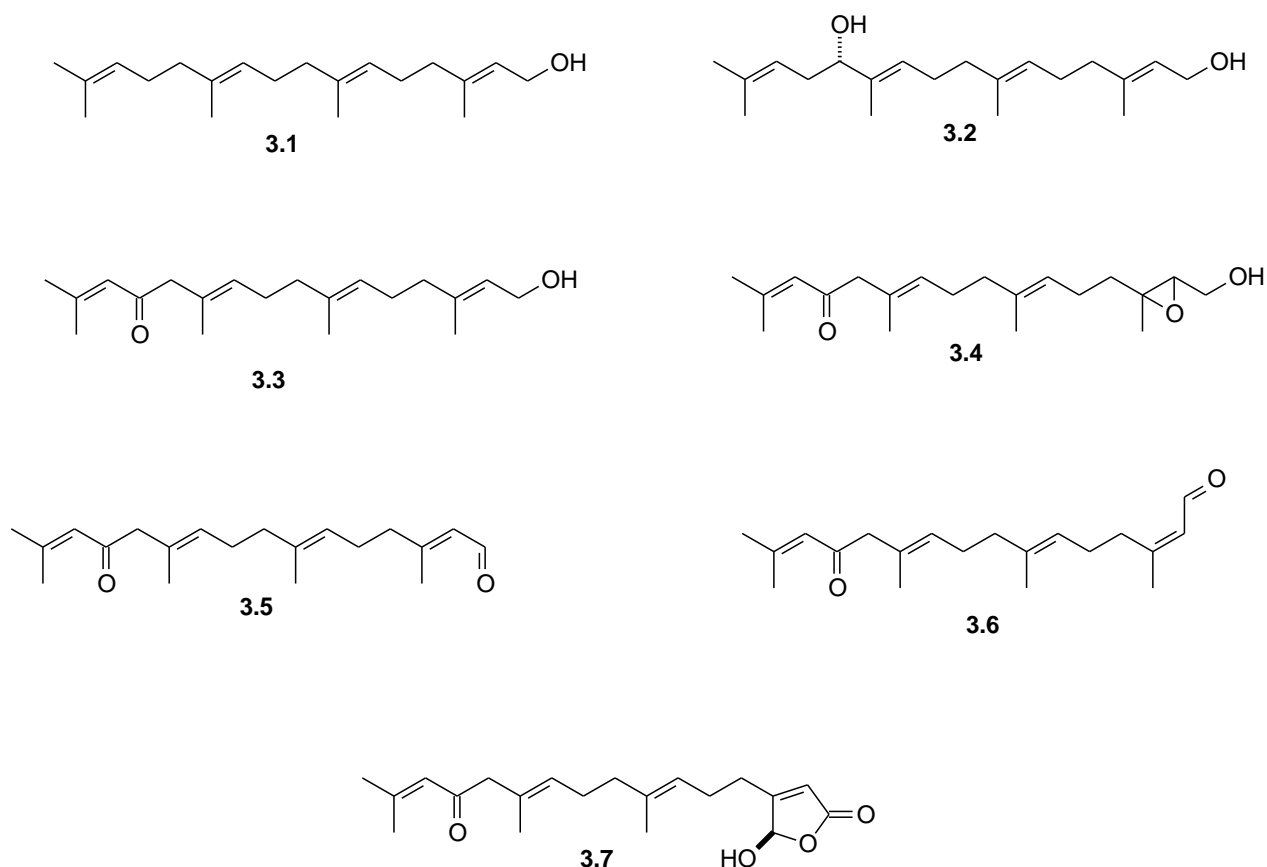
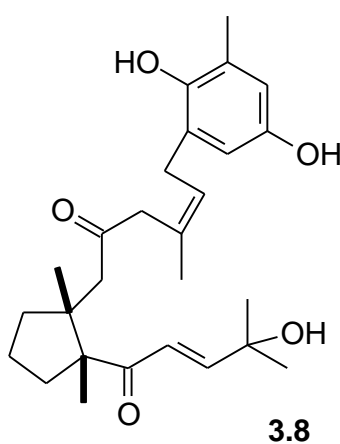
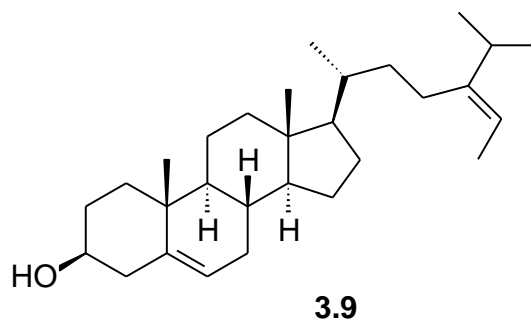


**Figure 3.1** Acyclic diterpenes isolated from *Bifurcaria bifurcata*

*B. galapagensis* produces monocyclic diterpenoid metabolites with a methyl hydroquinone moiety (Combaut and Piovetti, 1983). An example of this class of metabolite is bifurcarenone (**3.8**). However, *B. galapagensis* has been considered to be extinct as it has not been observed since 1983 (Muñoz et al., 2013).

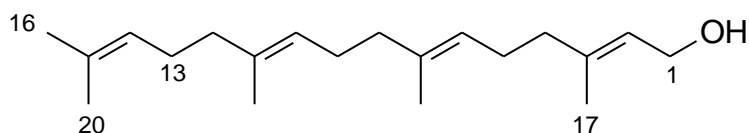


Fucosterol (**3.9**) is the only phytosterol isolated from organic extracts of *Bifurcaria brassicaeformis* which suggest that *B. brassicaeformis* preferentially synthesizes sterols since no diterpenes have been isolated (Daoudi *et al.*, 2001). In fact, studies have shown that fucosterol is the most abundant sterol produced by brown marine algae (Khanavi *et al.*, 2012).



### 3.1.2 Biosynthetic pathways for secondary metabolites from genus *Bifurcaria*

The linear terpenes isolated from *Bifurcaria* bear a C<sub>16</sub> chain with five methyl groups and four double bonds (Figure 3.2) (Muñoz *et al.*, 2013). Oxidation and isomerization occurs mainly at the C-1, C-12 and C-13 positions with the C-6/C-7 and C10/-C-11 positions being less prone to transformation (Muñoz *et al.*, 2013). These terpene metabolites have therefore been categorized into three main families: family A, B and C with family B being subdivided into family B1 and B2 (Table 3.2. structures **3.10-3.13**). Classification into these families depends on the position of oxidation in the diterpenes.

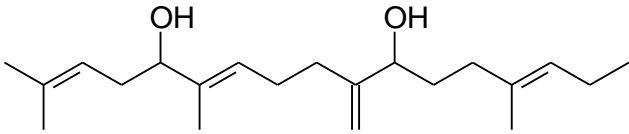
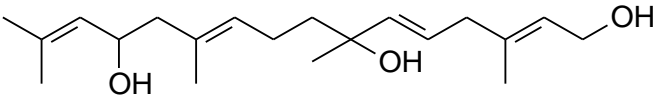
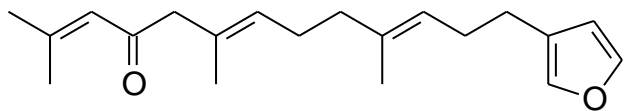
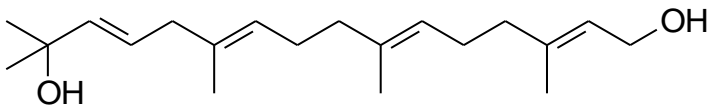


**Figure 3.2** C<sub>16</sub> scaffold for diterpene metabolites from genus *Bifurcaria* (Muñoz *et al.*, 2013)

The biosynthetic pathway of geranylgeraniol derivatives provides four major precursors to the three family classifications of metabolites from the genus *Bifurcaria*. These are geranylgeraniol (**3.1**), 12-hydroxygeranylgeraniol (**3.2**), eleganolone (**3.3**) and eleganediol (Figure 3.3). Of interest is the 1,4 dehydration of 12-hydroxygeranylgeraniol which results in a compound which belongs to both family A and C (Figure 3.3) (Muñoz *et al.*, 2013).

Meroditerpenes such as bifurcarenone (**3.8**) are formed from a mixed biogenesis pathway which results in a hydroquinone moiety linked to a diterpene. In this case, the hydroquinone is derived from shikimic acid and the diterpene chain from geranylgeraniol. Geranylgeraniol is therefore used by some species of Sargassaceae as an alkylating agent for the shikimic acid, an activated aromatic substrate, to result in linear, monocyclic, bicyclic and rearranged meroditerpene metabolites (Valls and Piovetti, 1995; Amico, 1995). Bifurcarenone for example, is derived from the intramolecular cyclization of a linear meroditerpene precursor (**3.14**) between C-7 and C-11 to form an amentane skeleton (Figure 3.4) (Valls and Piovetti, 1995).

**Table 3.2** Classification of diterpene metabolites isolated from genus *Bifurcaria*

Family	Description	Example
A	<u>C-12</u> oxidized terpenes	 <p style="text-align: center;"><b>3.10</b></p>
B1	<u>C-13</u> oxidized terpenes bearing an alcohol	 <p style="text-align: center;"><b>3.11</b></p>
B	<u>C-13</u> oxidized terpene bearing a ketone	 <p style="text-align: center;"><b>3.12</b></p>
C	<u>Non C-12/C-13</u> oxidized terpenes	 <p style="text-align: center;"><b>3.13</b></p>

Muñoz et al., 2013



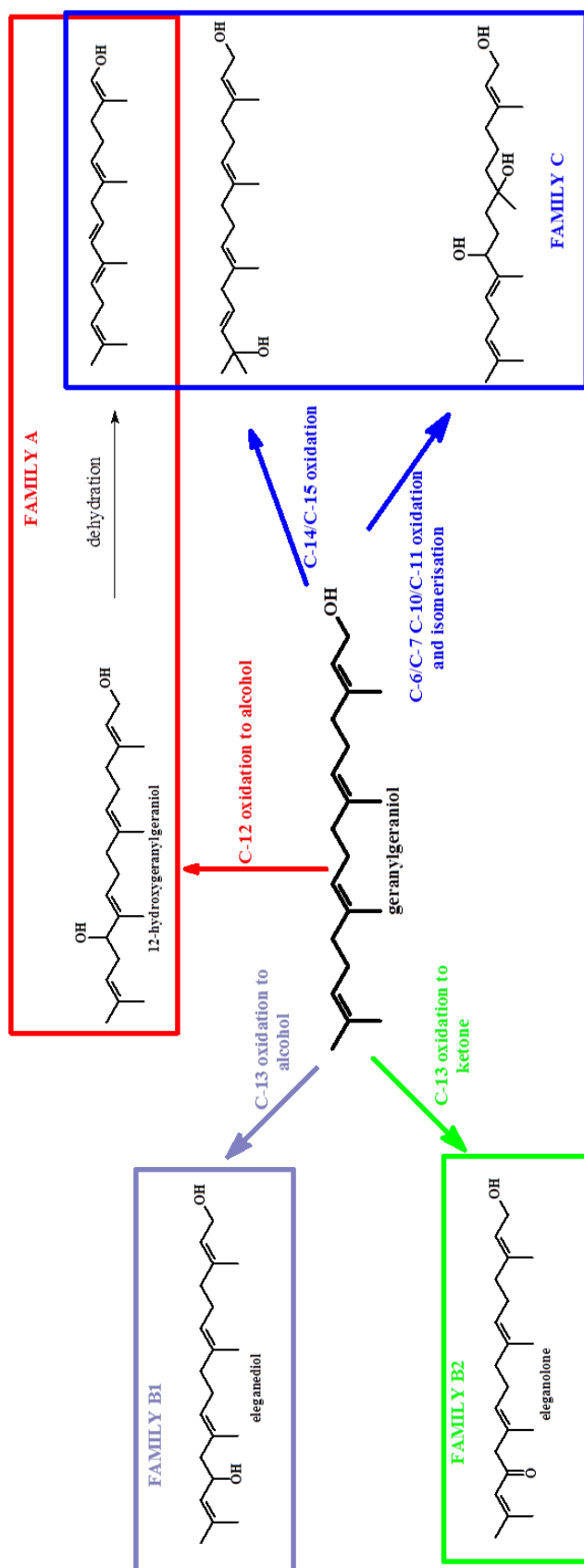


**Figure 3.3** A general biosynthetic scheme for geranylgeraniol derived secondary metabolites (Muñoz *et al.*, 2013)

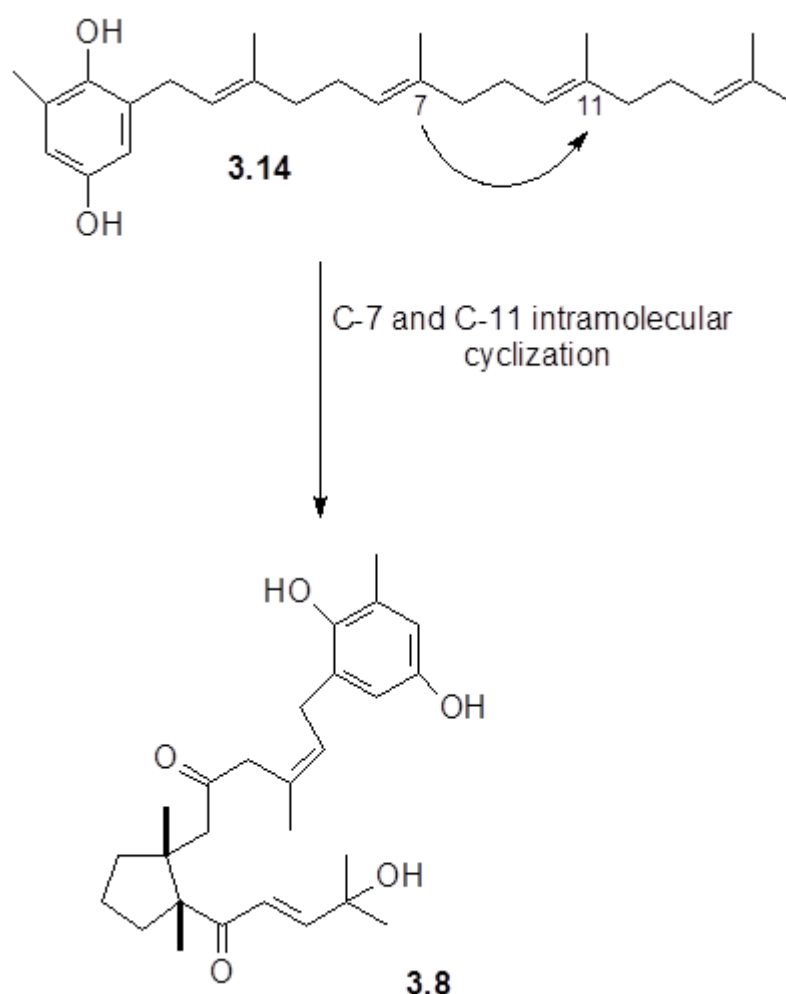
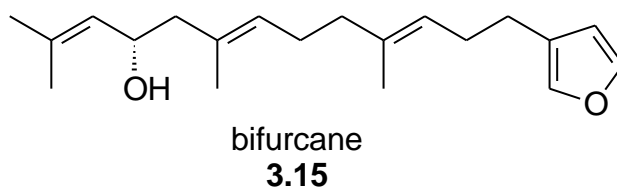


**Figure 3.4** Biogenetic formation of bifurcarenone (**3.8**) (Valls and Pioveti, 1995)

### 3.1.3 Biological activity of secondary metabolites from the genus *Bifurcaria*

Linear diterpenes isolated from the brown alga *B. bifurcata* have been shown to possess various biological activities including cytotoxic, antiulcer, antimitotic, antimicrobial and antifouling activities (Guardia *et al.*, 1999; Muñoz *et al.*, 2013). Eleganolone (**3.3**) was shown to be useful in the growth inhibition of several *Mycobacterium* strains such as *M. smegmatics* (75µg/ml), *M. ranae* (100µg/ml) and *M. avium* (100µg/ml) however, it was found to be ineffective against *M. tuberculosis* (Muñoz *et al.*, 2013).

The cytotoxicity of these secondary metabolites was assessed by the inhibition of sea urchin cell division which gives an overall indication of biological activity. Of interest is compound **3.13**, an allylic alcohol and bifurcane (**3.15**), a furan derivative which showed remarkable inhibition of fertilized sea urchin eggs *Paracentrotus lividus*. Both metabolites showed ED<sub>50</sub> values of 4 and 12 µg/ml respectively, showing their ability to inhibit rapidly growing cells at low concentrations (Muñoz *et al.*, 2013; Valls *et al.*, 1995a).



12-(*S*)-hydroxygeranylgeraniol (**3.2**) also possesses promising cytotoxic activity against human cell lines such as non-small cell lung adenocarcinoma (A549), colon (HCT15) and ovarian (SK-OV-3) cancer cell lines (Valls *et al.*, 1993; Zee *et al.*, 1999).

Fucosterol (**3.9**) has been isolated from a wide range of brown marine algae which include: *Pelvetia siliquosa*, found in craggy surfaces of the Korean peninsula (Lee *et al.*, 2003; Yeon *et al.*, 2004); *Hizikia fusiformis*, an edible brown algae in Korea and Japan (Huh *et al.*, 2012) and *Undaria pinnatifida*, also known as sea mustard, an edible delicacy from the Laminariaceae family (Bang *et al.*, 2011). Fucosterol has been shown to possess antioxidant, antidiabetic, cytotoxic and antifungal activities making it an invaluable source of novel, new chemical entities against diabetes and several cancers (Bang *et al.*, 2011; Huh *et al.*, 2012; Khanavi *et al.*, 2012; Lee *et al.*, 2003; Yeon *et al.*, 2004).

### 3.1.4 Chapter Aims and Objectives

#### Overall aim:

Brown algae of the family Sargassaceae are responsible for the production of the vast majority of known, biologically active brown algal secondary metabolites. The biological activities exhibited by these metabolites include cytotoxic, antimicrobial and antifouling activities. In continuation of our search for new biologically active metabolites from South African marine algae, the organic extracts of the alga, *Brassicophycus brassicaeformis* were examined.

#### Objectives of the study:

To isolate and characterize secondary metabolites from the organic extracts of *B. brassicaeformis*,



**Figure 3.5** Photograph of *Brassicophycus brassicaeformis*<sup>4</sup>

<sup>4</sup>Photograph taken in the Faculty of Pharmacy, Rhodes University, South Africa

Collected from Glencairn beach, Western Cape, South Africa on 1/9/2012 by Professor John Bolton (University of Capetown)

## 3.2 Results and Discussion

### 3.2.1 Isolation of secondary metabolites from *Brassicophycus brassicaeformis*

The organic extract from the alga was obtained by an initial MeOH soak for 1hr which was followed by liquid-liquid extraction using CH<sub>2</sub>Cl<sub>2</sub>-MeOH (2:1). The organic extracts were then pooled and collected by solvent evaporation *in vacuo* to give the crude extract (4.19% of the algal dry mass). The <sup>1</sup>H-NMR spectrum of the crude *B. brassicaeformis* extract (Figure 3.6) showed complex signals which demanded further fractionation.

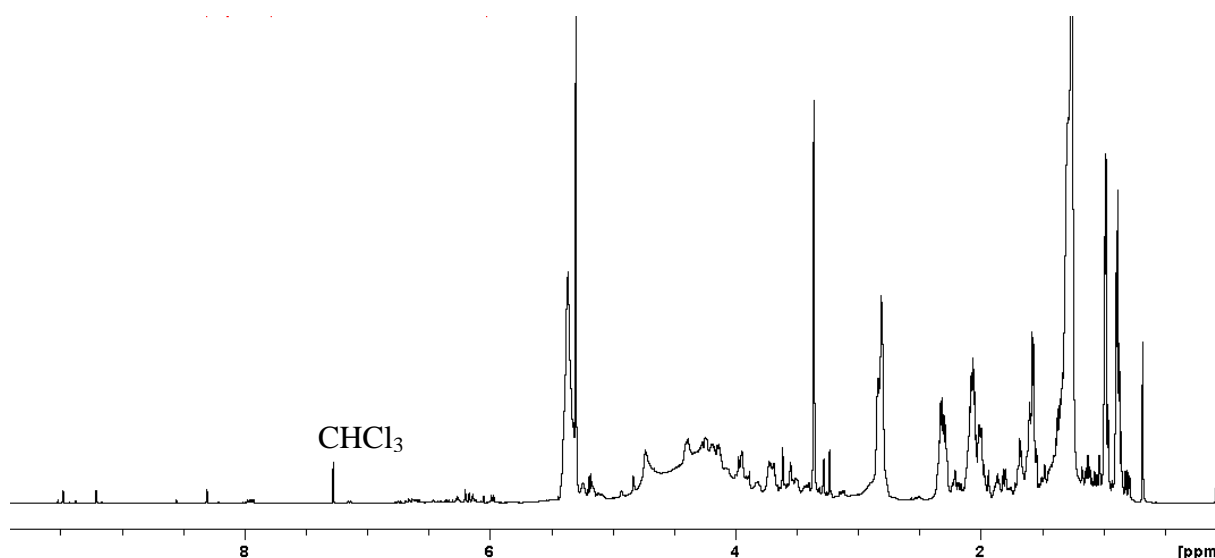
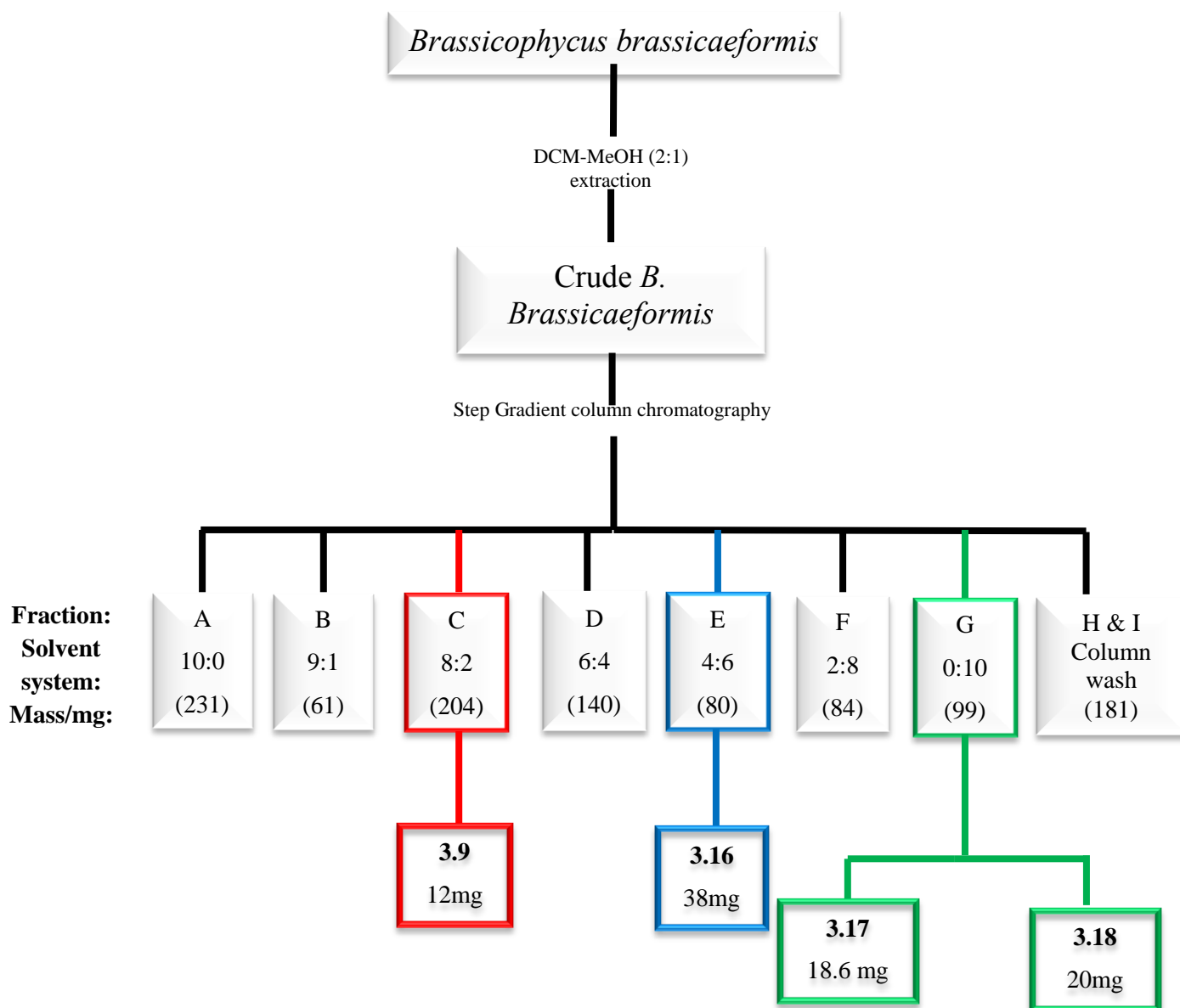


**Figure 3.6** <sup>1</sup>H-NMR (600MHz, CDCl<sub>3</sub>) spectrum of the crude *B. brassicaeformis* extract

The crude extract was fractionated by step gradient silica gel chromatography with Hexane-EtOAc in increasing polarity as the mobile phase (Scheme 3.1). This afforded nine fractions (A-I) which were analyzed by <sup>1</sup>H-NMR spectroscopy (Figure 3.7). The <sup>1</sup>H-NMR spectra of fractions C (Figure 3.8), E (Figure 3.9) and G (Figure 3.10) showed that they each contained one major metabolite worth further investigation. The overlapping signals in the methylene envelope  $\delta$  1-2.4 in <sup>1</sup>H-NMR spectrum of fraction C suggested a steroidal structure, whilst fraction E illustrated signals in the  $\delta$  6-7 region characteristic of fucoxanthin. Fraction G

showed  $^1\text{H-NMR}$  signals characteristic of a sugar moiety ( $\delta$  3-4) and an unsaturated system ( $\delta$  5.4) characteristic of fatty acids.

Therefore, fraction **C** and **G** were further purified by HPLC whilst fraction **E** was purified by silica gel column chromatography to obtain pure fractions, **3.9**, **3.16**, **3.17** and **3.18**.



**Scheme 3.1** Isolation of secondary metabolites **3.9** and **3.16-3.18** from *B. brassicaeformis*

Conditions: (i) Normal Phase HPLC, solvent: 7:3 Hexane-EtOAc

(ii) Silica gel column chromatography, solvent: 6:4 Hexane-EtOAc

(iii) Reversed Phase HPLC, solvent: 100% MeOH

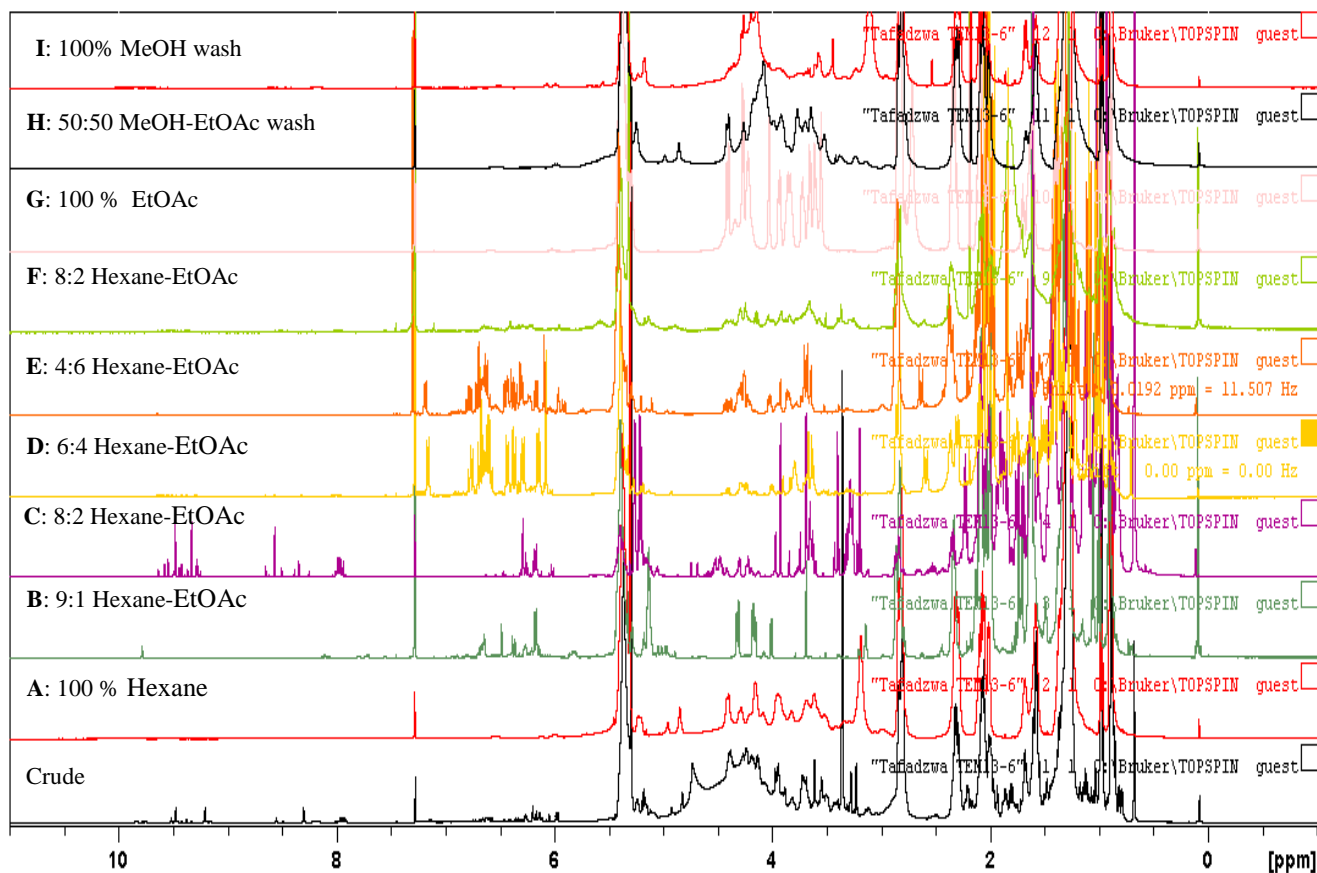


**Figure 3.7**  $^1\text{H-NMR}$  (600 MHz,  $\text{CDCl}_3$ ) spectra of the crude and fractions A-I

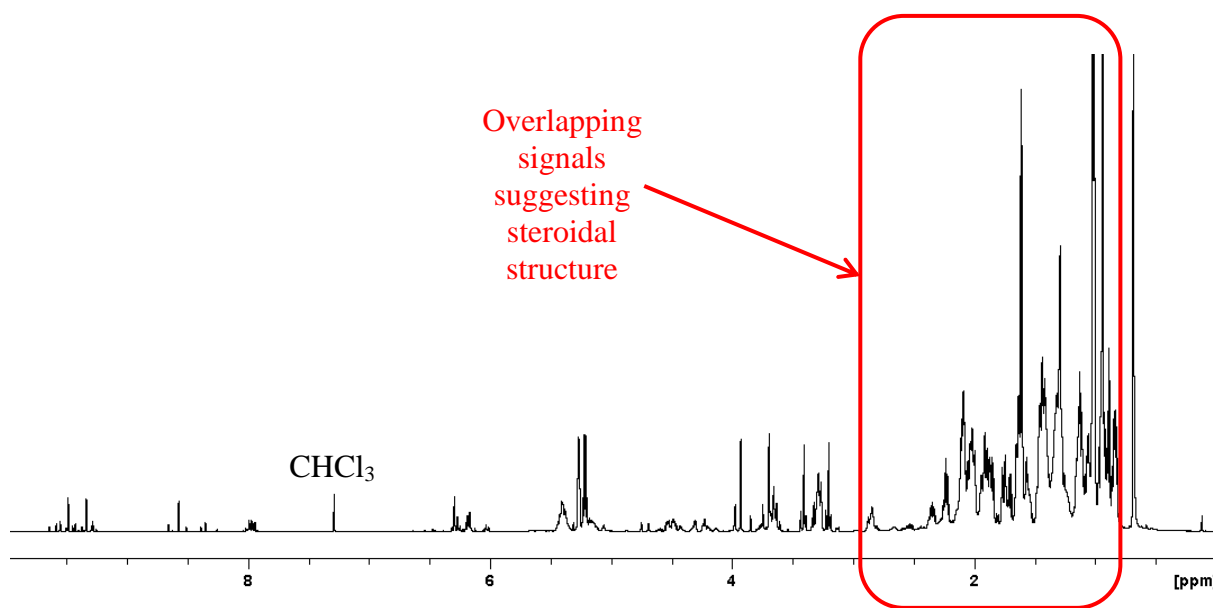


**Figure 3.8**  $^1\text{H-NMR}$  (600 MHz,  $\text{CDCl}_3$ ) spectrum of fraction C

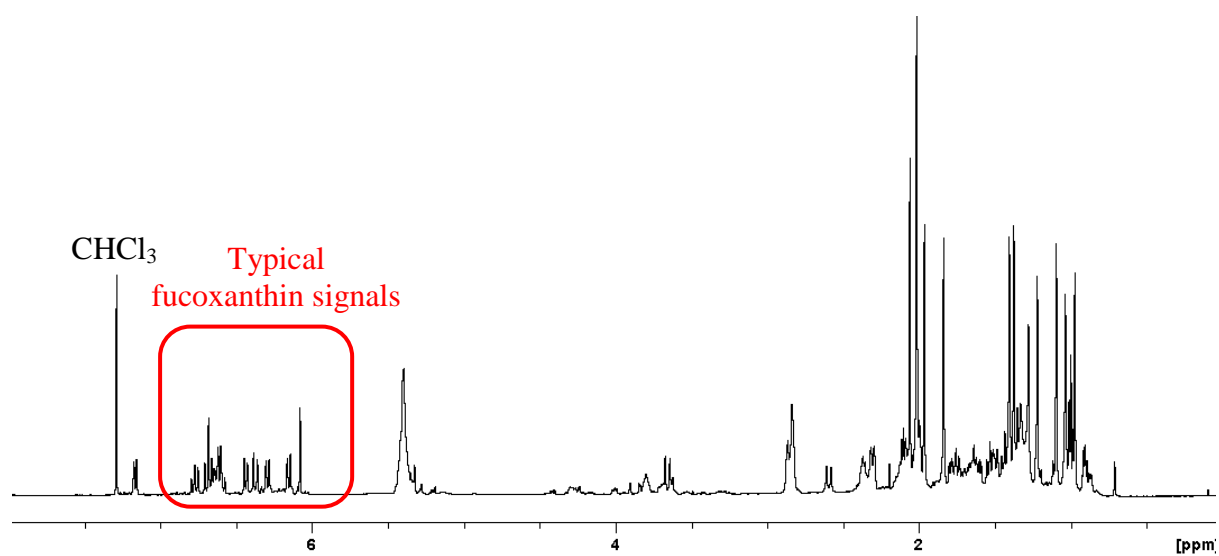


**Figure 3.9**  $^1\text{H-NMR}$  (600 MHz,  $\text{CDCl}_3$ ) spectrum of fraction **E**

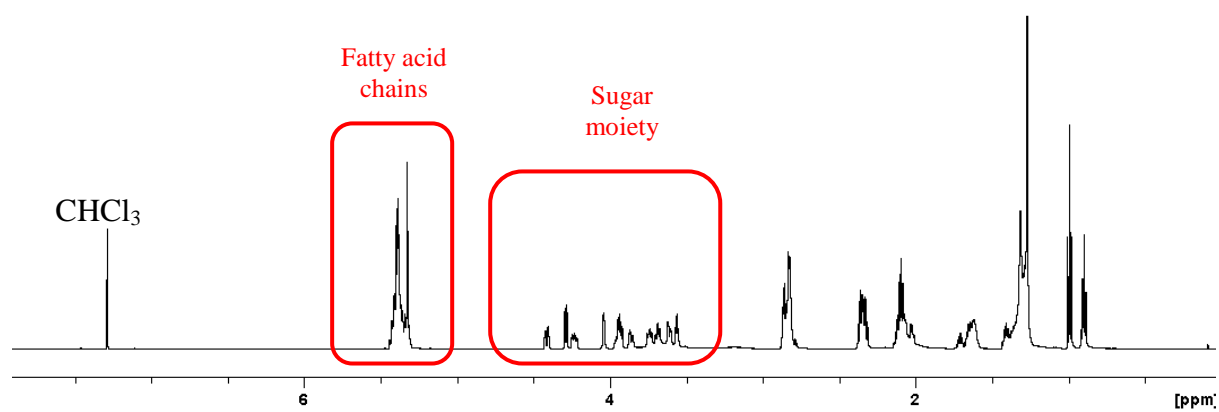


**Figure 3.10**  $^1\text{H-NMR}$  (600 MHz,  $\text{CDCl}_3$ ) spectrum of fraction **G**



### 3.2.2 Structure elucidation of secondary metabolites from *B. brassicaeformis*

#### 3.2.2.1 Structure elucidation of compound **3.9**

Compound **3.9** was isolated by reversed phase HPLC as a whitish-green solid. Its  $^1\text{H-NMR}$  (600 MHz,  $\text{CDCl}_3$ ) spectrum (Figure 3.11) displayed two olefinic methine protons at  $\delta$  5.36 (br. d,  $J = 4.9$  Hz) and  $\delta$  5.20 (q,  $J = 6.7$  Hz). An oxymethine proton is shown by the multiplet residing at  $\delta$  3.54, while the doublet at  $\delta$  1.59 (d,  $J = 6.7$  Hz) represents allylic methyl protons. Five methyl groups were indicated by signals at:  $\delta$  1.03 (s),  $\delta$  1.01 (d,  $J = 6.8$  Hz),  $\delta$  1.00 (d,  $J = 6.7$  Hz),  $\delta$  0.99 (d,  $J = 6.7$  Hz) and  $\delta$  0.70 (s). The  $^{13}\text{C-NMR}$  (150 MHz,  $\text{CDCl}_3$ ) spectrum of **3.9** (Figure 3.12) displayed 29 carbon signals which indicated the presence of two olefin quaternary carbons at  $\delta$  147.1 and 140.8, two olefin methine carbon signals at  $\delta$  121.8 and 115.7, an oxygenated methine carbon ( $\delta$  71.9) and two quaternary carbon signals at  $\delta$  42.4 and 36.5. The  $^{13}\text{C-NMR}$  spectrum together with the DEPT-135 and multiplicity edited-HSQC also indicated the presence of five methine carbons ( $\delta$  56.9, 55.8, 50.2, 34.8 and 31.9), eleven methylene carbons ( $\delta$  42.3, 39.8, 37.2, 36.5, 35.3, 31.9, 31.7, 28.3, 25.7, 24.3 and 21.1), five methyl carbons ( $\delta$  22.3, 22.1, 19.4, 18.8 and 11.7) and lastly one allylic methyl carbon at  $\delta$  13.2. The  $^1\text{H-NMR}$  and  $^{13}\text{C-NMR}$  data were compared with those from the literature and were found to be consistent with the known stigmastane sterol, fucosterol (Huh *et al.*, 2012). Two-dimensional NMR studies (COSY, HMBC, and HSQC) including DEPT-135 data (Table 3.3) confirmed this assignment. Figure 3.13 gives the key HMBC correlations observed for **3.9**.

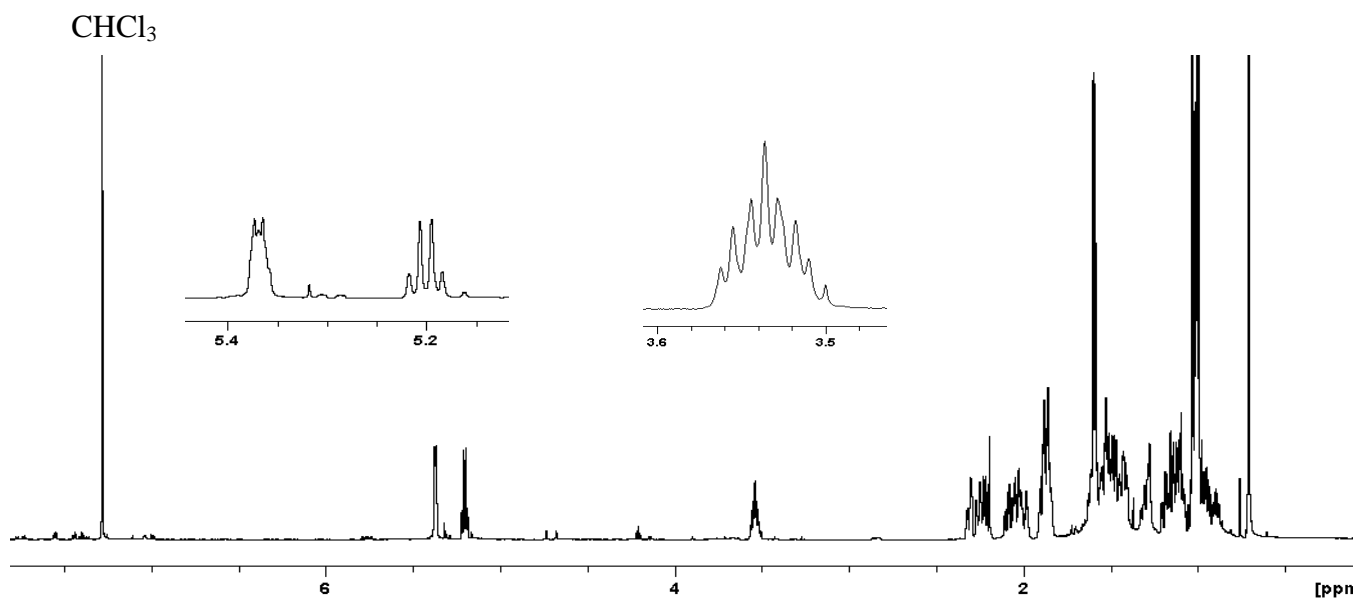


**Figure 3.11**  $^1\text{H-NMR}$  spectrum (600 MHz,  $\text{CDCl}_3$ ) of compound 3.9

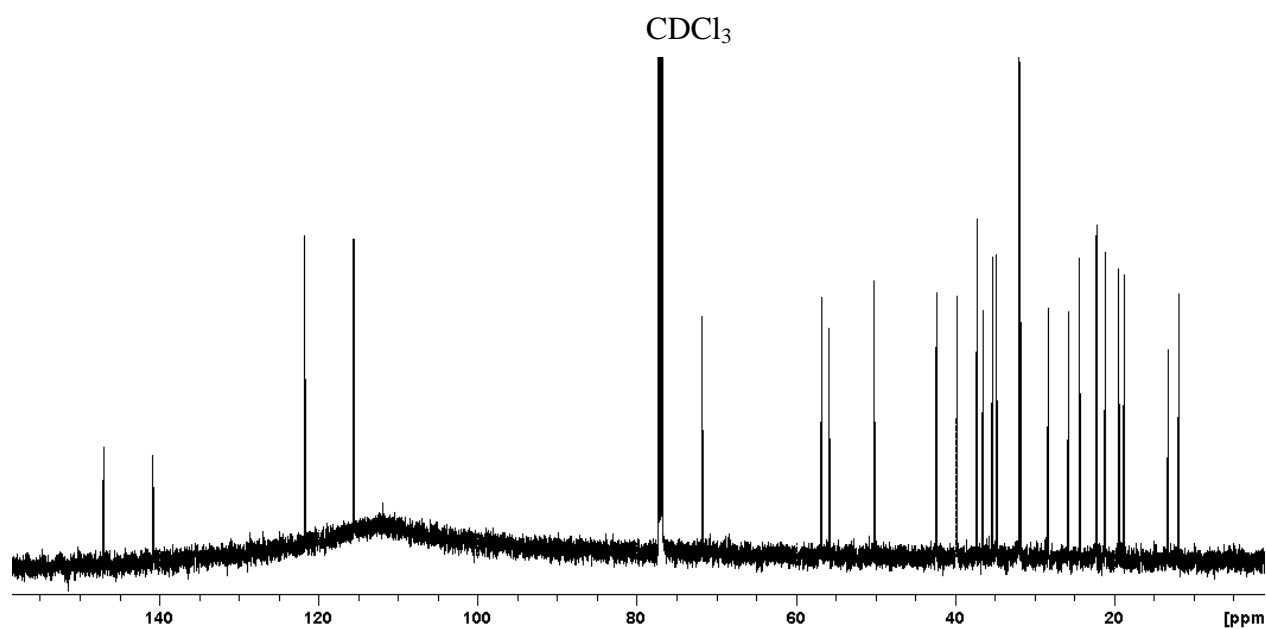


**Figure 3.12**  $^{13}\text{C-NMR}$  (150MHz,  $\text{CDCl}_3$ ) spectrum of compound 3.9

**Table 3.3** Comparison of observed and literature  $^1\text{H}$ -NMR (600 MHz,  $\text{CDCl}_3$ ) and  $^{13}\text{C}$ -NMR (150 MHz,  $\text{CDCl}_3$ ) and observed  $^1\text{H}$ - $^1\text{H}$ - COSY and HMBC correlations of fucosterol (**3.9**)

Carbon No	Observed			Literature <sup>5</sup>		Observed	
	$\delta_{\text{C}}$	$\delta_{\text{C}}$ , multi	$\delta_{\text{H}}$ (multi, <i>J</i> in Hz)	$\delta_{\text{C}}$	$\delta_{\text{H}}$ (multi, <i>J</i> in Hz)	COSY	HMBC
1	37.2	CH <sub>2</sub>		37.26			
2	31.7	CH <sub>2</sub>		31.58		H-3	C-4
3	71.9	CH	3.53 (m)	71.62	3.53 (m)	H-2, H-4	
4	42.3	CH <sub>2</sub>		42.24		H-3	
5	140.8	C		140.76			
6	121.8	CH	5.36 (d, 5.2)	121.52	5.31 (d, 4.8)	H-7	
7	31.9	CH <sub>2</sub>		31.89		H-6	
8	31.9	CH		31.86			
9	50.2	CH		50.14			
10	36.5	C		36.46			
11	21.1	CH <sub>2</sub>		21.05			
12	39.8	CH <sub>2</sub>		39.75			C-18
13	42.4	C		42.31			
14	56.9	CH		56.74			
15	24.3	CH <sub>2</sub>		24.28			
16	28.3	CH <sub>2</sub>		28.17			
17	55.8	CH		55.81			
18	11.7	CH <sub>3</sub>	0.70 (s)	11.79	0.66 (s)		
19	19.4	CH <sub>3</sub>	1.02 (s)	19.33	0.98 (s)		
20	36.6	CH		36.35			
21	18.8	CH <sub>3</sub>	1.01 (d, 6.8)	18.73	0.97 (d, 6.8)		
22	35.3	CH <sub>2</sub>		35.19			C-16, C-23
23	25.7	CH <sub>2</sub>		25.71			C-28
24	147.1	C		146.86			
25	34.8	CH		34.72			
26	22.3	CH <sub>3</sub>	0.99 (d, 6.8)	22.19	0.96 (d, 6.8)		C-25, C-28
27	22.1	CH <sub>3</sub>	1.01 (d, 6.8)	22.09	0.96 (d, 6.8)		
28	115.7	CH	5.20 (q, 6.8)	115.50	5.15 (q, 6.8)	H-29	
29	13.2	CH <sub>3</sub>	1.59 (d, 6.8)	13.11	1.54 (d, 6.8)	H-28	C-29, C-24

Assignments completed based on the COSY, HMBC and HSQC correlations observed

<sup>5</sup> Huh *et al.*, 2012

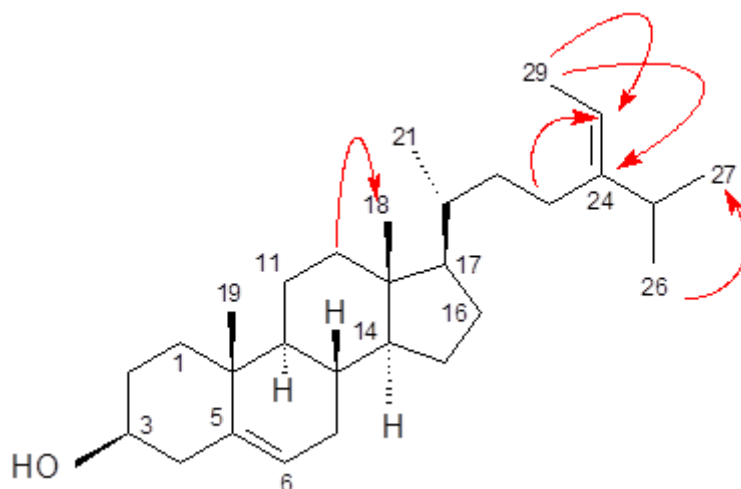


**Figure 3.13** Key HMBC correlations observed for compound **3.9**

The isolation of fucosterol from *B. brassicaeformis* is consistent with literature in stating that fucosterol is the most abundant sterol in *Bifurcaria brassicaeformis* (the former genus name for *Brassicophycus brassicaeformis*) (Daoudi *et al.*, 2001; Draisma *et al.*, 2010).

### 3.2.2.2 The structure elucidation of compound **3.16**

Compound **3.16** was isolated as a yellow-brown paste. Its  $^1\text{H-NMR}$  spectrum (Figure 3.14) was characterized by a cluster of signals in the region  $\delta$  6.07-6.78 together with a distinct doublet at  $\delta$  7.16 (d,  $J = 11.4$  Hz). The  $^{13}\text{C-NMR}$  spectrum (Figure 3.15) of **3.16** illustrated 42 resonances with most signals in the region  $\delta$  100-150 which are characteristic of olefin carbon signals, suggesting that the compound is rich in double bonds. Thirteen quaternary carbons signals were denoted from  $^{13}\text{C-NMR}$  spectra of compound **3.16**. Of importance is the oxygenated quaternary carbon at  $\delta$  72.8 (C-5') and the carbons associated epoxide at C-5 and 6 signalled by  $\delta$  66.2 and 67.1. Another characteristic signal includes a carbon associated with a conjugated ketone at  $\delta$  197.8 (C-8) and an oxymethine signal at  $\delta$  64.4 is present corresponding to C-3. The spectral region  $\delta$  10-35 presented ten characteristic methyl signals at  $\delta$  11.8 (C-19), 12.8 (C-20), 12.9 (C-20'), 14.0 (C-19'), 21.2 (C-18), 21.4 (C-16'), 25.1 (C-16), 28.1 (C-17), 31.3 (C-18') and 32.1 (C-17'). Moreover, the compound's yellow-brown colour also suggested the presence of a highly conjugated system such as those present in

carotenoid pigments. Due to overlapping signals in  $^1\text{H-NMR}$  spectrum of compound **3.16** it was difficult to analyze the spectrum; the data of compound **3.16** was therefore compared with the spectroscopic data available from literature (Mori *et al.*, 2004; Afolayan *et al.*, 2008) allowing the assignment of **3.16** as fucoxanthin.

Fucoxanthin is an abundant carotenoid in brown algae (Phaeophyceae) and has been postulated to be an accessory pigment in photosynthesis (Bonnett *et al.*, 1969). It is mostly isolated from the edible brown algae of some European and South East Asian countries which include; *Hizikia fusiformis* and *Undaria pinnatifida* (Peng *et al.*, 2011). Fucoxanthin has exhibited remarkable biological activities which have been linked to its unique carotenoid structure, possessing antioxidant, antimalarial, anti-inflammatory, anti-cancer and even anti-obesity activities. Fucoxanthin's broad spectrum of biological activities makes it lucrative as a potential new chemical entity in drug discovery (Jongaramruong *et al.*, 2007; Peng *et al.*, 2011).

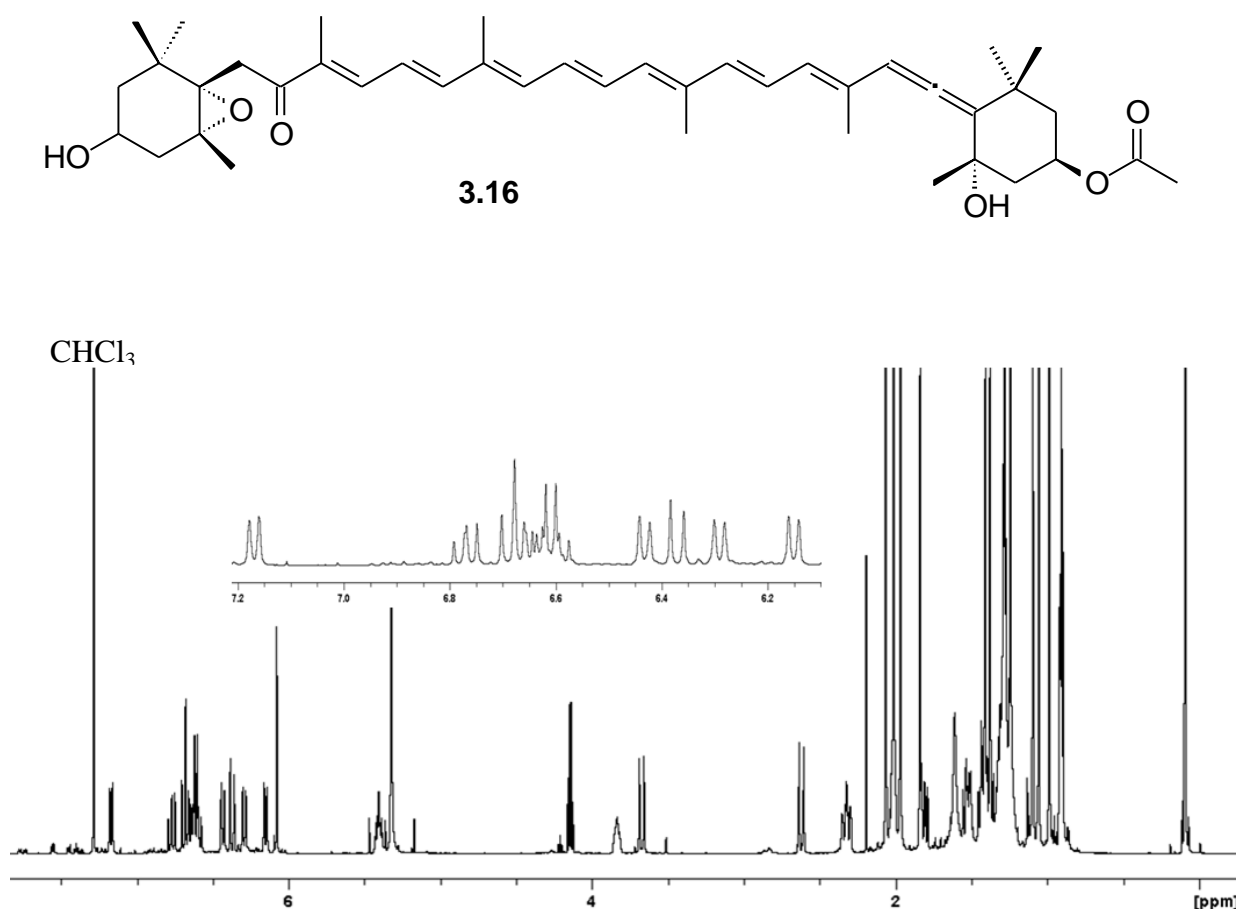


**Figure 3.14**  $^1\text{H-NMR}$  spectrum (600 MHz,  $\text{CDCl}_3$ ) of compound **3.16**

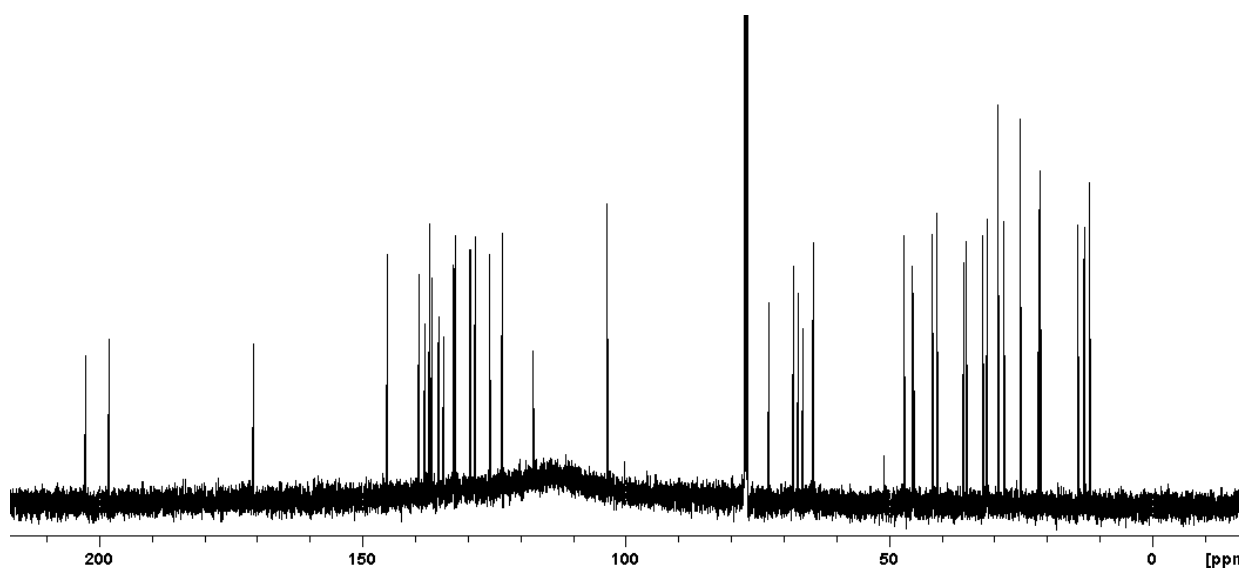


**Figure 3.15** <sup>13</sup>C-NMR spectrum (150 MHz, CDCl<sub>3</sub>) of compound **3.16**

### 3.2.2.3 The structure elucidation of compound **3.17** and **3.18**

Compounds **3.17** and **3.18** were isolated as colourless oils. The <sup>1</sup>H-NMR spectra of the compounds were similar, with three spectral regions characteristic of glycolipid molecules. The region  $\delta$  0.8- 2.9 showed complex overlapping signals characteristic of methylene and methyl protons within fatty acids, with differences in the spectra of **3.17** and **3.18** arising due to the degree of unsaturation of the fatty acids as seen by the allylic methylene protons at  $\delta$  2.8 (br m) (Figure 3.16). The terminal methyl protons are signalled at about  $\delta$  1.0. Furthermore, the cluster of signals at about  $\delta$  5.4 further supports the presence of an unsaturated linear system as observed in fatty acid chains. The sugar moiety is represented by the signals residing at  $\delta$  3.5-4.5. Due to the complexity of the signals in the <sup>1</sup>H-NMR spectra of compounds **3.17** and **3.18**, <sup>13</sup>C and two-dimensional NMR studies (COSY, HMBC, and HSQC), as well GC-MS and high resolution mass spectrometry were utilized in deducing the structures of these compounds.

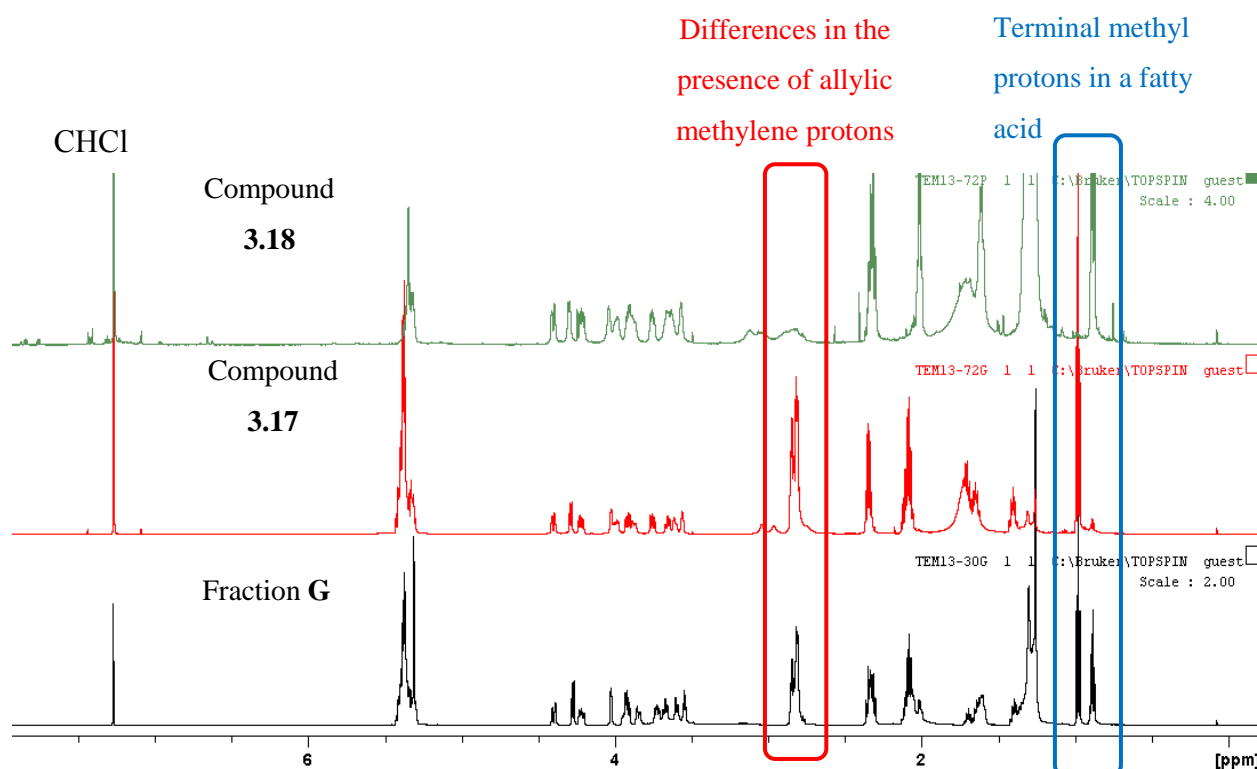
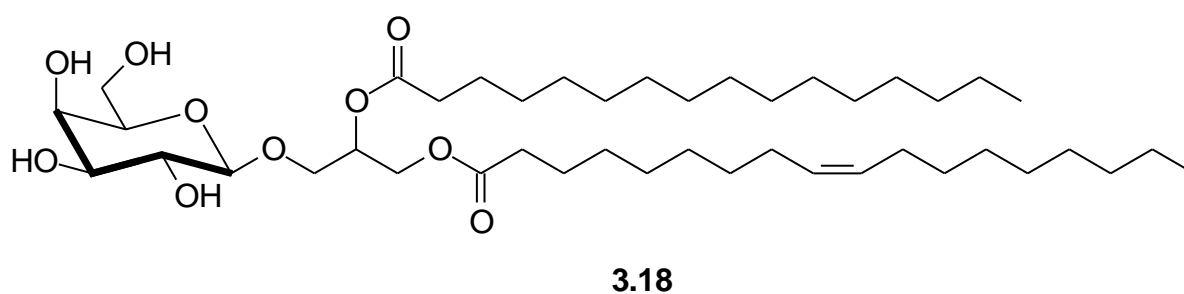
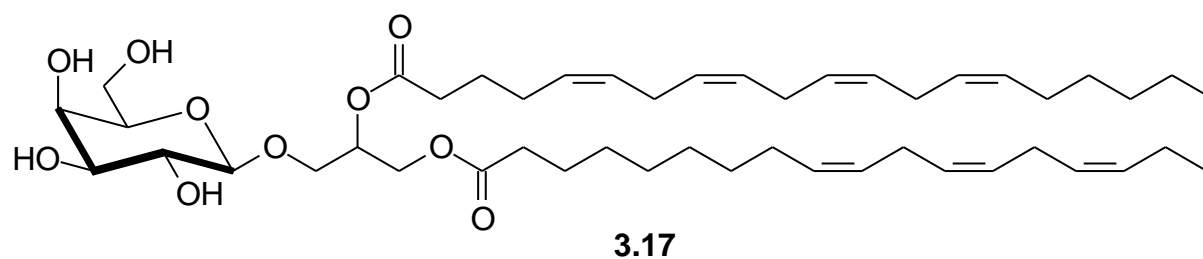


**Figure 3.16** <sup>1</sup>H-NMR spectra (600 MHz, CDCl<sub>3</sub>) of crude fraction **G** and purified compounds **3.17** and **3.18**

The  $^{13}\text{C}$ -NMR spectra of compounds **3.17** and **3.18** (Figure 3.17) showed resonances characteristic of the different types of carbons present in the two compounds. The signal at around  $\delta$  170 is characteristic of a carbonyl associated with an ester. The most important difference between the two spectra is in the olefinic region ( $\delta$  125-135). Compound **3.18** contains a single double bond ( $\delta$  129.9 and 130.3), while compound **3.17** contains seven methylene-interrupted double bond with carbon resonances in the cluster in the  $\delta$  126- 133.

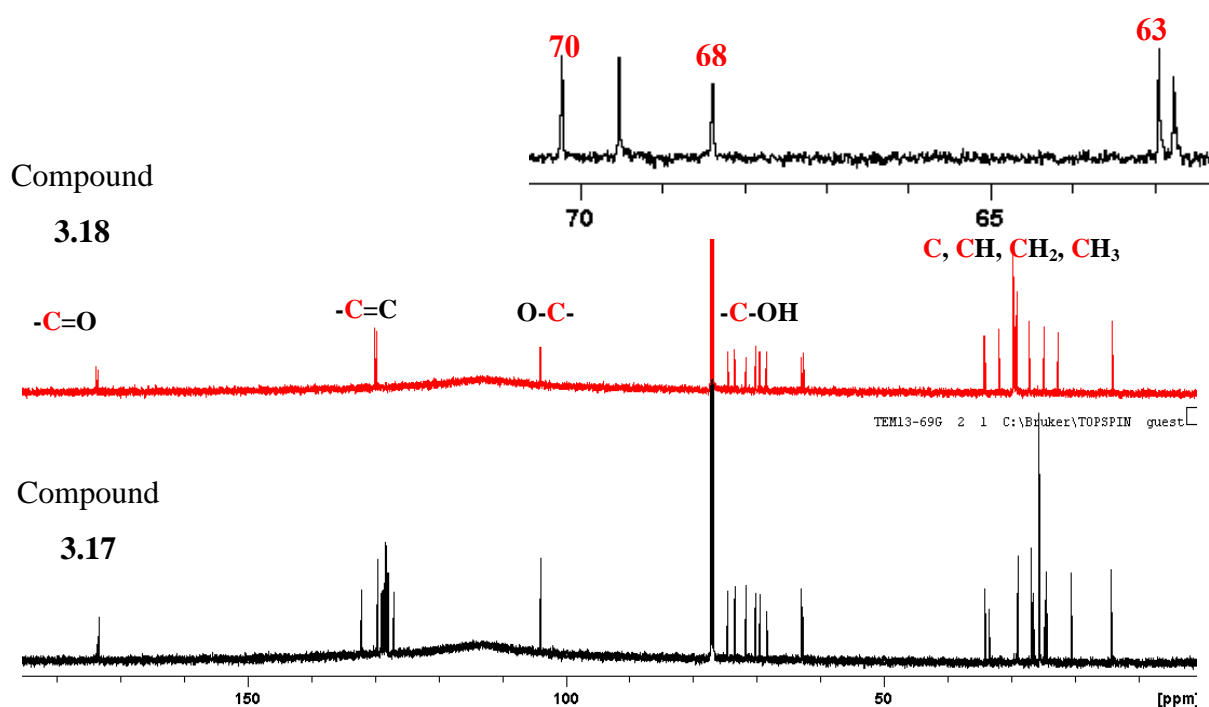


**Figure 3.17**  $^{13}\text{C}$ -NMR (150 MHz,  $\text{CDCl}_3$ ) spectra of **3.17** and **3.18**

The acetal carbon at about  $\delta$  105 is characteristic of an anomeric carbon linking a sugar moiety to a fatty acid chain. The carbon resonances characteristic of the sugar moiety had signals within the region  $\delta$  60-105. However the carbon signals due to the glycerol moiety are found in this same region and have been highlighted in Figure 3.17 ( $\delta$  63, 68 and 70). The quaternary carbon, methine, methylene and methyl groups forming the majority of the fatty acid carbon chain are represented in the  $\delta$  10-40 region. Analysis of the NMR spectroscopic data together with comparisons to literature allowed the assignment of two monogalactosylglycerol lipids which differ in fatty acid chain composition (Kim *et al.*, 2007; Imbs *et al.*, 2013).



**Table 3.4**  $^1\text{H}$ -NMR (600 MHz,  $\text{CDCl}_3$ ) and  $^{13}\text{C}$ -NMR (150 MHz,  $\text{CDCl}_3$ ) assignments for galactosylglycerol moieties of **3.17** and **3.18**

			<b>3.17</b>				<b>3.18</b>
Carbon no.	$\delta_{\text{C}}$	$\delta_{\text{C}}$ multi	$\delta_{\text{H}}$ (multi, <i>J</i> in Hz)	$\delta_{\text{C}}$	$\delta_{\text{H}}$ (multi, <i>J</i> in Hz)		
1	63.2	$\text{CH}_2$	4.40 (dd, 12.0, 2.3) 4.23 (dd, 12.0, 6.3)	63.2	4.41 (dd, 12.0, 2.3) 4.23 (dd, 12.0, 6.4)		
2	70.5	CH	5.36 (m)	70.4	5.35 (m)		
3	68.7	$\text{CH}_2$	3.99 (dd, 11.1, 5.4) 3.76 (dd, 11.3, 6.2)	68.7	4.00 (dd, 12.2, 5.8) 3.76 (dd, 11.3, 6.2)		
1'''	104.2	CH	4.29 (d, 7.4)	104.2	4.30 (d, 7.4)		
2'''	72.0	CH	3.64 (m)	72.0	3.65 (m)		
3'''	73.7	CH	3.89 (m)	73.7	3.89 (m)		
4'''	69.8	CH	3.93 (dd, 11.1, 5.4)	69.8	3.92 (dd, 11.1, 5.4)		
5''	74.8	CH	3.61 (m)	74.8	3.62 (m)		
6'''	63.0	$\text{CH}_2$	3.88 (dd, 10.8, 4.6) 3.62 (m)	62.9	3.88 (dd, 10.8, 4.6) 3.63 (m)		

Assignments completed based on the COSY and HMBC correlations observed

The linkage of the glycerol moiety to the galactosyl sugar was identified *via* a series of  $^1\text{H}$ - $^1\text{H}$ -COSY and HMBC experiments. The methylene protons of the glycerol unit at H-3 ( $\delta$  3.99 and 3.76) exhibited HMBC correlations to the anomeric carbon in the sugar moiety at C-1''' ( $\delta$  104.2) as well as correlations to the methylene carbon at C-1 ( $\delta$  63.2) on the glycerol unit. The methine proton at position H-3 ( $\delta$  5.36) of the glycerol showed HMBC correlations to methylene carbon at position C-1 ( $\delta$  63.2) in the same glycerol unit.  $^1\text{H}$ - $^1\text{H}$  COSY correlations were observed between the methine proton at position H-2 ( $\delta$  5.36) and the two methylene protons at position H-1 ( $\delta$  4.41) and H-3 ( $\delta$  3.76) in the determination of the glycerol unit. Table 3.4 illustrates these important spectroscopic correlations. The key  $^1\text{H}$ - $^1\text{H}$

COSY and HMBC correlations of the galactosylglycerol unit are shown in Figure 3.18 below.

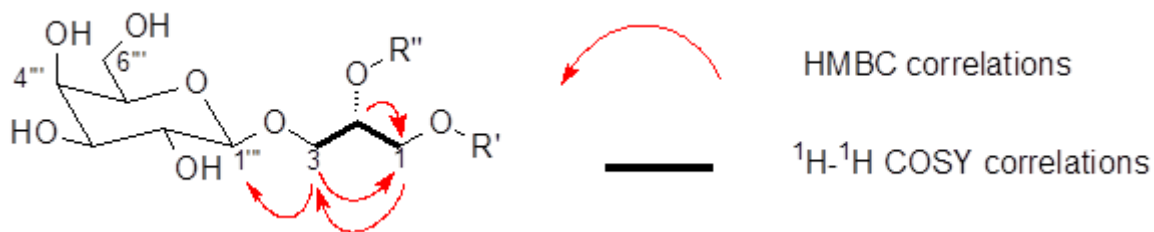
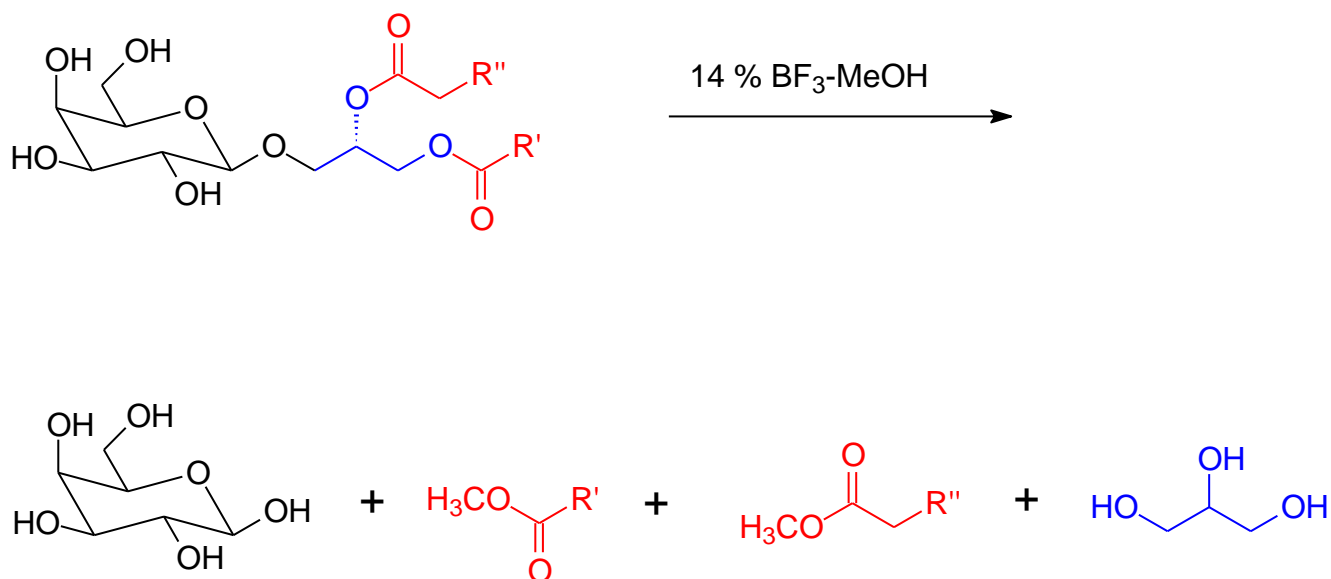


**Figure 3.18** Key  $^1\text{H}$ - $^1\text{H}$  COSY and HMBC correlations observed for the galactosylglycerol unit in compounds **3.17** and **3.18**

Overlapping NMR signals made it difficult to ascertain the fatty acid composition of both **3.17** and **3.18**; therefore fatty acid methyl ester (FAME) analysis studies were conducted in order to determine the composition of the fatty acid chains. Compounds **3.17** and **3.18** were each treated with a 14% boron trifluoride-MeOH reagent following the method reported by Metcalfe and Schmitz (1961) and Morrison and Smith (1964). The resultant fatty acid methyl esters were analyzed via Gas Chromatography-Mass spectrometry (GC-MS) (Metcalfe and Schmitz, 1961; Morrison and Smith, 1964) (Scheme 3.2).



### Scheme 3.2 FAME analysis of monogalactosylglycerol lipids

Conditions: i) Reflux for 30 min in MeOH

Mass spectral data from the fractions with the most abundant peaks on the gas chromatogram were considered to be the fractions containing the fatty acid methyl esters of **3.17** (Figure 3.19) and **3.18** (Figure 3.20). The fatty acid methyl esters were compared to a library of FAME esters of several fatty acids in the identification process.

Mass spectra of the FAME products of **3.17** obtained from GC, indicated that the peak at 15.8 min (Figure 3.19) contained one of the methyl esters of the compound. The  $m/z$  peak was obtained at  $m/z$  292.2 and corresponds to a molecular formula of C<sub>19</sub>H<sub>32</sub>O<sub>2</sub>. These values were compared to the fatty acid standards to determine that the peak corresponds to methyl 9Z,12Z,15Z-octadecatrienoate (FAME of linolenic acid (18:3) **3.17**<sup>1</sup>). The GC peak at 20.7 min (Figure 3.19) in the analysis of the methyl ester products compound of **3.17** represented the second fatty acid in this compound. The  $m/z$  peak in the mass spectrum was determined to be at  $m/z$  318.2 with a molecular formula C<sub>21</sub>H<sub>34</sub>O<sub>2</sub> which corresponds to the methyl 5Z,8Z,11Z,14Z-eicosatetraenoate (FAME of arachidonic acid (20:4) **3.17**<sup>2</sup>).

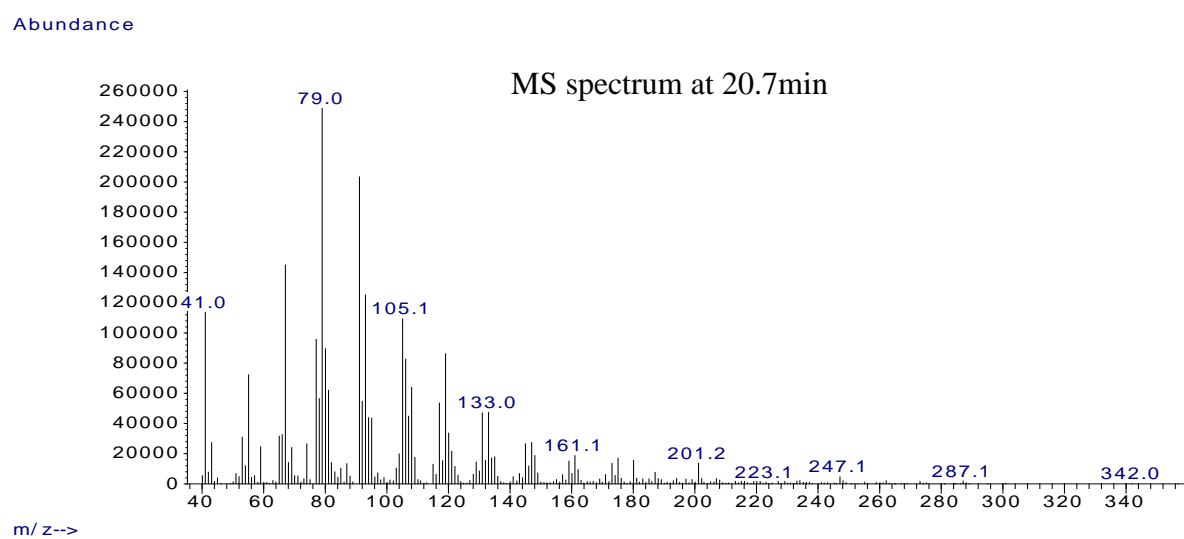
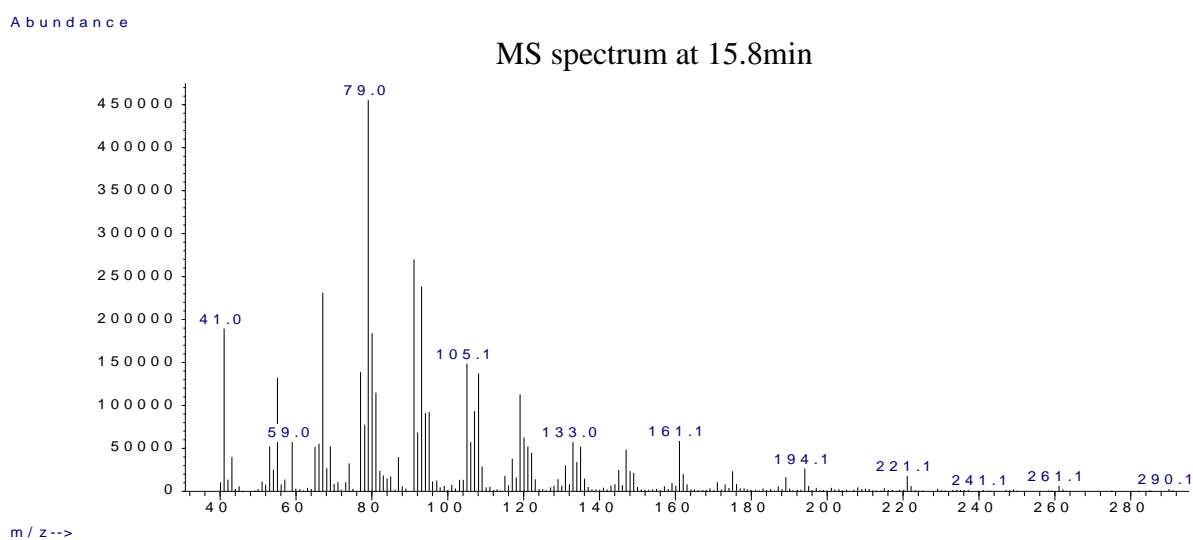
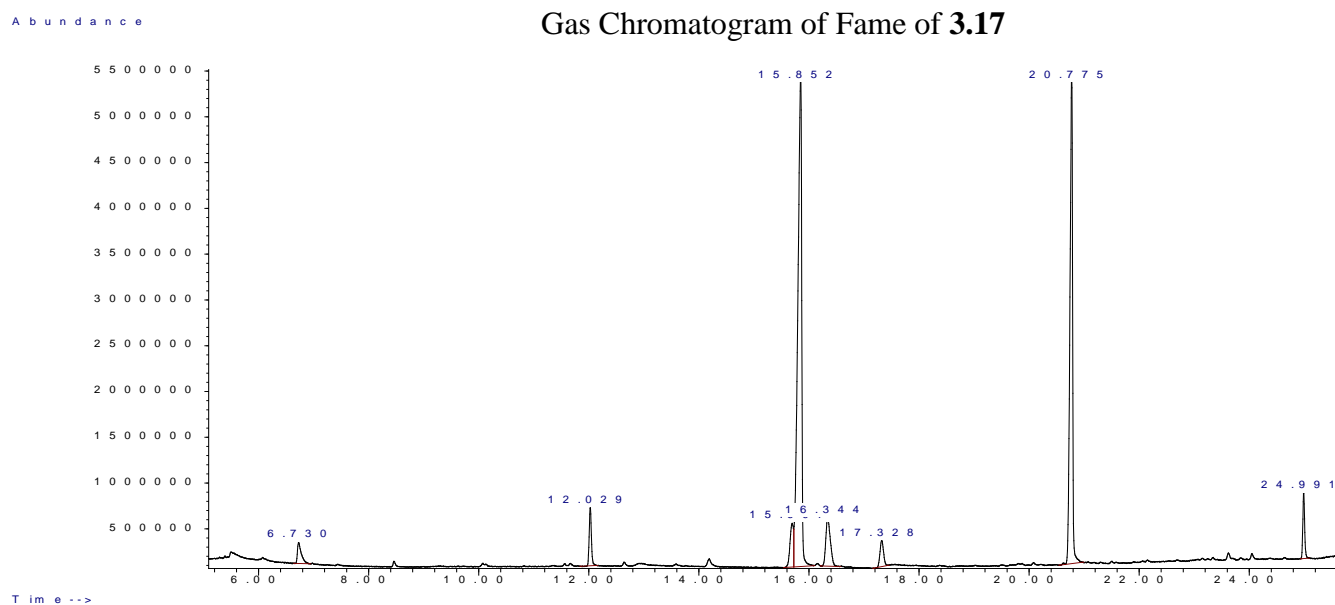


Figure 3.19 GC-MS data for FAME analysis of 3.17

The gas chromatogram for the FAME analysis carried out on **3.18** (Figure 3.20) showed a peak at 12.0 min which was one of the two abundant peaks observed. The mass spectra at this retention time gave a molecular ion  $m/z$  at 270.1 which corresponds to a molecular formula of  $C_{17}H_{34}O_2$ . The fatty acid methyl ester was identified as methyl hexadecanoate (FAME of palmitic acid (16:0) **3.18**<sup>1</sup>). Another GC peak at 16.5min gave a molecular ion peak at  $m/z$  296.3 in the mass spectrum with a molecular formula of  $C_{19}H_{36}O_2$ . This, however, suggested two possible fatty acids either the cis- isomer methyl 9Z-octadecenoate (FAME of oleic acid (18:1)) or the trans- isomer methyl 9E-octadecenoate (FAME of elaidic acid (18:1)). To identify the isomer further <sup>1</sup>H-NMR analysis of compound **3.18** was carried out. The multiplet present at  $\delta$  5.36 was observed as two triplets overlaying each other, due to the methine protons of the double bond. The coupling constants were determined for each triplet and found to be  $J= 9.97$  Hz for both triplets which is characteristic of a cis double bond. Therefore the fatty acid was determined to be methyl 9Z-octadecenoate **3.18**<sup>2</sup>).

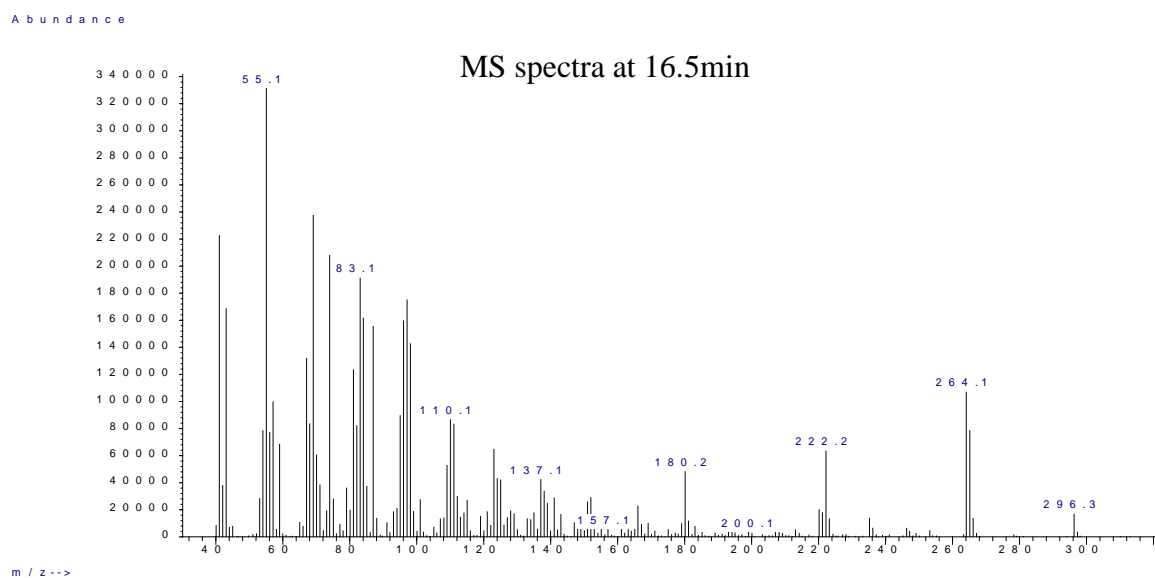
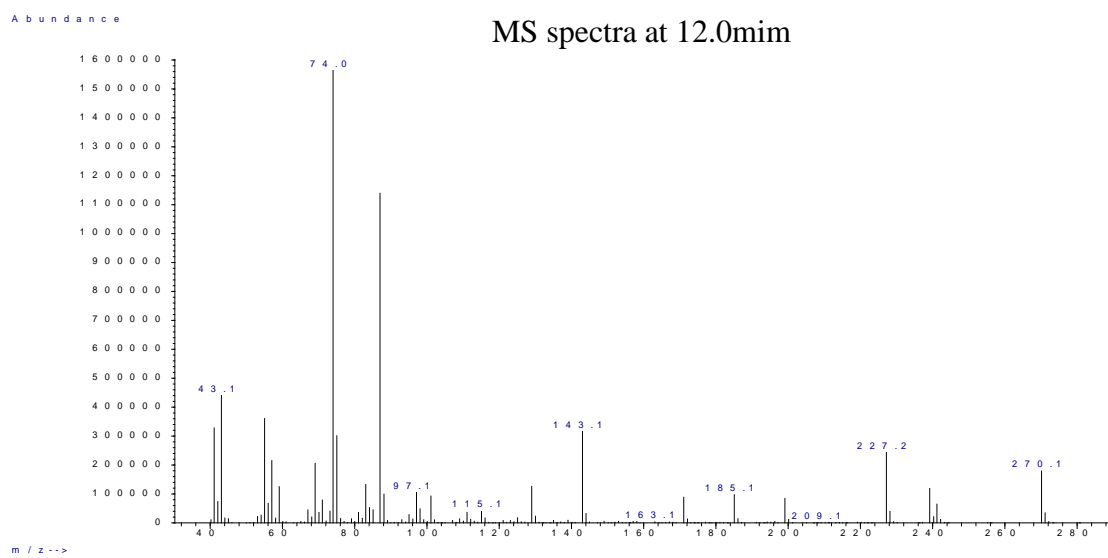
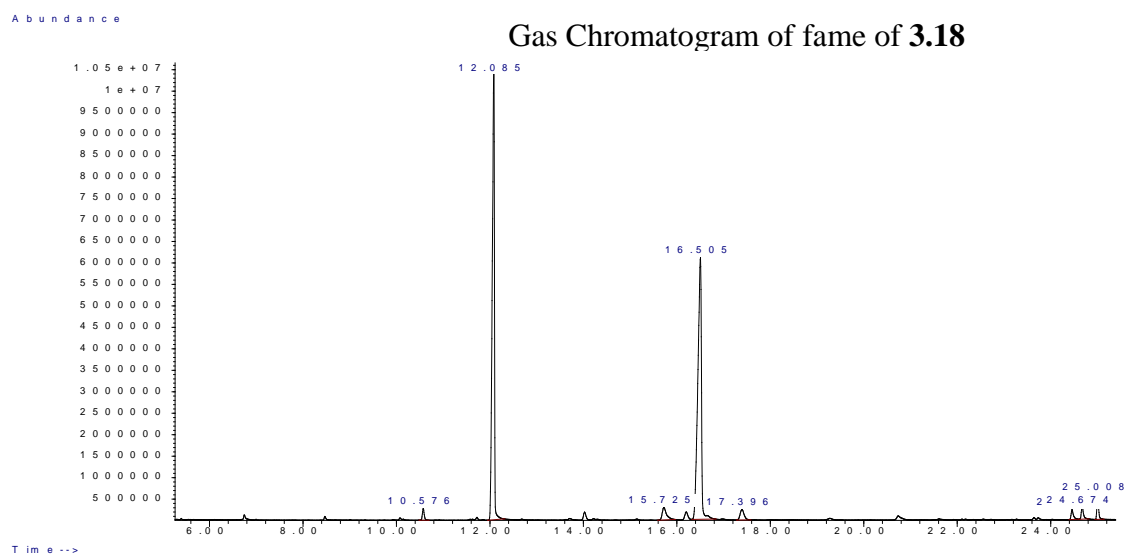


Figure 3.20 GC-MS data for FAME analysis of 3.18

High resolution mass spectrometry (HRESIMS) was conducted on compound **3.17** and **3.18** whilst Liquid Chromatography-Mass Spectrometry (LCMS) was conducted on the crude fraction **G** to assist with the FAME analysis data. The results are thus tabulated below (Table 3.5). The calculated mass of compound **3.18** matched the HRESIMS mass, as well as the low resolution mass spectrometry (LC-MS) giving the molecular formula as  $C_{43}H_{80}O_{10}$  for compound **3.18**. The HRESIMS for compound **3.17** could not be determined, probably due to its poor stability, and therefore low resolution mass spectrometry (LCMS) as well as FAME analysis data were used in determining the compound's molecular formula. With careful analysis, the molecular formula of **3.18** was determined to be  $C_{47}H_{76}O_{10}$ .

**Table 3.5** HRESIMS and LC-MS data for compound **3.17** and **3.18**

		<b>3.17</b>	<b>3.18</b>
	Proposed formula	$C_{43}H_{80}O_{10}$	$C_{47}H_{76}O_{10}$
	$^1H$	80.626	76.5947
	$^{12}C$	516	564
	$^{16}O$	159.9492	159.9492
	Calculated $m/z$ value	756.5752	800.5439
<b>ESI +</b> <b>(+Na)</b>	HRMS ESI $m/z$ value	779.5664	ND
	Calculated $m/z$ value	779.5649	823.5336
	Difference	0.00148	-
<b>ESI-</b> <b>(+<math>^{35}Cl</math>)</b>	HRMS $m/z$ value	791.5440	ND
	Calculated $m/z$ value	791.5440	835.5127
	Difference	0.0000	-
<b>ESI-</b> <b>(+<math>^{37}Cl</math>)</b>	HRMS $m/z$ value	793.5401	ND
	Calculated $m/z$ value	793.5411	837.5098
	Difference	0.001	-
<b>LC-MS</b> <b>(+Na)</b>	LC-MS $m/z$ value	779.51	823.64
	Calculated $m/z$ value	779.5649	823.5336
	Difference	0.05492	0.10638

ND= Not Determined

Differences

Therefore, **3.17** was assigned as 1-*O*-(5Z,8Z,11Z,14Z-eicosatetraenoyl)-2-*O*-(9Z,12Z,15Z-octadecatrienoyl)-3-*O*- $\beta$ -D-galactopyranosyl-*sn*-glycerol and **3.18** assigned as 1-*O*-(9Z-octadecenoyl)-2-*O*-(hexadecanoyl)-3-*O*- $\beta$ -D-galactopyranosyl-*sn*-glycerol.

Monogalactosyldiacylglycerols (MGDGs) are a major component of photosynthetic membranes in plants, algae and even bacteria. In some species of Phaeophyceae, MGDGs have been produced as herbivore deterrents (Deal *et al.*, 2003; Kim *et al.*, 2007). In the search for new, biologically active natural products, MGDGs have been found to possess numerous activities making them suitable candidates as novel drugs in medicinal chemistry. These MGDGs have been found to possess anti-tumor, anti-viral as well as anti-inflammatory activities. Bruno *et al.*, (2005) have postulated that the biological activities of these MGDGs are linked to the degree of unsaturation of the fatty acid chain; i.e. MGDGs with highly unsaturated fatty acid chains possess high biological activity (Imbs *et al.*, 2013).



## 3.3 Experimental

### 3.3.1 General experimental

#### Solvents

All solvents used for extraction and chromatography were of HPLC grade (LiChrosolv<sup>®</sup>; Merck<sup>®</sup>, Darmstadt, Germany).

#### Chromatographic procedures

Column Chromatographic purification procedures were achieved using Merck<sup>®</sup> silica gel 60 (0.040-0.063mm) 230-400 mesh ASTM product. All thin layer chromatography experiments were run on Merck<sup>®</sup> silica gel 60F<sub>254</sub> 20x20 aluminium sheets and visualization was done using Syngene UV lamp, with dual wavelengths 254nm and 365nm.

#### HPLC procedures

A Waters HPLC machine consisting of a Waters 1515 Isocratic HPLC Pump with a Waters 2414 Refractive Index Detector was used. Normal phase HPLC was done on a Whatman Partsil<sup>®</sup> 10 (50 x 1 cm) column while reverse phase HPLC was carried out on a Phenomex<sup>®</sup> C<sub>18</sub> (25 x 1 cm) column. All solvents were prepared by filtering under vacuum through a 0.45 µm membrane filter and degassed by sonicating for 20 min using an Ultrasonic Manufacturing Company<sup>®</sup> sonicator.

#### Nuclear magnetic resonance spectroscopy

NMR studies were conducted using a Bruker<sup>®</sup> Avance 600 MHz spectrometer with deuterated chloroform (CDCl<sub>3</sub>) as the NMR solvent. All chemical shifts were recorded in part per million ( $\delta$ ) and coupling constants  $J$  given in hertz (Hz). All spectra were referenced to residual solvent ( $\delta_{\text{H}}$  7.28,  $\delta_{\text{C}}$  77.0).

### **Gas chromatography-mass spectrometry**

GC-MS analyses were carried out at the Central Analytical Facilities (CAF), University of Stellenbosch. An Agilent 6890N GC with CTC CombiPAL Autosampler and Agilent 5975B MS equipped with a ZB 274305 SemiVolatiles column (30 m, 0.25 mm ID, 0.25 µm film thickness). Helium was used as carrier gas in all experiments with the temperature set at 280 °C. The ionization voltage was set at 70 eV.

### **High resolution mass spectrometry**

High resolution mass spectrometry analyses were also conducted at the CAF, University of Stellenbosch using a Waters Synapt G2 instrument.

### **Liquid chromatography-mass spectrometry**

LC-MS analyses were carried out in the positive ion mode in the Department of Chemistry at Rhodes University using a Finnigan MAT LCQ MS equipped with an ESI source and an ion trap.

### **3.3.2 Plant material**

*Brassicophycus brassicaeformis* was collected from Glencairn beach on the south-western coast in Simons Town on 1/9/2012. Plant material was hand-picked and identified by Professor John Bolton, Department of Botany, University of Cape Town. A voucher specimen was prepared and kept in the Department of Pharmaceutical Chemistry, Rhodes University. The alga was stored at -20 °C prior to extraction and then air dried following extraction.

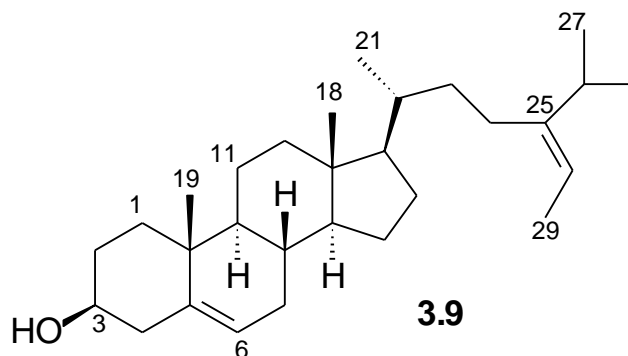
### **3.3.3 Isolation of secondary metabolites from *B. brassicaeformis***

Algal material (dry mass 36.40g) was thawed and washed with distilled water before an initial MeOH (850ml) soak for 1h at room temperature. The solvent was then decanted and

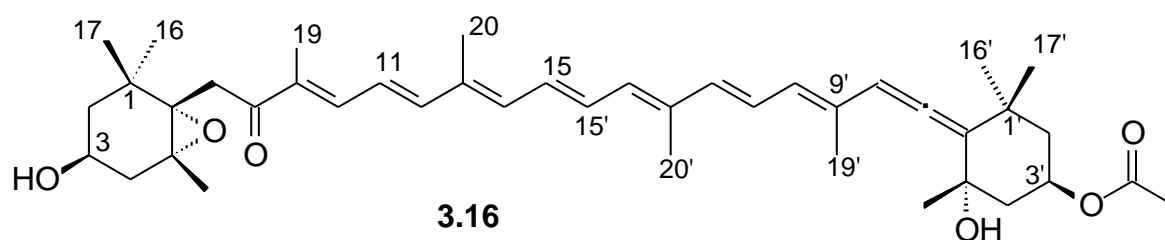
the plant material extracted with 2:1 CH<sub>2</sub>Cl<sub>2</sub>-MeOH (1200ml) at 40°C for 30 min. The organic CH<sub>2</sub>Cl<sub>2</sub> layer was separated from the aqueous methanolic layer by phase separation through the addition of water. The organic crude (1.59g) was concentrated by solvent evaporation under reduced pressure. Fractionation of the crude product (0.86g) was done by step gradient column chromatography eluted by Hexane-EtOAc in increasing polarity to obtain eight fractions (TEM13 A-H). Fraction C was further purified by normal phase HPLC (7:3 Hexane-EtOAc) to yield **3.9** (11.2mg). Fraction D was purified by passing through silica gel column chromatography (6:4 Hexane-EtOAc) to give **3.16** (38mg). Fraction D was purified to give compounds **3.17** (18.6mg) and **3.18** (20mg) by reversed phase HPLC (100 % MeOH). (Step gradient chromatography illustrated in Scheme 3.1 page 47).

### 3.3.3.1 Isolated secondary metabolites (**3.9**, **3.16**, **3.17**, **3.18**)

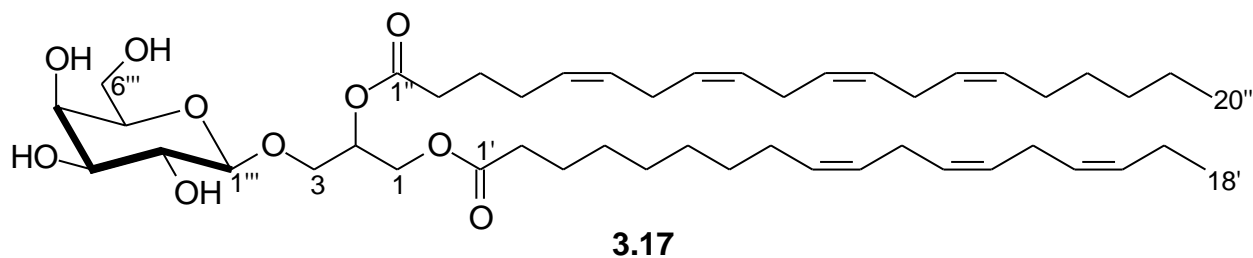
#### Compound **3.9** (Isolation code TEM13-16H)



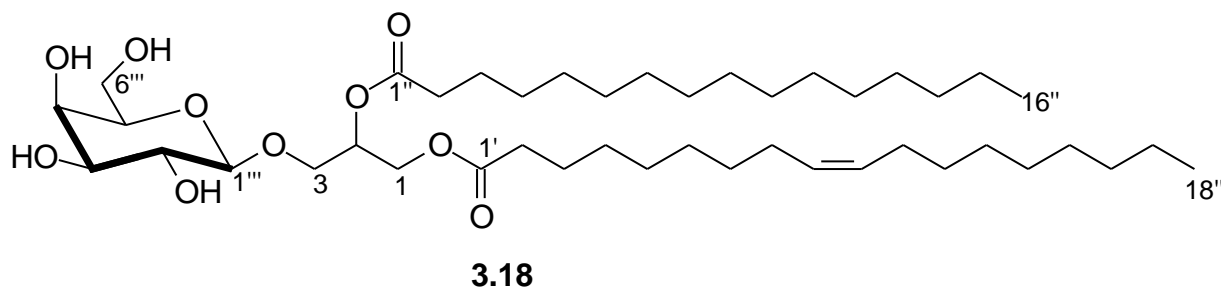
*3β-Hydroxy-5,24(28)-stigmastadiene* (**3.9**): White solid- <sup>1</sup>H NMR (600 MHz, CDCl<sub>3</sub>) and <sup>13</sup>C NMR (150 MHz, CDCl<sub>3</sub>) data available in Table 3.3 and are consistent with literature values (Huh *et al.*, 2012).

**Compound 3.16** (Isolation code TEM13-20H, K, L)

*Fucoxanthin* (**3.16**): Yellow Brown Paste-  $^1\text{H}$  NMR (600 MHz,  $\text{CDCl}_3$ ):  $\delta$  0.91 (s, Me-17),  $\delta$  0.99 (s, Me-16),  $\delta$  1.06 (s, Me-17'),  $\delta$  1.09 (s, H-18),  $\delta$  1.25 (s, H-18'),  $\delta$  1.28 (dd,  $J=7.2, 14.2$  Hz, H-2ax),  $\delta$  1.38 (s, Me-16'),  $\delta$  1.40 (dd,  $J= 10.3, 15.7$  Hz, H-2ax'),  $\delta$  1.51 (dd,  $J= 2.3, 12.4$  Hz, H-2eq),  $\delta$  1.53 (dd,  $J= 11.7, 16.4$  Hz, H-4'ax),  $\delta$  1.82 (dd,  $J= 7.2, 14.7$  Hz, H-4ax),  $\delta$  1.84 (s, H-19'),  $\delta$  1.97 (s, H-19),  $\delta$  2.01 (s, H-20),  $\delta$  2.01 (s, H-20'),  $\delta$  2.07 (dd,  $J= 2.9, 14.1$  Hz, H-2'eq),  $\delta$  2.19 (s, Me,C-3'OAc),  $\delta$  2.32 (dd,  $J= 2.3, 17.7$  Hz, H-4'eq),  $\delta$  2.32 (dd,  $J= 2.3, 17.7$  Hz, H-4eq),  $\delta$  2.62 (d,  $J= 17.9$ , H-7),  $\delta$  3.7 (d,  $J= 18.4$  H-7),  $\delta$  3.84 (m, H-3),  $\delta$  5.41 (tt,  $J= 8.5, 14.3$  Hz, H-3'),  $\delta$  6.08 (s, H-8'),  $\delta$  6.15 (d,  $J= 10.2$ , H-10'),  $\delta$  6.29 (d,  $J= 10.2$  Hz, H-14'),  $\delta$  6.37 (d,  $J= 14.8$ , H-12'),  $\delta$  6.43 (d,  $J= 11.5$ , H-14),  $\delta$  6.61 (m, H-11),  $\delta$  6.68 (t,  $J= 14.7$ , H-12),  $\delta$  6.72 (m, H-15),  $\delta$  6.76 (dd,  $J= 11.7, 14.5$  Hz, H-15'),  $\delta$  6.77 (t,  $J= 11.7$ , H-11'),  $\delta$  7.17 (d,  $J= 11.2$ , H-10).  $^{13}\text{C}$ -NMR (150 MHz,  $\text{CDCl}_3$ ):  $\delta$  35.8 (C-1),  $\delta$  35.2 (C-1'),  $\delta$  47.1 (C-2),  $\delta$  45.5 (C-2'),  $\delta$  64.4 (C-3),  $\delta$  68.1 (C-3'),  $\delta$  41.7 (C-4),  $\delta$  45.2 (C-4'),  $\delta$  66.2 (C-5),  $\delta$  72.8 (C-5'),  $\delta$  67.1 (C-6),  $\delta$  117.4 (C-6'),  $\delta$  40.8 (C-7),  $\delta$  202.4 (C-7'),  $\delta$  197.9 (C-8),  $\delta$  103.4 (C-8'),  $\delta$  134.5 (C-9),  $\delta$  132.5 (C-9'),  $\delta$  139.2 (C-10),  $\delta$  128.6 (C-10'),  $\delta$  123.4 (C-11),  $\delta$  125.7 (C-11'),  $\delta$  145.0 (C-12),  $\delta$  137.1 (C-12'),  $\delta$  135.5 (C-13),  $\delta$  17.8 (C-13'),  $\delta$  136.8 (C-14),  $\delta$  132.2 (C-14'),  $\delta$  129.5 (C-15),  $\delta$  132.5 (C-15'),  $\delta$  25.1 (C-16),  $\delta$  21.4 (C-16'),  $\delta$  28.1 (C-17),  $\delta$  32.1 (C-17'),  $\delta$  21.2 (C-18),  $\delta$  31.3 (C-18'),  $\delta$  11.8 (C-19),  $\delta$  14.0 (C-19'),  $\delta$  12.8 (C-20),  $\delta$  12.9 (C-20'),  $\delta$  21.5 and 170.6 (3'-OAc). All  $^1\text{H}$ - NMR and  $^{13}\text{C}$ -NMR data were consistent with literature values (Mori *et al.*, 2004, Afolayan *et al.*, 2008).

**Compound 3.17** (Isolation code TEM13-69G)

*1-O-(5Z,8Z,11Z,14Z-eicosatetraenoyl)-2-O-(9Z,12Z,15Z-octadecatrienoyl)-3-O-β-D-galactopyranosyl-sn-glycerol (3.17)*: Colourless oil-  $^1\text{H}$  NMR and  $^{13}\text{C}$  NMR data available in Table 3.4; LC-MS (positive mode)  $m/z$  823.64 (calculated 823.5336)  $\text{C}_{47}\text{H}_{76}\text{O}_{10}\text{Na}$   $[\text{M}+\text{Na}]$

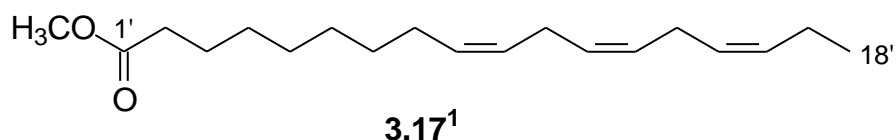
**Compound 3.18** (Isolation code TEM13-69P)

*1-O-(9Z-octadecenoyl)-2-O-(hexadecanoyl)-3-O-β-D-galactopyranosyl-sn-glycerol (3.18)*: Colourless oil-  $^1\text{H}$  NMR and  $^{13}\text{C}$  NMR data available in Table 3.4; HRESIMS (positive mode),  $m/z$  779.5664 (calculated 779.56492)  $\text{C}_{43}\text{H}_{80}\text{O}_{10}\text{Na}$   $[\text{M}+\text{Na}]$ .

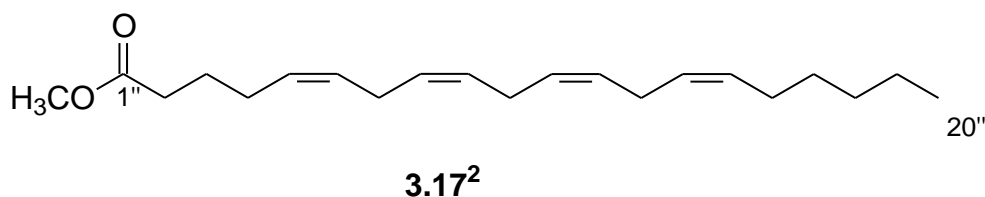
### Derivatization of fatty acid methyl esters of compounds 3.17 and 3.18

A solution of MGDG (**3.17** (6mg); **3.18** (4mg)) in MeOH (9ml) was treated with 14 %  $\text{BF}_3$ -MeOH reagent and the mixture refluxed for 30 min. Progress of the reaction was monitored by TLC on a silica gel plate which was developed by charring with 50% sulphuric acid. Methyl esters were isolated by phase separation between Hexane (30ml) and water (15ml). The lipophilic hexane layer containing the methyl esters was concentrated under reduced pressure and the samples analyzed using an Agilent 6890NGC GC-MS with CTC CombiPAL Autosampler and Agilent 5975B MS, Column ZB 274305 SemiVolatiles (30 m, 0.25 mm ID, 0.25  $\mu\text{m}$  film thickness) at the Central Analytical Facility, University of Stellenbosch.

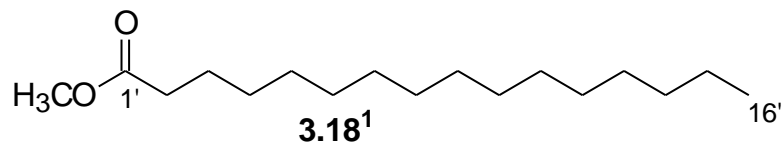
#### Fatty acid methyl esters of 3.17 Isolation code TEM14-86G



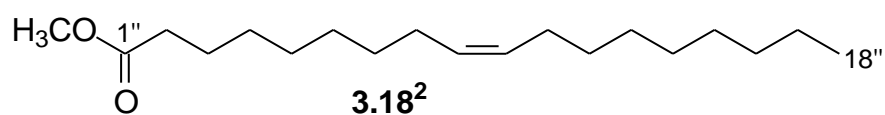
*Methyl 9Z,12Z,15Z-octadecatrienoate (3.17<sup>1</sup>):* Colourless oil : ESIMS (positive mode)  $m/z$  292.2 (calculated 292.24023)  $\text{C}_{19}\text{H}_{32}\text{O}_2$  [M+1]



*Methyl 5Z,8Z,11Z,14Z-eicosatetraenoate (3.17<sup>2</sup>):* Colourless oil: ESIMS (positive mode)  $m/z$  318.2 (calculated 318.2559)  $\text{C}_{21}\text{H}_{34}\text{O}_2$  [M+1]

**Fatty acid methyl esters of 3.18** Isolation code TEM14-86P

*Methyl hexadecanoate* (**3.18<sup>1</sup>**): Colourless oil: ESIMS (positive mode)  $m/z$  270.2 (calculated 270.25588)  $C_{17}H_{34}O_2$  [M+1].



*Methyl 9Z-octadecenoate* (**3.18<sup>2</sup>**): Colourless oil- ESIMS (positive mode)  $m/z$  296 (calculated 296.27153)  $C_{19}H_{36}O_2$  [M+1].

### 3.4 References

- Afolayan A.F., Bolton J.J., Lategan C.A., Smith P.J., Beukes D.R. (2008). Fucoxanthin, tetraprenylated toluquinone and toluhydroquinone metabolites from *Sargassum heterophyllum* inhibit the *in vitro* growth of malaria parasite *Plasmodium falciparum*. *Zeitschrift für Naturforschung B* 63: 848-852
- Amico V. (1995). Marine brown algae of family cystoseiraceae: chemistry and chemotaxonomy. *Phytochemistry* 39: 1257-1279
- Bang M., Kim H., Lee D., Han M., Baek Y., Chung D.K., Baek N. (2011). Anti-osteoporotic activities of fucoxerol from sea mustard (*Undaria pinnatifida*). *Food Science and Biotechnology* 20: 343-347
- Bonnett R., Mallams A.K., Spark A.A., Tee J.L., Weedon B.C.L. (1969). Carotenoids and related compounds. Part XX.<sup>1</sup> Structure and reactions of fucoxanthin. *Journal of Chemical Society C* 429-454
- Bruno A., Rossi C., Marcolongo G., Di Lena A., Venzo A., Berrie C.P., Corda D. (2005). Selective *in vivo* anti-inflammatory action of the galactolipid monogalactosyldiacylglycerol. *European Journal of Pharmacology* 524: 159-168
- Combaut G., Piovetti L. (1983). A novel acyclic diterpene from the brown alga *Bifurcaria bifurcata*. *Phytochemistry* 22: 1787-1789
- Culioli G., Mesguiche V., Piovetti L., Valls R. (1999). Geranylgeraniol and geranylgeraniol-derived diterpenes from the brown alga *Bifurcaria bifurcata* (Cystoseiraceae). *Biochemical Systematics and Ecology* 27: 665-668
- Culioli G., Daoudi M., Mesguiche V., Valls R., Piovetti L. (1999). Geranylgeraniol-derived diterpenoids from the brown alga *Bifurcaria bifurcata*. *Phytochemistry* 52: 1447-1454
- Culioli G., Ortalo-Magné A., Daoudi M., Thomas-Gyon H., Valls R., Piovetti L. (2004). Trihydroxylated linear diterpenes from the brown alga *Bifurcaria bifurcata*. *Phytochemistry* 65: 2063-2069



- Daoudi M., Bakkas S., Culioli G., Ortalo-Magné A., Piovetti L., Guiry MD. (2001). Acyclic diterpenes and sterols from genera *Bifurcaria* and *Bifurcariopsis* (Cystoseiraceae, Phaeophyceae). *Biochemical Systematics and Ecology* 29: 973-978
- Deal M.S., Hay M.E., Wilson D., Fenical W. (2003). Galactolipids rather than phlorotannins as herbivore deterrents in the brown seaweed *Fucus vesiculosus*. *Oecologia* 136: 107-114
- Draisma S.G.A., Ballesteros E., Rousseau F., Thibaut T. (2010). DNA sequence data demonstrate the polyphyly of the genus *Cystoseira* and other Sargassaceae genera (Phaeophyceae). *Journal of Phycology* 46: 1329-1345
- Guardia S., Valls R., Mesguiche V., Brunel J., Culioli G. (1999). Enantioselective synthesis of (-)-Bifurcadiol: A Natural Antitumor Marine Product. *Tetrahedron Letters* 40: 8359-8360
- Huh G., Lee D., In S., Lee D., Park S., Yi T., Kang H., Seo W., Baek N. (2012). Fucosterols from *Hizikia fusiformis* and their proliferative activities on osteosarcoma-derived cell MG63. *Journal of the Korean Society for Applied Biological Chemistry* 55: 551-555
- Imbs T.I., Ermakova S.P., Fedoreyev S.A., Anastyuk S.D., Zvyagintseva T.N. (2013). Isolation of fucoxanthin and highly unsaturated monogalactosyldiacylglycerol from brown alga *Fucus evanescens* C Agardh and *in vitro* investigation of their antitumor activity. *Marine Biotechnology* 15: 606-612
- Jongaramruong J., Kongkam N. (2007). Novel diterpenes with cytotoxic, anti-malarial and anti-tuberculosis activities from a brown alga *Dictyota* sp. *Journal of Asian Natural Products Research* 9: 743-751
- Khanavi M., Gheidarloo R., Sadati N., Ardekani M.R.S., Nabavi S.M.B., Tavajohi S., Ostad S.N. (2012). Cytotoxicity of fucosterol containing fraction of marine algae against breast and colon carcinoma cell line. *Pharmacognosy Magazine* 8: 60-64
- Kim Y.H., Kim E., Lee C., Kim M., Rho J. (2007). Two new monogalactosyl diacylglycerols from brown alga *Sargassum thunbergii*. *Lipids* 42: 395-399
- Lee S., Lee Y.S., Jung S.H., Kang S.S., Shin K.H. (2003). Anti-oxidant activities of fucosterol from the marine algae *Pelvetia siliquosa*. *Archives of Pharmacal Research* 26: 719-722

- Lee Y.S., Shin K.H., Kim B., Lee S. (2004). Anti-diabetic activities of fucosterol from *Pelvetia siliquosa*. *Archives of Pharmacal Research* 27: 1120-1122
- Metcalf L.D., Schmitz A.A. (1961). The rapid preparation of fatty acid esters for GC analysis. *Armour Industrial Chemical Co., McCook III* 33: 363-364
- Mori K., Ooi T., Hiraoka M., Oka N., Hamada H., Tamura M., Kusumi T. (2004). Fucoxanthin and its metabolites in edible brown algae cultivated in deep seawater. *Marine Drugs* 2: 63-72
- Morrison W.R., Smith L.M. (1964). Preparation of fatty acid methyl esters and dimethylacetals from lipids with boron trifluoride-MeOH. *Journal of Lipids Research* 5: 600-608
- Muñoz J., Culioli G., Köck M. (2013). Linear diterpenes from the brown marine alga *Bifurcaria bifurcata*: a chemical perspective. *Phytochemistry Reviews* 12: 407-424
- Peng J., Yuan J., Wu C., Wang J. (2011). Fucoxanthin, a marine carotenoid present in brown seaweeds and diatoms: metabolism and bioactivities relevant to human health. *Marine Drugs* 9: 1806-1828
- Silva P.C., Basson P.W., Moe R.L. (1996). Catalogue of benthic marine algae of the Indian Ocean. *University of California Publications in Botany* 79: 1259
- Stegenga H., Bolton J.J., Anderson R.J. (1997). *Bolus Herbarium*. University of Cape Town, Cape Town
- Valls R., Banaigs B., Piovetti L., Archavlis A., Artaud J. (1993). Linear diterpene with antimitotic Activity from the brown alga *Bifurcaria bifurcata*. *Phytochemistry* 34:1585-1588
- Valls R., Piovetti L., Archavlis A., Pellegrini M. (1995). (S)-13-Hydroxygeranylgeraniol-derived furanoditerpenes from *Bifurcaria bifurcata*. *Phytochemistry* 39: 145-149
- Valls R., Piovetti L. (1995). The chemistry of the Cystoseiraceae (fucales: Pheophyceae): chemotaxonomic relationships. *Biochemical Systematics and Ecology* 23: 723-745
- Zee O.P., Kim D.K., Choi S.U., Lee C.O., Lee K.R. (1999). A new cytotoxic acyclic diterpene from *Carpesium divaricatum*. *Archives of Pharmacal Research* 22: 225-227

# Chapter 4

## Biomimetic oxidation and its application to selected natural products and their analogues

### Abstract

In the drug discovery and development process, drug metabolism studies have been established as a necessity early in the process in order to predict the pharmacokinetics and metabolic processes a potential drug may undergo. With this in mind, biomimetic oxidation models mimicking cytochrome P450 oxidative processes were developed in this chapter using the non-steroidal anti-inflammatory drugs such as phenylbutazone and acetanilide as model substrates.

The developed biomimetic oxidations were applied to a selected number of natural products with known biological activity and successful oxidation was achieved with lapachol and sargahydroquinoic acid. The oxidation of sargahydroquinoic acid (**4.20**) yielded sargaquinoic acid (**4.32**), an active metabolite with cytotoxic and antioxidant activity, while lapachol (**4.21**) yielded three naphthoquinone derivatives. Of importance was the dehydro- $\alpha$ -lapachone (**4.33**), a metabolite isolated from *in vivo* drug metabolism animal models of lapachol, thus alluding to the potential of biomimetic oxidation models in predicting the *in vivo* metabolism of drug molecules.

# Chapter 4

## Biomimetic oxidation and its application to selected natural products and their analogues

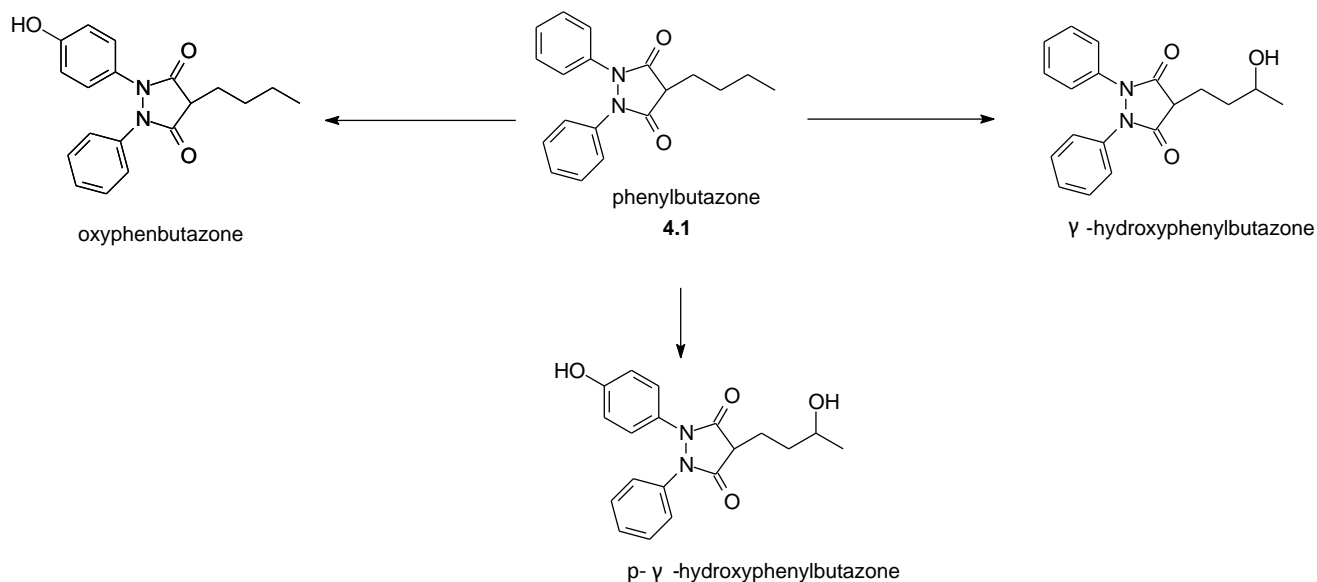
### 4.1 General introduction

In this chapter we explored the application of metalloporphyrins in the oxidation of selected natural products isolated in our research group. Metalloporphyrins have been shown to be a versatile catalyst for the assessment of *in vitro* drug metabolism of a variety of medicinally important and biologically active compounds (Lohmann and Karst, 2008; MacLeod *et al.*, 2008). Non-steroidal anti-inflammatory drugs (NSAIDs) have been studied extensively and their drug metabolites are well known (Balogh and Keserű, 2004; Othman *et al.*, 2000). This drug class is metabolized mainly *via* extensive oxidation in hepatic drug transformation (Nakajima *et al.*, 1998). As a result, NSAIDs are deemed to be the most suitable to study *in vitro* phase I drug metabolism. It is on this basis that they were chosen as suitable model compounds to develop and optimize methods for biomimetic oxidation. For the purpose of this research, the focus was on the following NSAIDs: phenylbutazone (**4.1**), ibuprofen (**4.2**), indomethacin (**4.3**) and acetanilide (**4.4**).

#### Phenylbutazone

Phenylbutazone (**4.1**) was first introduced in the 1950s as an anti-inflammatory drug, in the short term, and chronic management of various forms of arthritis. It is a highly metabolized drug molecule with only about 1% of the drug excreted in urine unchanged (Lees and Toutain, 2012). Oxyphenbutazone,  $\gamma$ -hydroxyphenylbutazone and p- $\gamma$ -dihydroxyphenylbutazone are some of the metabolites produced in its metabolism in the

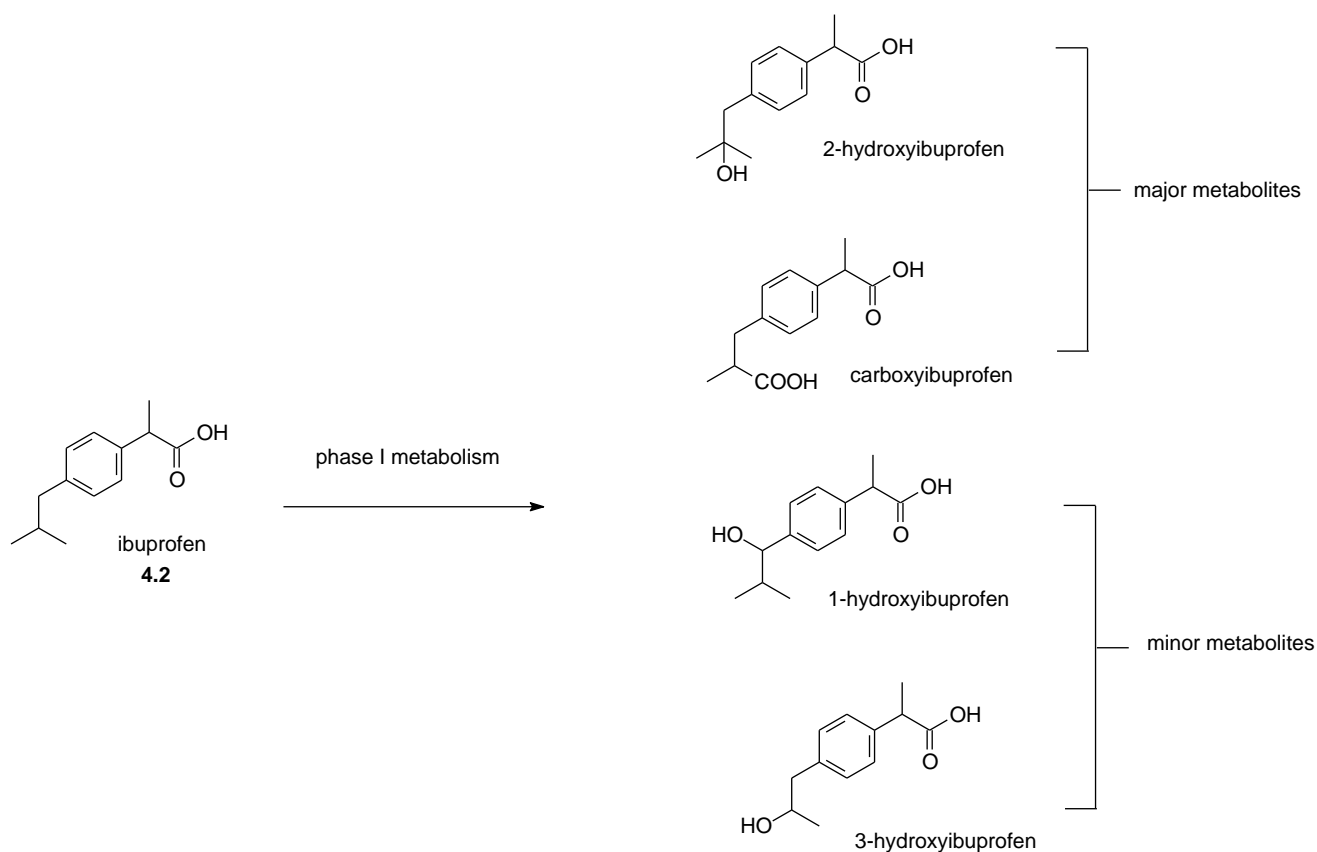
body, with oxyphenbutazone and  $\gamma$ -hydroxyphenylbutazone being the most predominant phase I metabolites with biological activity (Dieterle *et al.*, 1976; Lees and Toutain, 2012). Scheme 4.1 below illustrates phase I metabolism of phenylbutazone in the human body.



**Scheme 4.1** Phase I metabolites of phenylbutazone (**4.1**) (Adapted from Dieterle *et al.*, 1976)

## Ibuprofen

Ibuprofen (**4.2**) is metabolized mainly via phase I metabolism to produce a number of metabolites which are ultimately excreted from the human body in urine as glucuronide conjugates (Kepp *et al.*, 1997; Neunzig *et al.*, 2012). The two major metabolites formed in the human body are 2-hydroxyibuprofen and carboxyibuprofen, whilst 1-hydroxyibuprofen and 3-hydroxyibuprofen are minor metabolites (Kepp *et al.*, 1997; Neunzig *et al.*, 2012). The overall phase I metabolism of ibuprofen has been summarised in Scheme 4.2.



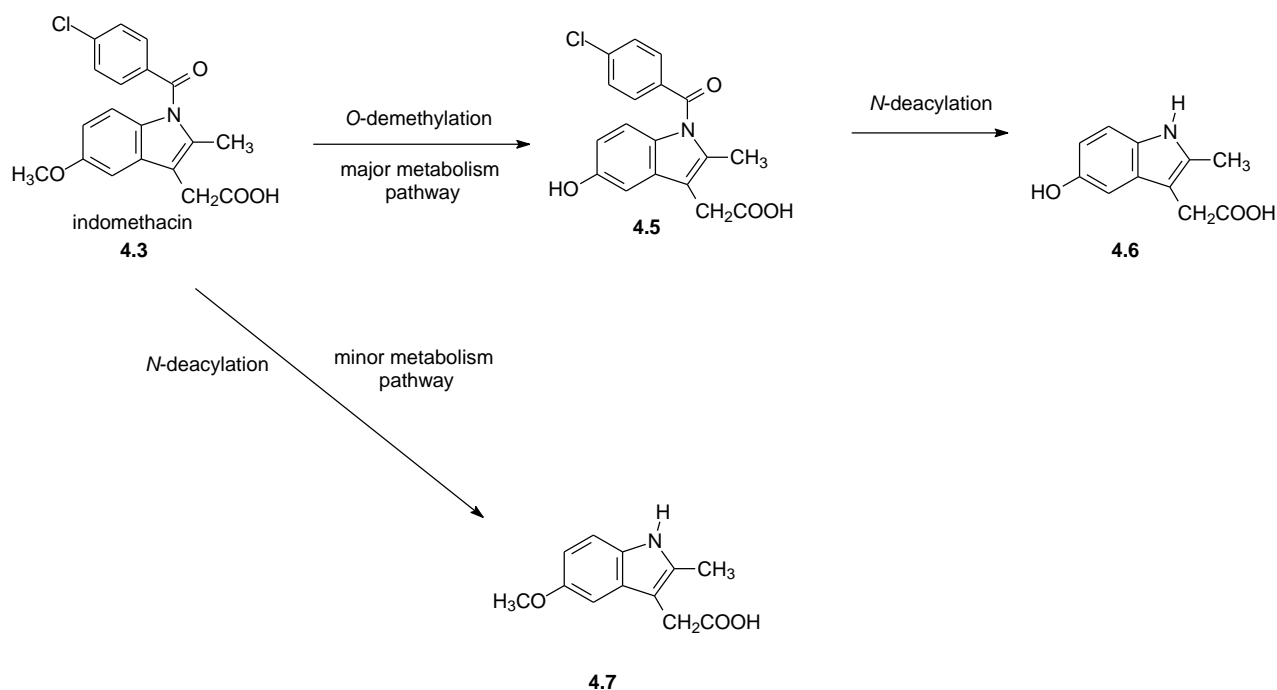
**Scheme 4.2** Phase I metabolism of ibuprofen (4.2)

(Adapted from Kepp *et al.*, 1997; Neunzig *et al.*, 2012)

## Indomethacin

Indomethacin (4.3) is a widely used anti-inflammatory drug which has mainly been used in treating arthritic conditions such as rheumatoid arthritis (Nakajima *et al.*, 1998; Rimmel *et al.*, 2004). Indomethacin undergoes *O*-demethylation to form its main metabolite *O*-desmethyindomethacin (4.5), an inactive metabolite which is conjugated with glucuronic acid and eliminated in urine (Duggan *et al.*, 1972; Nakajima *et al.*, 1998). *N*-deacylation of *O*-desmethyindomethacin also occurs as part of the major metabolism pathway to form *O*-desmethyl-*N*-deschlorobenzoylindomethacin (4.6), whilst direct *N*-deacylation of indomethacin constitutes its minor metabolism pathway to form *N*-

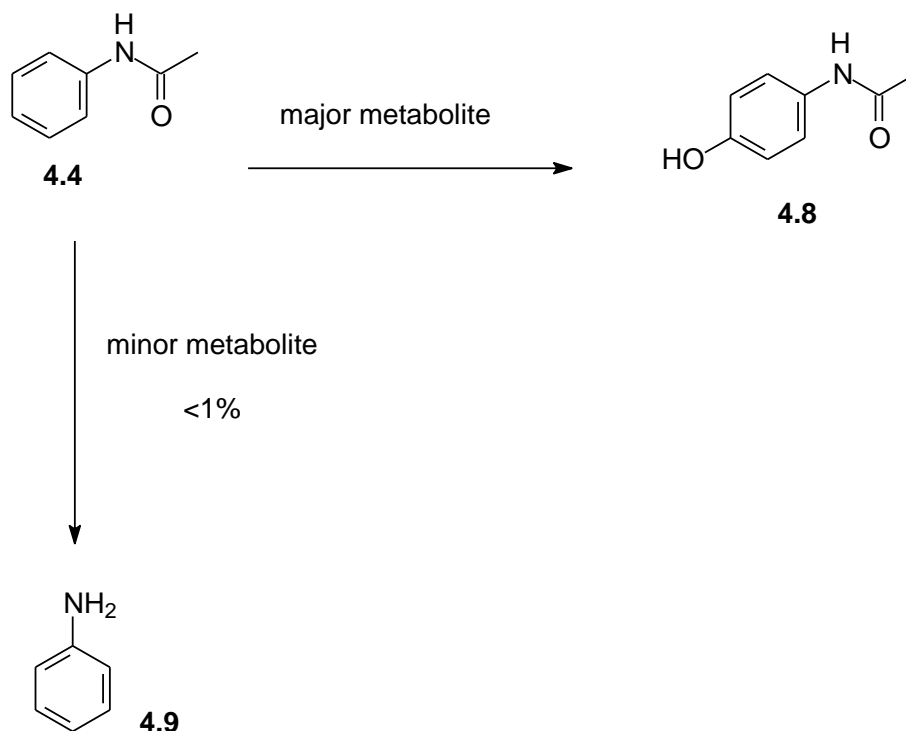
deschlorobenzoylindomethacin (**4.7**) (Duggan *et al.*, 1972; Nakajima *et al.*, 1998). The phase I metabolism of indomethacin has been illustrated in Scheme 4.3 below.



**Scheme 4.3** Phase I metabolism of indomethacin (**4.1**) (Adapted from Nakajima *et al.*, 1998)

### Acetanilide

In the human body, acetanilide is metabolized via two routes. The major metabolic route involves para-hydroxylation of acetanilide to form acetaminophen (**4.8**), the active metabolite with anti-pyretic activity. Acetaminophen is eliminated by conjugation with glucuronic acid. In a minor metabolism route, deacetylation of acetanilide occurs to form aniline (**4.9**) with no activity (Atkinson and Markey, 2012) (Scheme 4.4).



**Scheme 4.4** Phase I metabolism of acetanilide (**4.4**) (Adapted from Atkinson and Markey, 2012)

#### 4.1.1 Models for biomimetic oxidation

Metalloporphyrins have been used for more than 20 years in understanding the functional groups of drug molecules most susceptible to metabolism as well as in understanding their *in vivo* metabolism processes (Gotardo *et al.*, 2006). In this chapter, two biomimetic oxidation models were developed and optimized in the oxidation of NSAIDs as model compounds and selected natural products.

##### Biomimetic oxidation model (catalyst-hydrogen peroxide)

The model was adapted from Segrestaa *et al.*, 2002 and involved the oxidation of phenylbutazone and ibuprofen in the presence of a second generation lipophilic catalyst manganese (III) tetrakis-(2,6-dichlorophenyl) porphyrin (Mn(TDCPP)Cl (**4.10**) (Figure 4.1), imidazole as the co-catalyst and hydrogen peroxide (30% v/v) (H<sub>2</sub>O<sub>2</sub>) as a single oxygen donor at room temperature. In this reaction, formic acid was added to improve the oxidation



efficiency of the substrate. Throughout this chapter, this biomimetic oxidation model shall be referred to as catalyst-H<sub>2</sub>O<sub>2</sub> where ‘catalyst’ is replaced by the abbreviated name of the metalloporphyrin catalyst used.

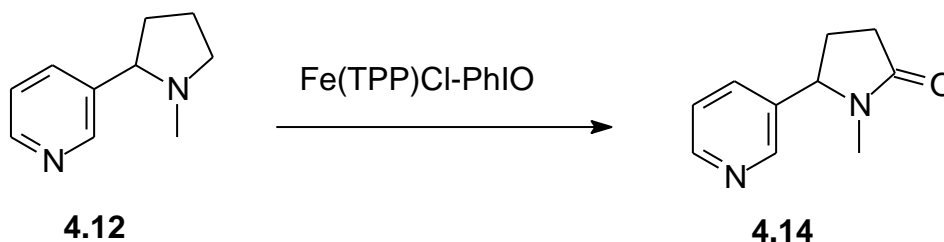
### **Biomimetic oxidation model (catalyst-iodosobenzene diacetate)**

This biomimetic model involved the use of an efficient oxygen donor iodosylbenzene (PhIO), derived from iodobenzene diacetate (PhIO(Ac)<sub>2</sub>) in the presence of a metalloporphyrin catalyst. The biomimetic model was adapted from In *et al.*, (2003), where iodobenzene diacetate was used as an efficient oxygen donor in the oxidation of olefins and alkanes, this time in the presence of an iron (III) metalloporphyrin iron *meso*-tetrakis(pentafluorophenyl)porphyrinato chloride (Fe(TPFPP)Cl) (**4.11**) (Figure 4.1) at room temperature. In these reactions, iodobenzene diacetate was hydrolysed to form iodosylbenzene *in situ*, the terminal oxidant. The hydrolysis of iodobenzene diacetate was preferred over iodosylbenzene because it is soluble in organic solvents and additionally the potential to explode at room temperature conditions was eliminated (In *et al.*, 2003; Stang and Zhdankin, 1996). In this model by In *et al.*, (2003), two different concentrations of iodobenzene diacetate were used for the olefin epoxidation reactions and alkane hydroxylation. These were 0.3 mmol and 0.05 mmol, were respectively added to 1:200 catalyst to substrate ratio in a reaction medium. Throughout this chapter, this biomimetic oxidation model shall be referred to as catalyst-PhIO(Ac)<sub>2</sub> where catalyst is replaced by the abbreviated name of the metalloporphyrin catalyst used.

### **4.1.2 Success of the biomimetic models in mimicking *in vivo* drug metabolism**

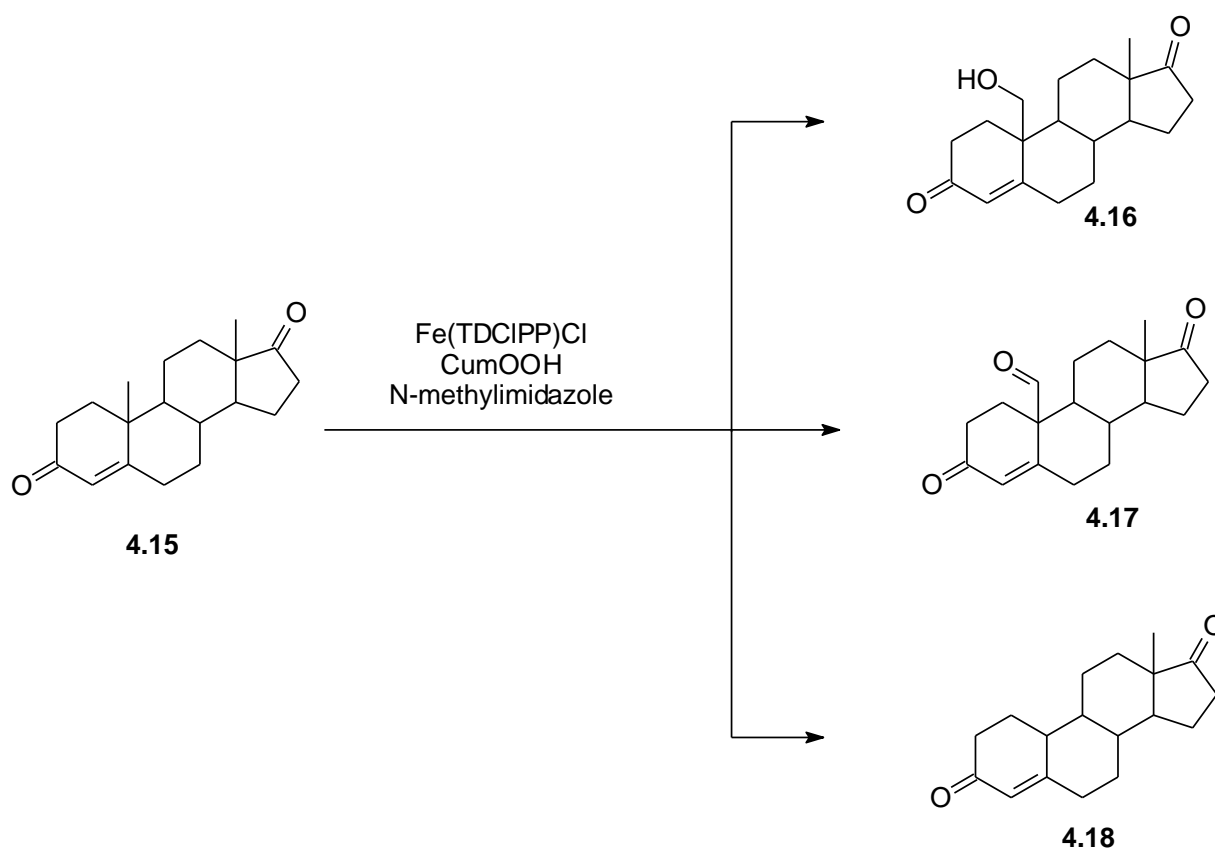
The importance of using biomimetic models in drug metabolism studies is to determine any possible metabolites of potential drug molecules and to isolate them in large quantities to facilitate toxicological, histopathologic, and pathologic or genotoxic testing (Chorgade *et al.*, 1996). Some biomimetic studies have produced unique metabolites, whilst other studies have managed to produce metabolites which have been isolated in human metabolism studies. For example, the oxidation of nicotine (**4.12**) in the presence of the *meso*-tetraphenylporphyrin iron (III) chloride (Fe(TPP)Cl) catalyst (**4.13**) (Figure 4.1) and PhIO, i.e. Fe(TPP)Cl-PhIO

produced cotinine (**4.14**), a major *in vivo* metabolite of nicotine produced in humans (Scheme 4.5) (Balogh and Keserű, 2004).



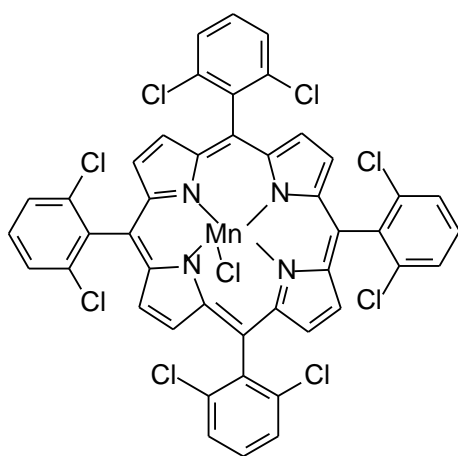
**Scheme 4.5** Biomimetic oxidation of nicotine (Balogh and Keserű, 2004)

Another example where biomimetic oxidation products have been translated into *in vivo* metabolism products is the oxidation of androst-4-en-3,17-dione (**4.15**). This androgen undergoes biotransformation in the presence of microsomal cytochrome P450 aromatase, a member of the monooxygenase family of heme enzymes to produce: 19-hydroxyandrost-4-en-3,17-dione (**4.16**), androst-4-en-3,17,19-trione (**4.17**) and estrone (**4.18**) (estrogens) (Vijayarahavan and Chauhan, 1990; Balough and Keserű, 2004). The same metabolites **4.16**, **4.17** and **4.18** were isolated when androst-4-en-3,17-dione was oxidized by the metalloporphyrin iron (III) tetrakis-(2,6-dichlorophenyl) porphyrin Fe(TDCIPP)Cl (**4.19**) (Figure 4.1) and CumOOH in the presence of N-methylimidazole (Scheme 4.6) (Vijayarahavan and Chauhan, 1990; Balough and Keserű, 2004).

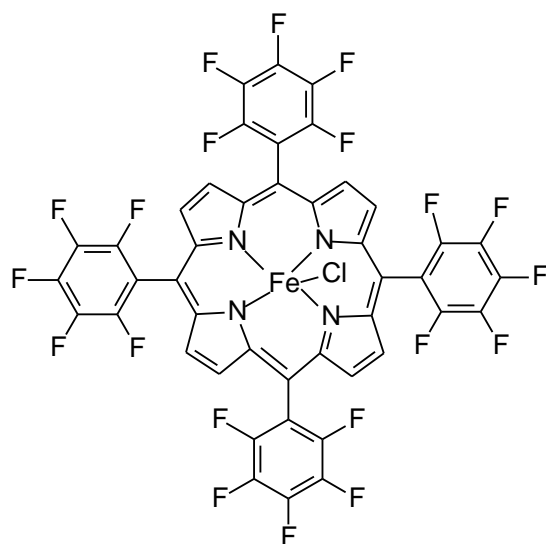


**Scheme 4.6** Biomimetic biotransformation of androst-4-en-3,17-dione (**4.15**) (Vijayarahavan and Chauhan, 1990; Balough and Keserü, 2004)

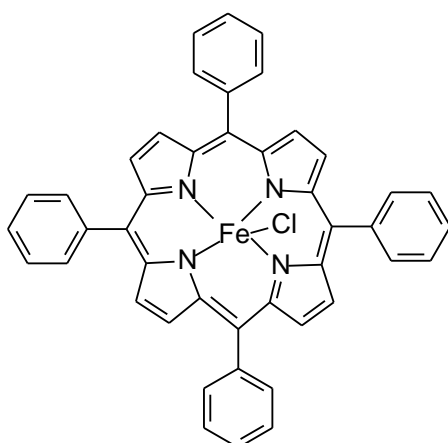
The above discussion clearly indicates the potential of biomimetic metabolism studies during drug development. These studies generate potential drug metabolites in sufficient quantities enabling assessment of their activity, toxicity and potential contribution to the side-effect profile of a potential new drug. In addition, when applied to new natural products, these studies are capable of generating new “natural product-like” chemical entities that can also be part of the studies in drug discovery and development.



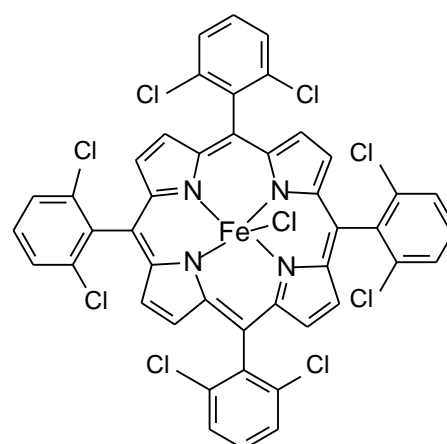
Mn(TDCIPP)Cl

**4.10**

Fe(TPFPP)Cl

**4.11**

Fe(TPP)Cl

**4.13**

Fe(TDCIPP)Cl

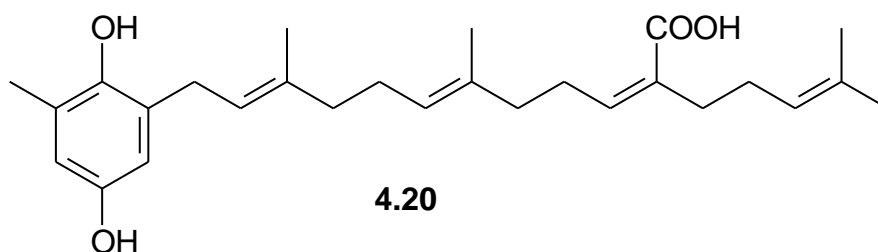
**4.19****Figure 4.1** The most common metalloporphyrins used in biomimetic oxidation studies

### 4.1.3 Natural products selected for biomimetic studies

The natural products that were available in sufficient quantity for biomimetic studies were: sargahydroquinolic acid (**4.20**), sargaquinolic acid, sargachromenol, fucoxanthin, lapachol (**4.21**), sclareol, cinnamic acid and cholesterol.

#### Sargahydroquinolic acid

Sargahydroquinolic acid (**4.20**) is a prenylated quinone-type secondary metabolite which has been isolated from the *Sargassum* species of brown algae (Kim *et al.*, 2008; Kim *et al.*, 2011).

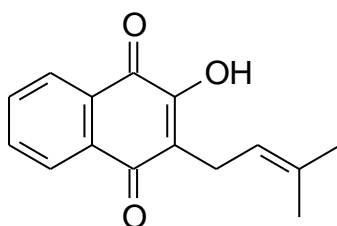


Sargahydroquinolic acid has shown antioxidant activity, moderate antimalarial activity, as well as an ability to induce peroxisome proliferator activator receptor (PPAR $\alpha/\gamma$ ) activity which has been implicated in the treatment of metabolic disorders such as diabetes mellitus (Afolayan *et al.*, 2008; Kim *et al.*, 2008; Kim *et al.*, 2011).

#### Lapachol

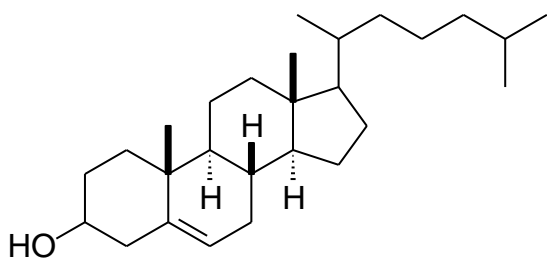
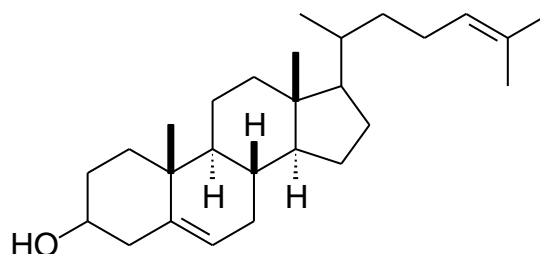
Lapachol (**4.21**) is a naphthoquinone natural product which has been mainly isolated from the *Tabebuia* plant species of the family Bignoniaceae (Niehues *et al.*, 2012). Lapachol has been shown to possess many biological activities which include trypanocidal, antimalarial and cytotoxic activities (de Almeida, 2009; Niehues *et al.*, 2012). Lapachol reached early clinical studies as an anti-cancer agent due to its ability to induce oxidative stress, as well as its ability to carry out the alkylation of cell nucleophiles. However, its progress to market was impeded by the toxic side effects of its metabolites at therapeutic doses. Lapachol's success

was also limited by its low serum concentration following administration of a therapeutic dose (Niehues *et al.*, 2012).

**4.21**

### Cholesterol

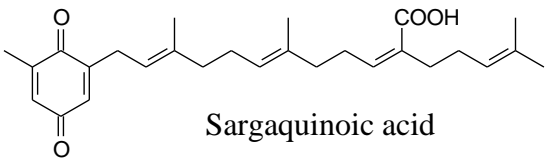
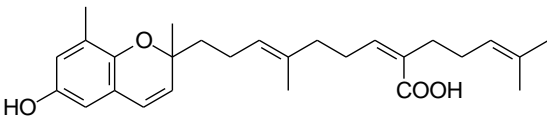
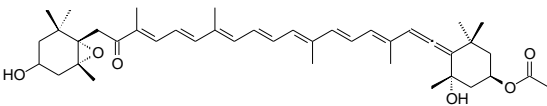
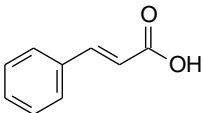
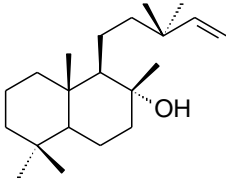
Cholesterol (**4.22**) is an animal sterol but it has been isolated from the green alga *Ulva lactuca*. It has been isolated together with cholesta-5,24 (25)-dien-3 $\beta$ -ol (**4.23**), a precursor for cholesterol (Kanazawa *et al.*, 1972; Kapetanovic *et al.*, 2005; Zivanovic, 2012).

**4.22****4.23**

Cholesterol is an important component of the lipid bilayer of the biological membrane. It acts as a structural scaffold for steroids and steroidal hormones within the human body and it is important in the formation of bile salts. Humans obtain cholesterol mainly from the diet and from biogenesis (Valenzuela *et al.*, 2003).

A summary of the other natural products pertinent to this research has been given in Table 4.1 below.

Table 4.1 Summary of natural products

Natural product	Source	Biological activity	Reference
 <p>Sargaquinoic acid</p>	Synthetic analogue of sargahydroquinoic acid	Antidiabetic activity, regulation of adipogenesis	Kim <i>et al.</i> , 2008
 <p>Sargachromenol</p>	Synthetic analogue of sargahydroquinoic acid	Anti-inflammatory activity	Kim <i>et al.</i> , 2014
 <p>Fucoxanthin</p>	<i>Sargassum incisifolium</i>	Antioxidant, anti-diabetic, anti-obesity, anticancer activities	Peng <i>et al.</i> , 2011
 <p>Cinnamic acid</p>	Chinese rhubarb <i>Rheum officinale</i>	Potential anticancer activity	Liu <i>et al.</i> , 1995
 <p>Sclareol</p>	Plant <i>Salvia sclarea</i>	Antifungal and antimicrobial activities	Bombarda <i>et al.</i> , 1997

#### 4.1.4 Chapter Aims and Objectives

Natural products research has resulted in the identification of promising molecules with interesting chemistry which can combat many disease states such as cancer and malaria. In a drug discovery and development process, metabolism studies have become one of the first studies carried out in the process in order to evaluate the therapeutic efficacy of a new drug molecule. Therefore, this chapter has been divided into two sections. The first section deals with the development of two biomimetic oxidation models which act as chemical *in vitro* drug metabolism models. The second section focuses on the oxidative drug metabolism reactions (using the developed biomimetic oxidation models with metalloporphyrins as biomimetic catalysts) of a selected range of natural products with therapeutic importance and the potential metabolites that can be obtained from the oxidation process.

#### **Objectives:**

1. To develop simple biomimetic oxidation models using the NSAIDs such as acetanilide and phenylbutazone.
2. To apply the developed biomimetic oxidation systems to a few selected natural products of therapeutic importance.

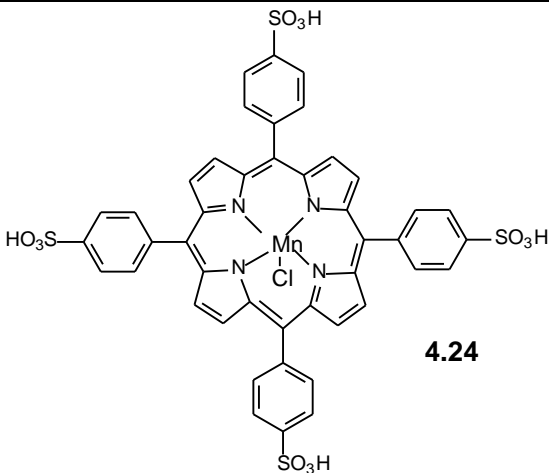
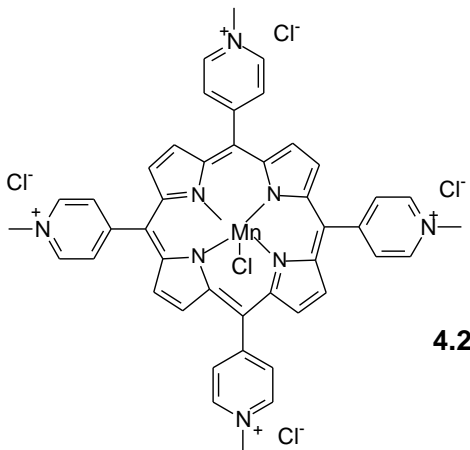


## 4.2 Results and Discussion

### 4.2.1 Biomimetic oxidation models

Biomimetic drug metabolism models were developed in the oxidation of selected NSAIDs and success was achieved with, phenylbutazone (**4.1**) and acetanilide (**4.4**) in the presence of two water soluble catalysts 5,10,15,20-Tetrakis(4-sulfonatophenyl)-21H,23H-porphine manganese (III) chloride (MnTPPs) (**4.24**) and Manganese (III) 5,10,15,20-tetra(4-pyridyl)-21H,23H-porphine chloride tetrakis methochloride (MnPYP) (**4.25**) (Table 4.2). The two biomimetic drug metabolism models employed were either: 1) catalyst-H<sub>2</sub>O<sub>2</sub> or 2) catalyst-PhIO(Ac)<sub>2</sub>.

**Table 4.2** Metalloporphyrins used in biomimetic oxidation models

Catalyst name	Structure
5,10,15,20-Tetrakis(4-sulfonatophenyl)-21H,23H-porphine manganese (III) chloride (MnTPPs)	 <p style="text-align: right;"><b>4.24</b></p>
Manganese (III) 5,10,15,20-tetra(4-pyridyl)-21H,23H-porphine chloride tetrakis methochloride (MnPYP)	 <p style="text-align: right;"><b>4.25</b></p>

#### 4.2.1.1 Biomimetic oxidation of phenylbutazone (4.1)

Phenylbutazone was reacted with either catalyst-H<sub>2</sub>O<sub>2</sub> or catalyst-PhIO(Ac)<sub>2</sub> where the catalyst was MnTPPs (4.24) or MnPYP (4.25) and stirred for 4h and 30 min respectively. The reaction progress was followed by thin layer chromatography (TLC). After the 4h and 30 min reaction time for each reaction model, the aqueous medium was extracted with dichloromethane (DCM) and the DCM extract dried and analyzed by <sup>1</sup>H-NMR spectroscopy. Figure 4.2 shows the <sup>1</sup>H-NMR spectra for the starting material and reaction product (4.26).

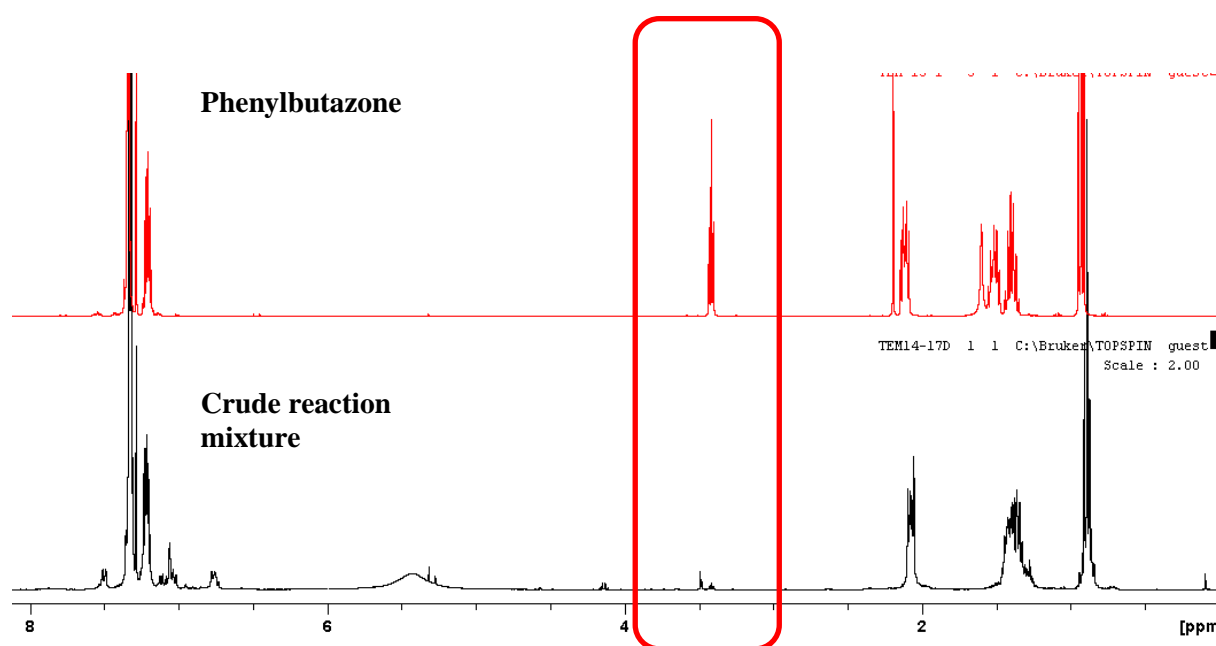


**Figure 4.2** <sup>1</sup>H-NMR (400MHz, CDCl<sub>3</sub>) spectrum of phenylbutazone (4.1) and reaction product of phenylbutazone containing compound 4.26

The <sup>1</sup>H-NMR spectra of the oxidation product of phenylbutazone showed important spectral features which suggested oxidation at the C-4 position. The spectrum of the crude reaction mixture included signals at  $\delta$  0.88 (3H, t,  $J$  = 7.2 Hz),  $\delta$  1.36 (2x CH<sub>2</sub>, m),  $\delta$  2.07 (CH<sub>2</sub>, t,  $J$  = 7.3 Hz),  $\delta$  3.48 (CH, s), and the aromatic signals at  $\delta$  7.21-7.35 (10H, m, 2x phenyl). Formation of a hydroxyl group on position 4 was revealed by the presence of a singlet at  $\delta$  3.48. However, a small amount of the phenylbutazone was still found to be present in the reaction product (4.26) as seen by the methine triplet of the pyrazolidine ring at  $\delta$  3.41. In addition, a change in the multiplicity for the methylene protons at  $\delta$  2.11 from a multiplet to a triplet at  $\delta$  2.07 also suggested the formation of the hydroxyl moiety.

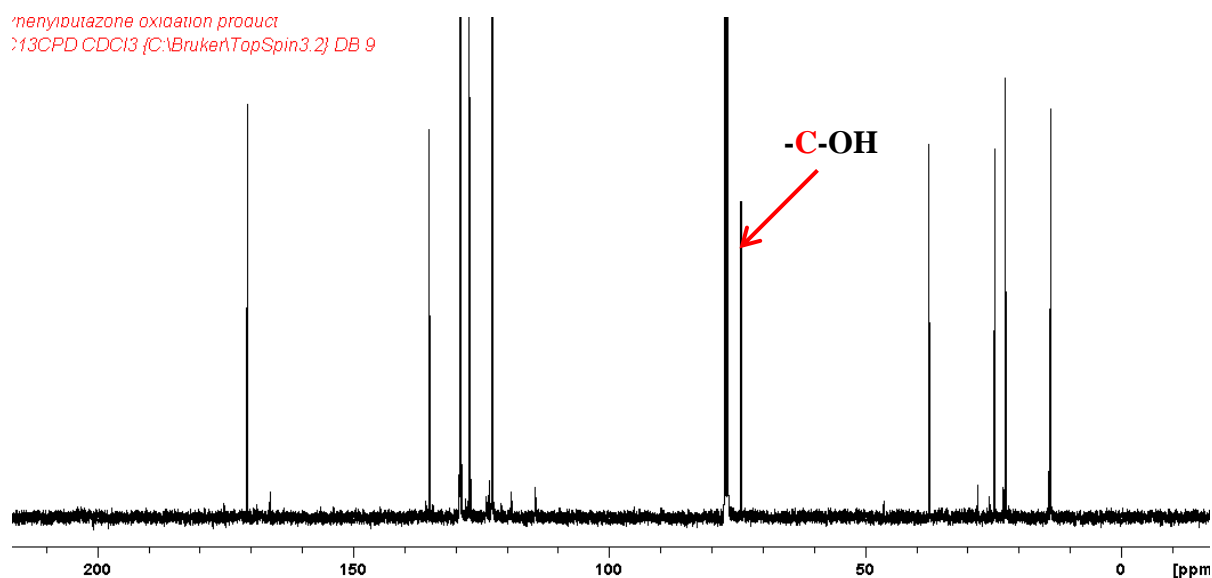


**Figure 4.3**  $^{13}\text{C}$ -NMR (100 MHz,  $\text{CDCl}_3$ ) spectrum of compound **4.26**

The  $^{13}\text{C}$ -NMR (100 MHz,  $\text{CDCl}_3$ ) (Figure 4.3) of **4.26** revealed the presence of 10 carbon signals: the carbonyl signals in the pyrazolidine ring are represented by a signal at  $\delta$  170.7, the olefin methine and quaternary carbon signals in the phenyl ring were present at  $\delta$  135.3, 129.3, 127.5, 123.0, the oxygenated methine carbon was found to reside at  $\delta$  74.2, three methylene carbon signals for the butyl chain were observed at  $\delta$  37.4, 24.7, 22.5 and lastly the methyl carbon of the butyl chain at  $\delta$  14.0. All  $^1\text{H}$  and  $^{13}\text{C}$ -NMR data were consistent with literature values and assisted in identifying the reaction product as 4-hydroxy-4-*n*-butyl-1,2-diphenylpyrazolidine-3,5-dione (**4.26**) (Segrestaa *et al.*, 2002; Chauhan *et al.*, 1999).

Two-dimensional NMR analyses (HMBC, HSQC, and COSY) of **4.26** were also carried out to determine the structure of the hydroxyl metabolite of phenylbutazone. These values were compared with the data for phenylbutazone (**4.1**) itself (Table 4.3). Figure 4.4 shows some of the key HMBC correlations identified in determining structure of **4.26**.

**Table 4.3** Comparison of **4.1** and **4.26**  $^1\text{H}$ -NMR (400 MHz,  $\text{CDCl}_3$ ) and  $^{13}\text{C}$ -NMR (100MHz,  $\text{CDCl}_3$ ) and 2D NMR ( $^1\text{H}$ - $^1\text{H}$  COSY and HMBC) spectroscopic data for compound **4.26**

	<b>4.1</b>			<b>4.26</b>				
<b>Carbon no</b>	$\delta_{\text{C}}$	$\delta_{\text{C}}$ <b>multi</b>	$\delta_{\text{H}}$ ( <b>multi, J=</b> <b>Hz)</b>	$\delta_{\text{C}}$	$\delta_{\text{H}}$ ( <b>multi, J=</b> <b>Hz)</b>	<b>Observed</b> <b>COSY</b>	<b>Observed</b> <b>HMBC</b>	
<b>3</b>	170.5	C	-	170.7	-			
<b>4</b>	46.1	CH	3.41 (t, 5.7)	74.2	3.48 (s)	H-6		
<b>5</b>	170.5	C	-	170.7	-			
<b>6</b>	27.94	CH <sub>2</sub>	2.11 (m)	37.7	2.07 (t, 7.1)	H-4	C-9,C-4,C-5,C-3	
<b>7</b>	27.91	CH <sub>2</sub>	1.39 (m)	24.7	1.30-1.45 (m)	H-8	C-8,C-9	
<b>8</b>	22.7	CH <sub>2</sub>	1.50 (m)	22.7		H-7, H-9		
<b>9</b>	13.8	CH <sub>3</sub>	0.93 (t, 7.3 )	13.8	0.88 (t, 7.2)	H-8		
<b>10</b>	136.0	C	-	135.5	-			
<b>11</b>	122.8	CH	7.31-7.34 (m)	123.0	7.29-7.75 (m)			
<b>12</b>	129.3	CH		129.6				
<b>13</b>	127.0	CH	7.20 (m)	127.5	7.21 (m)			

Assignments completed based on the COSY, HMBC and HSQC correlations observed

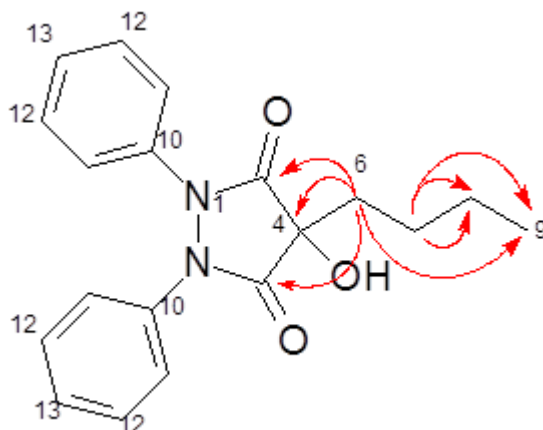


**Figure 4.4** Key HMBC correlations for compound **4.26**

Control oxidation reactions for phenylbutazone were carried out. Each reaction model (catalyst- $\text{H}_2\text{O}_2$  and catalyst- $\text{PhIO}(\text{Ac})_2$ ) had two controls: one in the absence of metalloporphyrin catalyst (referred to as control 1) and the other in the absence of the oxidant (referred to as control 2). The control reactions also revealed the presence of the 4-hydroxy metabolite of phenylbutazone (**4.26**). However the metabolite was isolated in smaller yields when metalloporphyrin catalyst was omitted as opposed to the catalyzed reactions. The percentage conversion of phenylbutazone to **4.26** in Table 4.4 was determined by weighing the mass of the isolated product **4.26**. In Table 4.5, the percentage conversion of phenylbutazone to **4.26** was determined by assessing the  $^1\text{H-NMR}$  spectra of the crude reaction mixtures (i.e. by observing the absence of the methine signal at  $\delta$  3.41). Masses of crude reaction mixtures were not determined in cases where reaction products were not isolated.

**Table 4.4** Percentage conversion of phenylbutazone to **4.26** with biomimetic oxidation model catalyst-H<sub>2</sub>O<sub>2</sub>

% conversion of phenylbutazone to 4-hydroxy-4- <i>n</i> -butyl-1,2-diphenylpyrazolidine-3,5-dione			
Catalysts	Catalyzed reaction	Control reaction 1	Control reaction 2
MnTPPs ( <b>4.24</b> )	66	29	ND
MnPYP ( <b>4.25</b> )	64	ND	ND

ND= Not Determined

**Table 4.5** Percentage conversion of phenylbutazone to **4.26** with biomimetic oxidation model catalyst-PhIO(Ac)<sub>2</sub>

% conversion of phenylbutazone to 4-hydroxy-4- <i>n</i> -butyl-1,2-diphenylpyrazolidine-3,5-dione			
Catalysts	Catalyzed reaction	Control reaction 1	Control reaction 2
MnTPPs ( <b>4.24</b> )	100	100	ND
MnPYP ( <b>4.25</b> )	100	ND	ND

ND= Not Determined

Interestingly, the biomimetic oxidation of phenylbutazone to **4.26**, occurred in the absence of the oxidant but in the presence of the both catalysts (MnTPPs and MnPYP) (control 2). The <sup>1</sup>H-NMR spectra of the control reaction showed the disappearance of the triplet at δ 3.41 (t, *J* = 5.7 Hz). This was not expected in control 1 because the reactions were carried out in the absence of oxidant. The control experiments were carried out under normal atmospheric conditions; i.e. the reaction vials were not flushed with nitrogen to exclude the presence of molecular oxygen, which suggests that the methine proton is prone to oxidation even in the presence of molecular oxygen only, under biomimetic conditions. The biomimetic oxidation

system proceeded to completion in 4 hours, with complete oxidation of phenylbutazone to its hydroxyl metabolite (Figure 4.5).

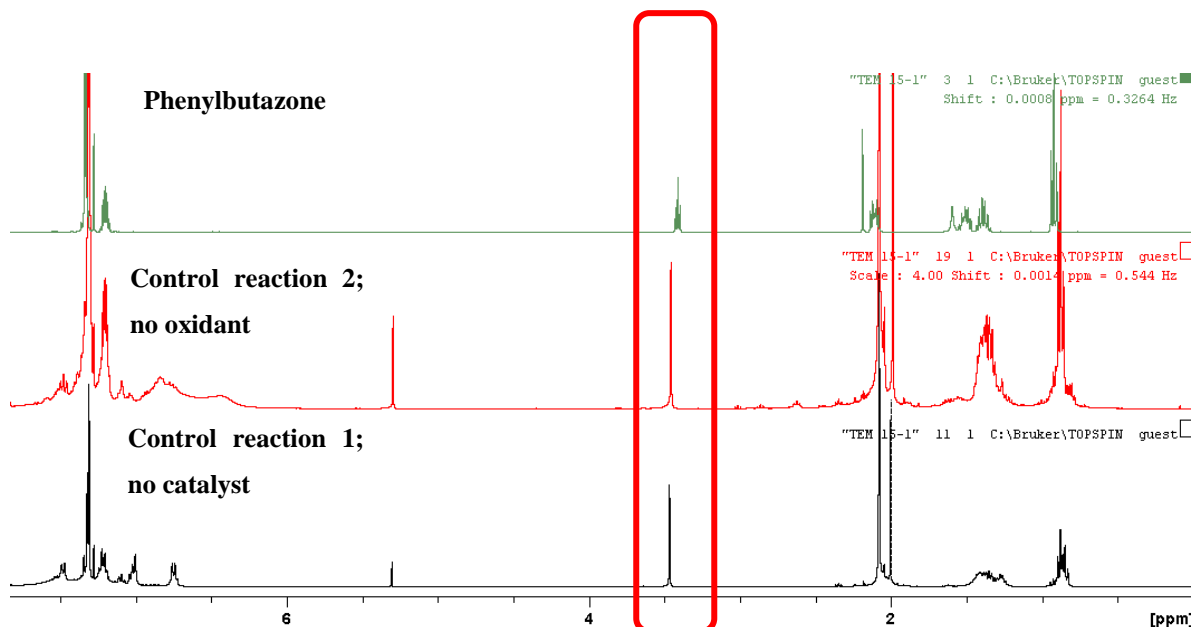


**Figure 4.5**  $^1\text{H-NMR}$  (400 MHz,  $\text{CDCl}_3$ ) spectra comparing control 1, control 2 and the starting material (catalyst- $\text{H}_2\text{O}_2$  model)

However, with the control reactions for the second model (catalyst- $\text{PhIO}(\text{Ac})_2$ ) control 2, where the reaction proceeded for 30 min, a reaction mixture containing both phenylbutazone and 4-hydroxy-4-*n*-butyl-1,2-diphenylpyrazolidine-3,5-dione was observed (Figure 4.6). This was probably due to a shorter reaction time. Therefore, it is possible that complete oxidation of phenylbutazone by molecular oxygen can be achieved if stirred in the presence of the catalyst for at least 4 hours.

The aromatic signals that are found with oxidation models in the presence of catalyst  $\text{PhIO}(\text{Ac})_2$  were unknown but were suspected to be by-products of the hydrolysis of iodobenzene diacetate as they do not resemble any of the known oxidation products of phenylbutazone (i.e. meta or para oxidation of the phenyl rings). Additional work would have to be carried out to identify these compounds.

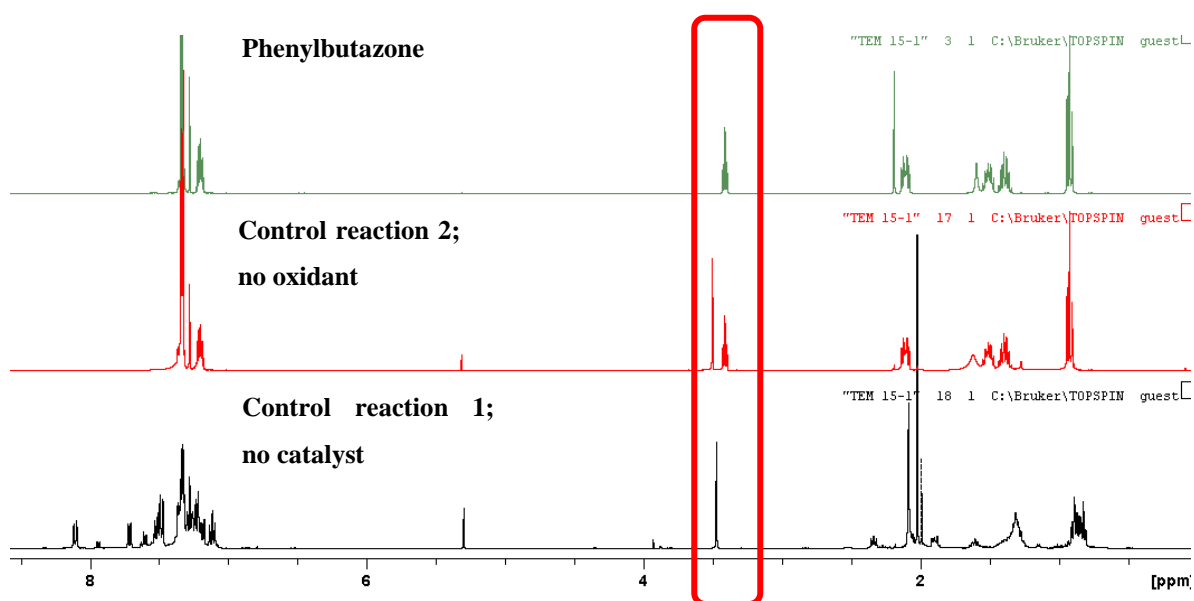


**Figure 4.6**  $^1\text{H-NMR}$  (400 MHz,  $\text{CDCl}_3$ ) spectra comparing control 1, control 2 and starting material (catalyst- $\text{PhIO}(\text{Ac})_2$  model)

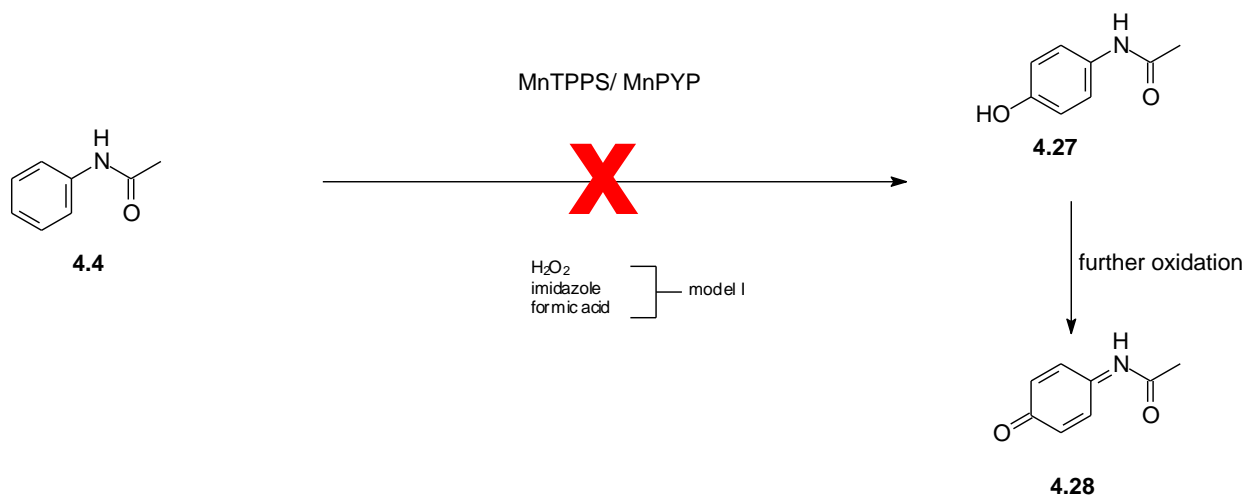
The *in vivo* metabolites of phenylbutazone (oxyphenbutazone and  $\gamma$ -hydroxyphenylbutazone) differ from the isolated product from the biomimetic oxidation of phenylbutazone. 4-hydroxy-4-*n*-butyl-1,2-diphenylpyrazolidine-3,5-dione has been tested as a possible immunosuppressant but the metabolite showed weak anti-cytokine activity suggesting that it is an inactive biomimetic metabolite of phenylbutazone.

#### 4.2.1.2 Biomimetic oxidation of acetanilide

##### Biomimetic oxidation of acetanilide using $\text{H}_2\text{O}_2$

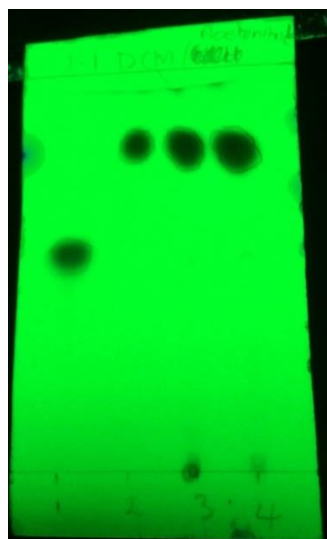
The biomimetic oxidation of acetanilide (**4.4**) was aimed at mimicking the metabolism of acetanilide taking place in humans. The oxidized products that were expected in these reactions were acetaminophen (**4.27**) as well as further oxidation of acetaminophen to the imino-quinone N-acetyl-p-benzoquinone imine (NAPQI) (**4.28**), a toxic metabolite which causes liver damage in humans (Atkinson and Markey, 2012) (Scheme 4.7).





**Scheme 4.7** Proposed oxidation of acetanilide using the biomimetic model catalyst- $\text{H}_2\text{O}_2$

However, oxidation of acetanilide by  $\text{H}_2\text{O}_2$  in a biomimetic oxidation model did not yield any of the desired oxidized products for acetanilide after 4 hours. The completion of each reaction progress was monitored by TLC, where the reaction mixtures and the control reactions were compared to acetanilide and acetaminophen. TLC analyses confirmed the presence of the starting material in each of the reactions after a four hour reaction time (Figure 4.7).



TLC elution solvent:  
 $\text{CH}_2\text{Cl}_2/\text{Acetonitrile}$  (1:1)

1= Acetaminophen  
 2= Acetanilide  
 3=Reaction mixture  
 4=Control Reaction (no catalyst)

**Figure 4.7** TLC assessment of reaction of acetanilide using catalyst- $\text{H}_2\text{O}_2$  biomimetic oxidation model

**Biomimetic oxidation of acetanilide using PhIO(Ac)<sub>2</sub>**

Acetanilide (**4.4**) was oxidized using iodobenzene diacetate (PhIO(Ac)<sub>2</sub>) at the concentration used for olefin epoxidation (In *et al.*, 2003) to yield a complex reaction mixture which was analyzed by NMR spectroscopic methods.

The <sup>1</sup>H-NMR spectra of the oxidation product of acetanilide revealed the presence of starting material ( $\delta$  2.19 (3H, s),  $\delta$  7.06 (t,  $J$ = 7.3 Hz),  $\delta$  7.33 (t,  $J$ = 7.9 Hz),  $\delta$  7.56 (d,  $J$ = 7.9 Hz)) and a singlet at  $\delta$  6.80 which suggested the presence of 1,4-benzoquinone (BQ) (**4.29**) (Figure 4.8). <sup>1</sup>H-NMR data was consistent with the literature value for 1,4-benzoquinone (Tedeschi and Rezende, 2009).

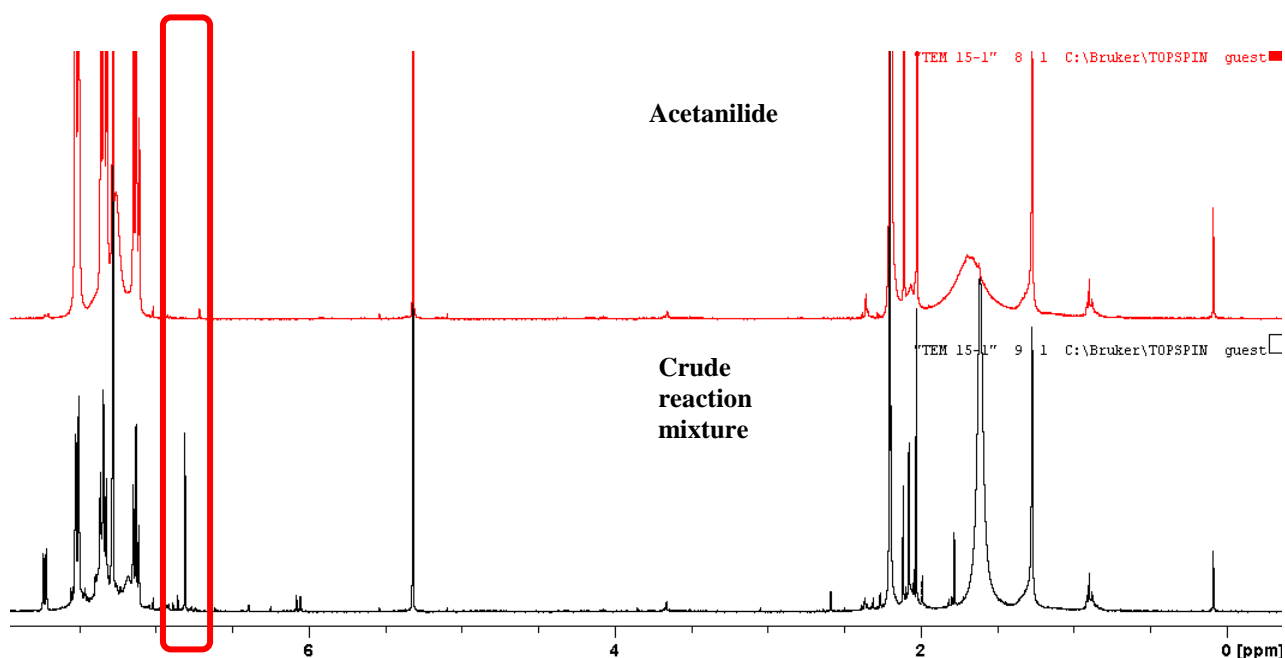


**Figure 4.8** <sup>1</sup>H-NMR (400 MHz, CDCl<sub>3</sub>) spectra of the starting material (**4.4**) and crude reaction mixture

HSQC correlations proved useful in determining the composition of the crude mixture composition. The methine singlet at  $\delta$  6.80 correlated to a methine carbon at  $\delta$  136.6, typically associated with a methine carbon in the benzoquinone ring. Typical proton-carbon correlations for acetanilide were also apparent in the HSQC spectrum. The following <sup>13</sup>C-

NMR (100 MHz,  $\text{CDCl}_3$ ) nuclei were deemed to belong to acetanilide including the methyl signal at  $\delta$  24.4 and three methine signals at  $\delta$  119.9, 122.0 and 129.5. However, the crude oxidation product contained the reaction by-product iodobenzene. The presence of iodobenzene was suspected to be denoted by the doublet signal in the  $^1\text{H}$ -NMR spectrum at  $\delta$  7.72 (d,  $J=7.9$ ), a consistent doublet observed in all oxidation reactions in the presence of  $\text{PhIO}(\text{Ac})_2$ . This doublet signal corresponded to the methine signal at  $\delta$  137.4 in the iodobenzene ring. Figure 4.9 below shows the HSQC spectrum for the crude oxidation product of acetanilide.

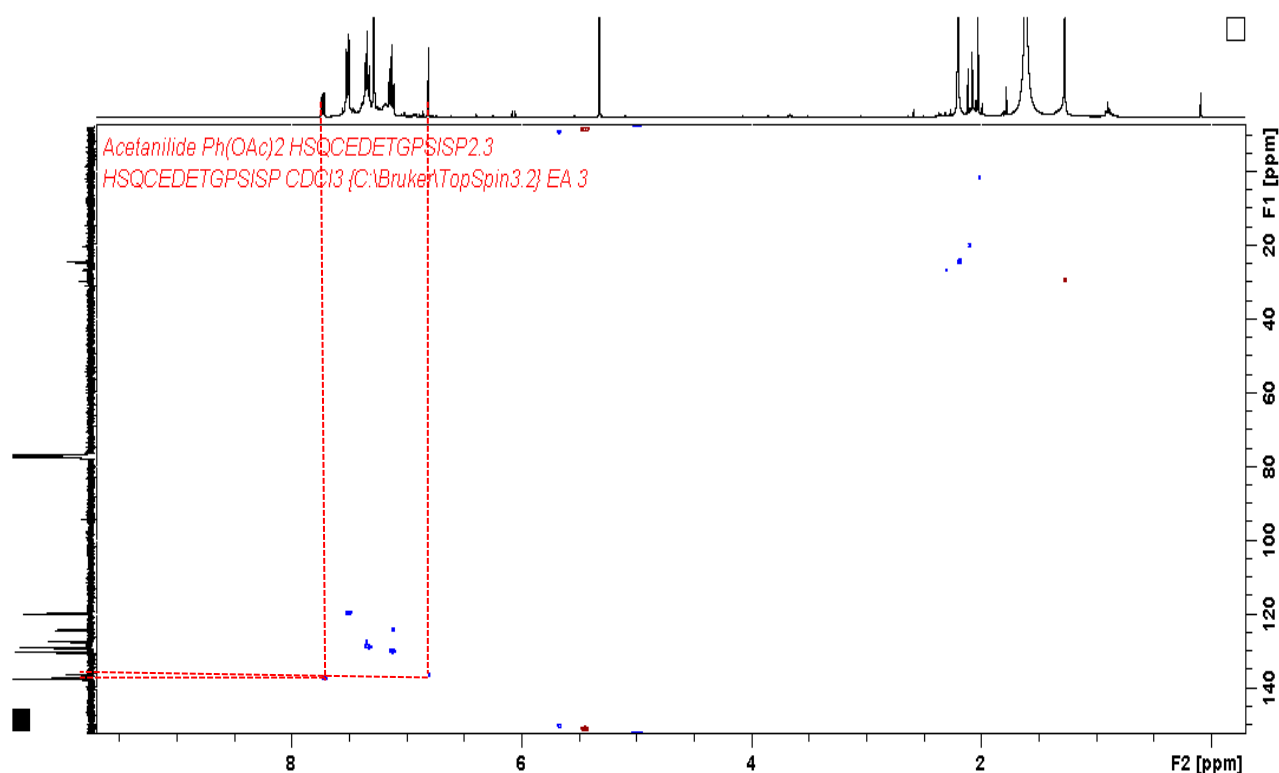
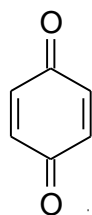
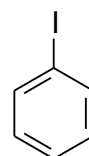


**Figure 4.9** HSQC spectrum of crude oxidation product of acetanilide biomimetic oxidation reaction highlighting some important correlations



4.29



iodobenzene

Acetanilide is less likely to be oxidized in a biomimetic oxidation reaction model due to the presence of the acetamide group on the para-position, a moderately activating group for electrophilic aromatic substitution (Fox and Whitesell, 2004). However the presence an efficient oxidant such as iodobenzene diacetate catalyzed by metalloporphyrin facilitated the oxidation of acetanilide to produce BQ. These products were not observed in the control reactions.

In summary, the selected metalloporphyrin catalysts used for carrying out biomimetic oxidation reactions were found to be suitable since the formation of highly reactive manganese (IV) oxo species responsible for substrate oxidation occurs. Both the catalysts MnTPPs and MnPYP contained electron withdrawing ligands (i.e. sulfonic acid and pyridyl moieties, respectively) on the porphyrin macrocycle which results in the high reactivity of the subsequent oxo species formed thus facilitating olefin epoxidation and alkane hydroxylation reactions (Goh and Nam, 1999; Jeong *et al.*, 2008; Lee *et al.*, 2009).

The use of single oxygen donors as terminal oxidants such as iodosylbenzene in biomimetic oxidation reactions is preferred since these do not facilitate the free radical side chain reactions associated with alkyl hydroperoxides and hydrogen peroxide. Free radical chain reactions have been shown to be the result of the weak O-H bonds in alkyl hydroperoxide which therefore diminish the efficiency of the oxidant as a result of the low turnover of the high valent oxo species of the metalloporphyrin. As a result, olefin epoxide and alkane hydroxyl product yields are low (De Faria *et al.*, 2011; Meunier, 1992; Mansuy *et al.*, 1989). However, alkyl hydroperoxides and hydrogen peroxide are more environmentally friendly as opposed to iodosylbenzene with water as the only by-product (De Faria *et al.*, 2011). Iodosylbenzene which was once a common oxidant used in the biomimetic oxidation models has seen diminished use due to its hazardous nature (De Faria *et al.*, 2011; Stang and Zhdankin, 1996). For this set of biomimetic oxidation models, iodobenzene diacetate was used in place of iodosylbenzene as it is less toxic and it was able to form the efficient oxidant iodosylbenzene *in situ* (In *et al.*, 2003). Overall, iodobenzene diacetate was the most efficient oxidant as it was efficient in the oxidation of both phenylbutazone and acetanilide in the biomimetic oxidation model whilst hydrogen peroxide is most environmentally friendly and closely resembles molecular oxygen.

### 4.2.1.3 Biomimetic oxidation of natural products

The biomimetic oxidation models MnTPPs-H<sub>2</sub>O<sub>2</sub> and MnTPPs-PhIO(Ac)<sub>2</sub> were applied to a selected number of natural products namely: sargahydroquinolic acid, sargaquinolic acid, sargachromenol, fucoxanthin, lapachol, cholesterol, cinnamic acid and sclareol. The main focus of this section is on the natural products that underwent conversion in both biomimetic oxidation models.

#### Biomimetic oxidation of sargahydroquinolic acid (4.20)

The biomimetic oxidation of sargahydroquinolic acid (SHQA) using both biomimetic oxidation models resulted in the oxidation of the hydroquinone moiety to form sargaquinolic acid (SQA) (4.30). The <sup>1</sup>H-NMR spectrum of sargahydroquinolic acid (4.20) (Figure 4.10) showed similarities to that of sargaquinolic acid (4.30) as expected, where the main difference is the proton signals attributed to the hydroquinone moiety; i.e. a change in multiplicity of the two doublets at  $\delta$  6.50 (d,  $J$ = 2.8 Hz) and  $\delta$  6.49 (d,  $J$ = 2.9 Hz) in 4.20 to two broad singlet signals at  $\delta$  6.56 and 6.48 in 4.30 respectively, was observed.

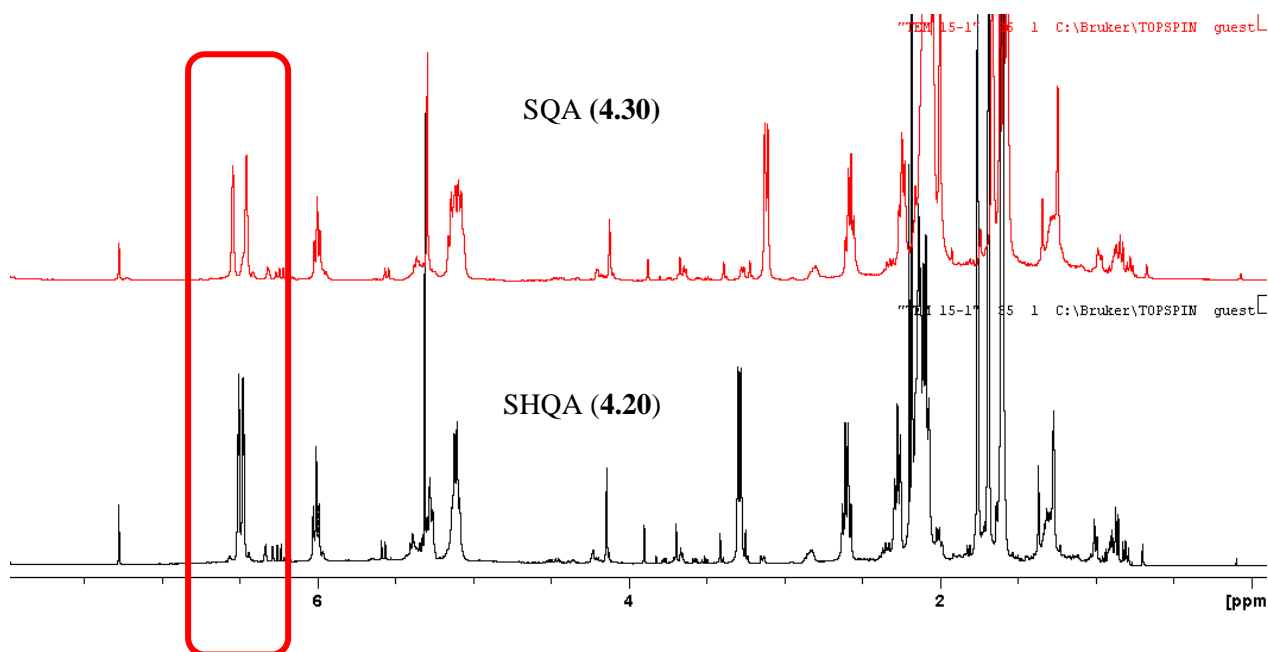
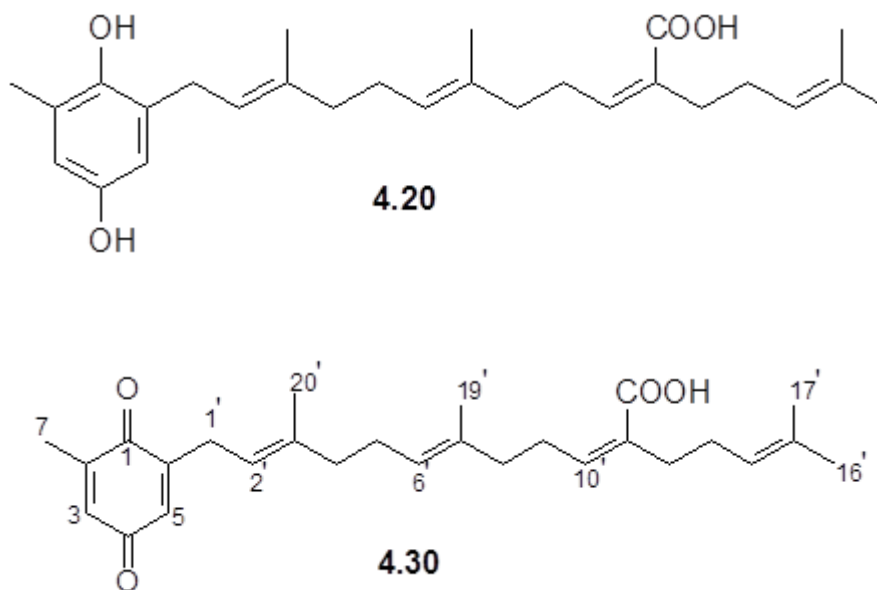


**Figure 4.10** <sup>1</sup>H-NMR (400 MHz, CDCl<sub>3</sub>) spectrum of sargahydroquinolic acid (4.20) and sargaquinolic acid (4.30)



The  $^{13}\text{C}$ -NMR (100 MHz,  $\text{CDCl}_3$ ) spectrum of compound **4.30** (Figure 4.11) revealed a signal at  $\delta$  188.1, characteristic of a quaternary carbon attached to a ketone, further confirming the change in the hydroquinone moiety of sargahydroquinonic acid to a quinone in sargaquinoic acid. All NMR data was found to be in agreement with literature values (Afolayan *et al.*, 2008). Table 4.6 compares the  $^1\text{H}$ -NMR data of compounds **4.20** and **4.30**.

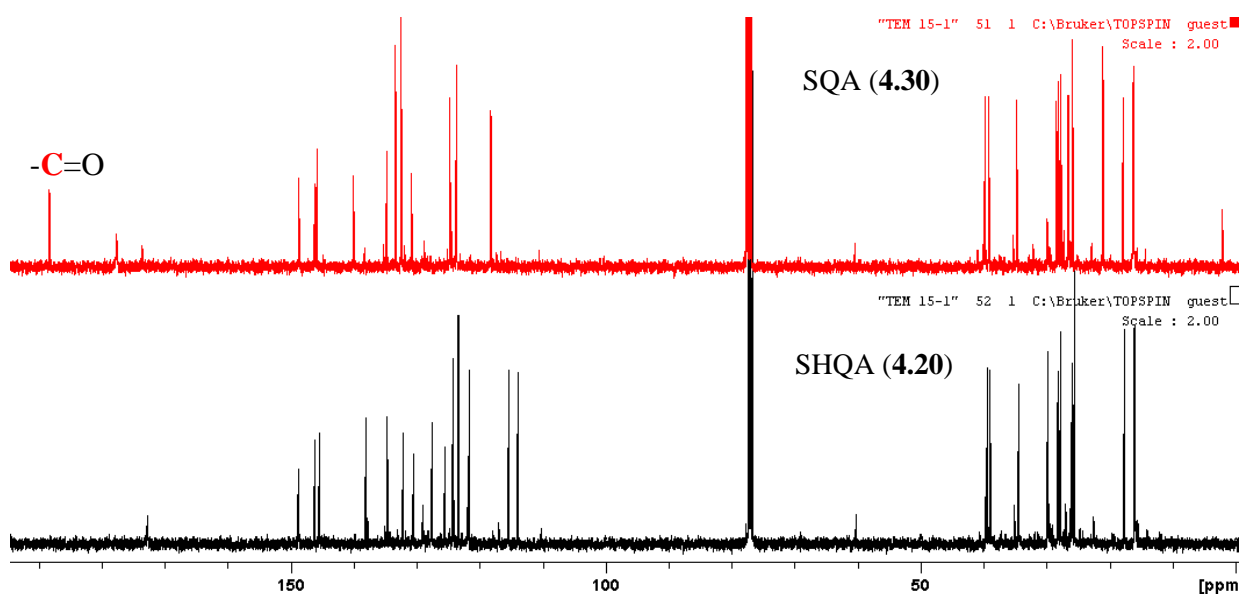


**Figure 4.11**  $^{13}\text{C}$ -NMR (100 MHz,  $\text{CDCl}_3$ ) spectrum of sargahydroquinonic acid (**4.20**) and sargaquinoic acid (**4.30**)

**Table 4.6**  $^1\text{H}$ -NMR spectroscopic data,  $^1\text{H}$ -NMR (400 MHz,  $\text{CDCl}_3$ ) and  $^{13}\text{C}$ -NMR (100 MHz,  $\text{CDCl}_3$ ) comparing compounds **4.20** and **4.30**

Carbon no	4.20			4.30		Literature values for 4.30 <sup>6</sup>	
	$\delta_{\text{C}}$	$\delta_{\text{C}}$ multi	$\delta_{\text{H}}$ , multi, $J=$ Hz	$\delta_{\text{C}}$	$\delta_{\text{H}}$ , multi, $J=$ Hz	$\delta_{\text{C}}$	$\delta_{\text{H}}$ , multi, $J=$ Hz
1	146.3	C	-	188.1		188.0	
2	125.6	C	-	145.9		145.2	
3	115.5	CH	6.50, br.s	132.5	6.56, q, 1.4	132.2	6.56,q, 1.5
4	148.7	C	-	188.2		187.9	
5	113.9	CH	6.48, br.s	132.5	6.46, m	132.2	6.46, m
6	127.6	C	-	148.9		148.5	
7	16.0	CH <sub>3</sub>	2.18, s	16.4	2.07, d, 1.5	16.0	2.05,d, 1.5
1'	29.8	CH <sub>2</sub>	3.27, d, 7.13	28.4	3.13,d, 7.3	28.2	3.12, d, 7.1
2'	121.6	CH	5.28, t, 6.74	118.3	5.03-5.18, m	118.0	5.10, m
3'	138.2	C	-	140.1		139.8	
4'	39.5	CH <sub>2</sub>	2.05-2.17, m	39.8	2.02-2.17, m	39.6	2.08, m
5'	26.0	CH <sub>2</sub>	2.05-2.17, m	26.6	2.02-2.17, m	26.3	2.08, m
6'	124.3	CH	5.07-5.15, m	124.8	5.03-5.18, m	124.5	5.10, m
7'	134.7	C	-	134.7		134.6	
8'	38.9	CH <sub>2</sub>	2.05-2.17, m	39.3	2.03-2.17, m	39.1	2.09, m
9'	28.3	CH <sub>2</sub>	2.60, q, 7.73	27.7	2.58, q, 7.5	27.6	2.58, q, 7.4
10'	145.5	CH	6.01, t, 7.33	146.2	6.00, t, 7.3	145.9	5.99, t, 7.3
11'	130.5	C	-	130.9		130.5	
12'	34.5	CH <sub>2</sub>	2.28, t, 7.33	34.7	2.25, t, 7.3	34.6	2.25, t, 7.2
13'	27.8	CH <sub>2</sub>	2.05-2.17, m	28.1	2.03-2.17, m	27.9	2.15, m
14'	123.5	CH	5.07-5.15, m	123.8	5.03-5.18, m	123.5	5.10, m
15'	132.3	C	-	133.4		133.1	
16'	25.6	CH <sub>3</sub>	1.69, s	25.8	1.66, s	25.7	1.66, s
17'	17.1	CH <sub>3</sub>	1.60, s	17.9	1.57, s	17.7	1.57, s
18'	172.9	C	-	173.6		172.2	
19'	16.1	CH <sub>3</sub>	1.61, s	16.1	1.59, s	16.0	1.59, s
20'	16.1	CH <sub>3</sub>	1.76, s	16.2	1.62, s	16.1	1.59, s

<sup>6</sup> Afolayan *et al.*, 2008

The hydroquinone moiety of sargahydroquinolic acid is very reactive and it therefore undergoes slow oxidation to form sargaquinolic acid in the presence of air. This reaction however, takes place over a prolonged period of time. When sargahydroquinolic acid was stirred at room temperature for the biomimetic oxidation reactions, sargaquinone was formed after 4 hours (using MnTPPs-H<sub>2</sub>O<sub>2</sub>) and 1h 30 min (using MnTPPs-PhIO(Ac)<sub>2</sub>). Moreover, the oxidation reaction in the presence of iodobenzene diacetate only (i.e. with no catalyst), still yielded the quinone derivative (Figure 4.12) which was not observed in a similar experiment where H<sub>2</sub>O<sub>2</sub> alone was used (also with no catalyst).

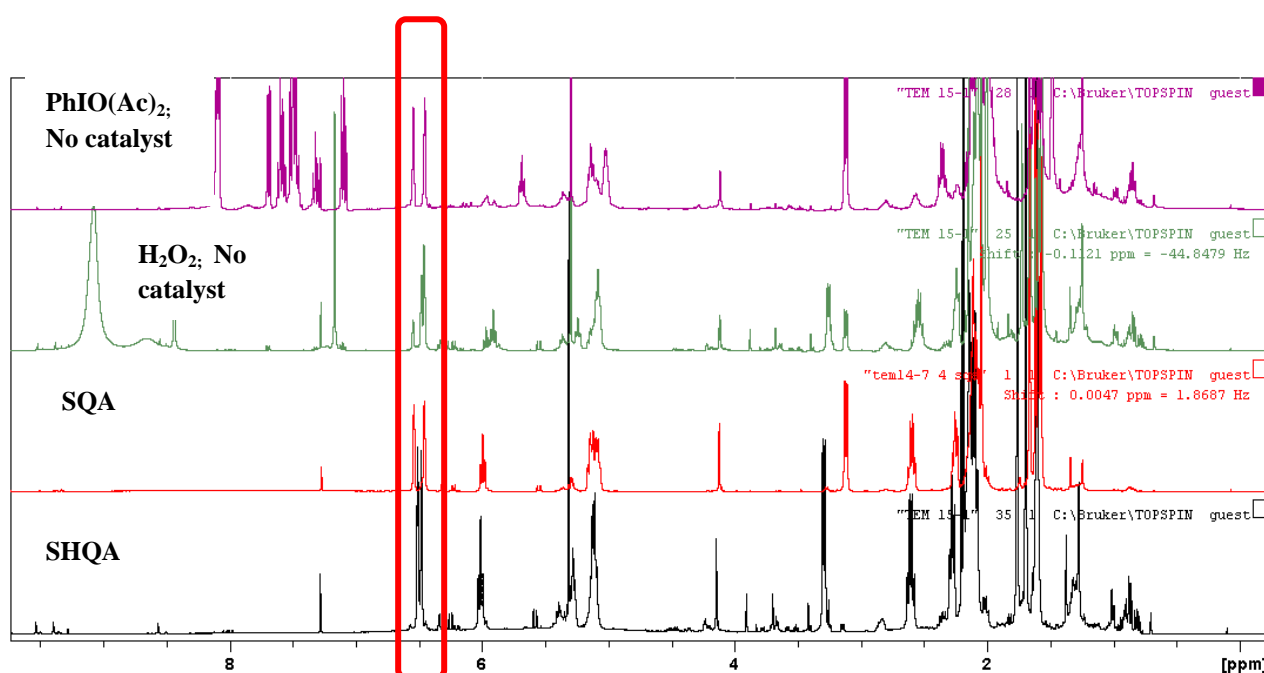
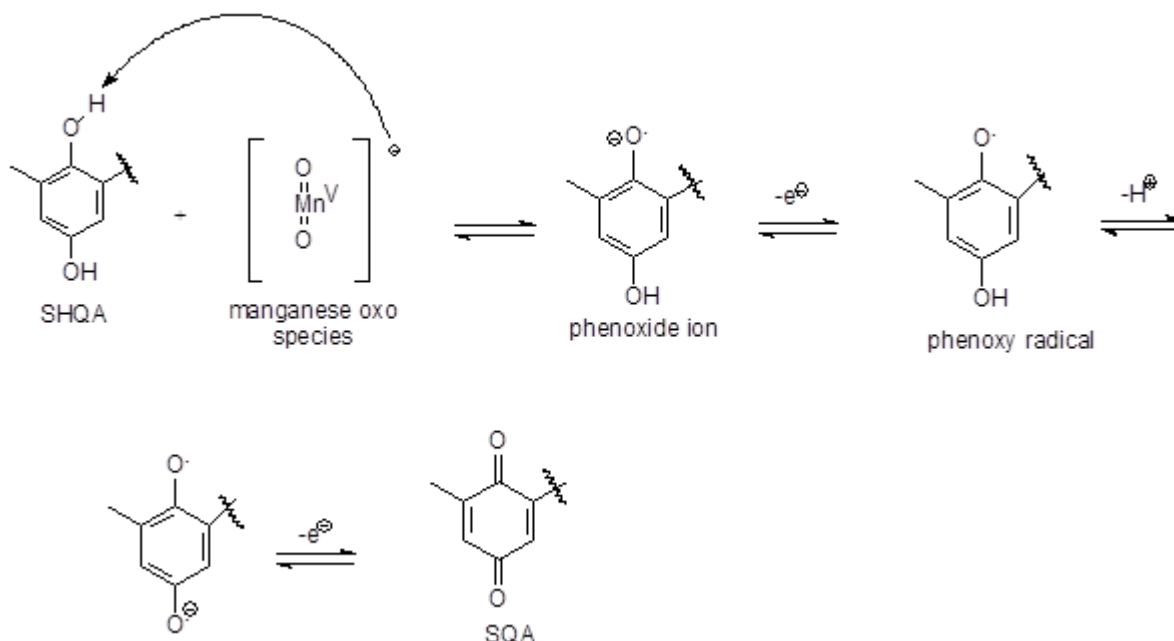


**Figure 4.12** <sup>1</sup>H-NMR (400 MHz, CDCl<sub>3</sub>) spectrum of the control reactions of **4.20**, SHQA and SQA highlighting the region  $\delta$  6.40-6.60

The presence of a catalyst in the biomimetic model MnTPPs-H<sub>2</sub>O<sub>2</sub> reactions facilitated the formation of sargaquinolic acid in the presence of the weak oxidant H<sub>2</sub>O<sub>2</sub>. However, iodobenzene diacetate fully oxidized sargahydroquinolic acid in 1h 30 min in the absence of catalyst, illustrating the high reactivity of the hydroquinone moiety and the efficient oxidation capacity of iodobenzene diacetate. Scheme 4.8 outlines the proposal for the formation of sargaquinolic acid from sargahydroquinolic acid in a biomimetic oxidation model. The high valent manganese oxo species catalyzes the oxidation reaction by an initial deprotonation



reaction which then facilitates the formation of the phenoxide. The phenoxy radical then undergoes further deprotonation and a loss of electrons to form the quinone.



**Scheme 4.8** Proposed mechanism for sargahydroquinone acid oxidation catalyzed by metalloporphyrin catalyst

Sargaquinone acid is a secondary metabolite which has been isolated from several species of *Sargassum* such as *S. incisifolium* and *S. serratifolium*. It has been shown to possess biological activities which include antimalarial, antioxidant and anti-diabetic activities (Afolayan *et al.*, 2008; Kim *et al.*, 2008). This metabolism study therefore suggests that sargahydroquinone acid as a potential new chemical entity may undergo *in vivo* oxidation catalyzed by cytochrome P450 enzymes to give sargaquinone acid, the active metabolite.

#### **Biomimetic oxidation of lapachol (4.21)**

The biomimetic oxidation of lapachol was also carried out using both biomimetic oxidation models MnTPPs-H<sub>2</sub>O<sub>2</sub> (over 4 hours) and MnTPPs-PhIO(Ac)<sub>2</sub> (over 1h 30 min), to give the naphthoquinone derivatives of lapachol. Further separation of the metabolites of the lapachol

oxidation reaction was avoided to ensure that there was no loss of any possible volatile products likely to form (Pires *et al.*, 2011). The reaction mixture for each model was therefore analyzed by NMR to identify the different lapachol metabolites present. The reaction mixture for the biomimetic oxidation model catalyst-H<sub>2</sub>O<sub>2</sub> gave a clear <sup>1</sup>H-NMR spectrum which was useful in identifying the naphthoquinone derivatives of lapachol (Figure 4.13).

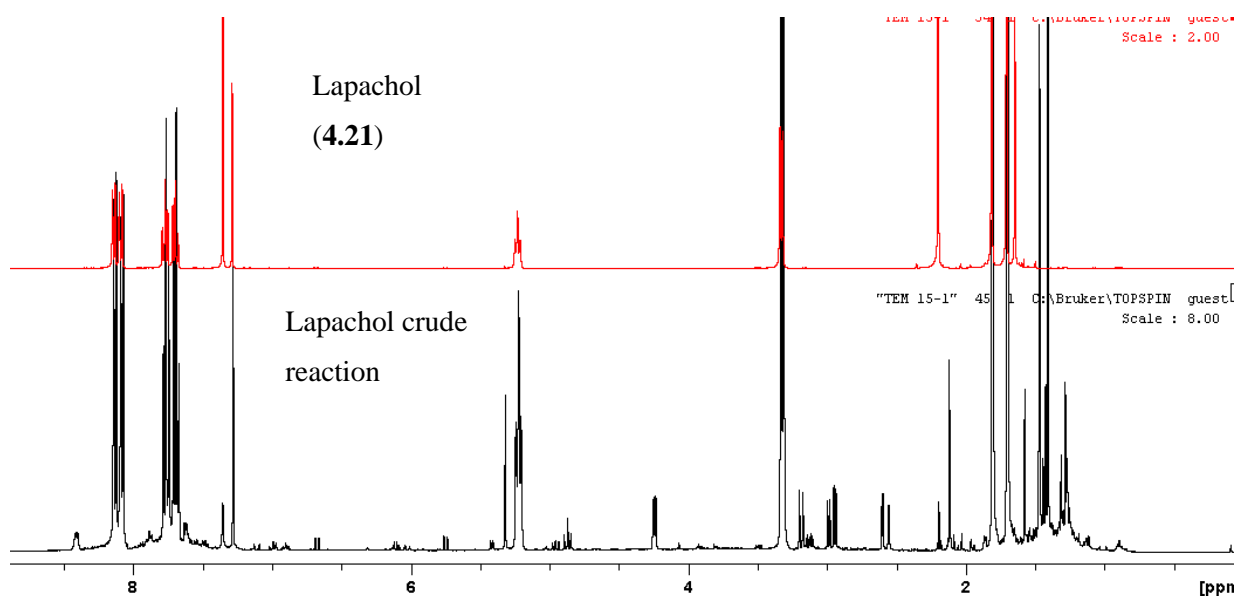


**Figure 4.13** <sup>1</sup>H-NMR (400 MHz, CDCl<sub>3</sub>) spectrum of lapachol crude reaction mixture and starting material (**4.21**)

The spectrum (Figure 4.13) was zoomed into the regions of interest to identify key <sup>1</sup>H-NMR signals specific for the various lapachol metabolites formed. The aromatic protons within the metabolites (**4.31** and **4.32**) were masked by the aromatic protons in lapachol which was still present in the crude reaction mixture.

The first region enlarged was  $\delta$  5.25- 6.25 (Figure 4.14). In this region, two doublets at  $\delta$  5.41 (d,  $J$ = 6.6 Hz) and  $\delta$  6.10 (d,  $J$ = 6.6 Hz) were identified as the two olefinic methine protons in the lactone ring suggesting cyclization of the alkene side chain of the lapachol into a six membered lactone ring. These values were compared with literature values, as well as

through the use of Mestrenova<sup>®</sup> NMR prediction software (Figure 4.15). These assisted in the identification of the metabolite as dehydro- $\alpha$ -lapachone (**4.31**) (Pires *et al.*, 2011).

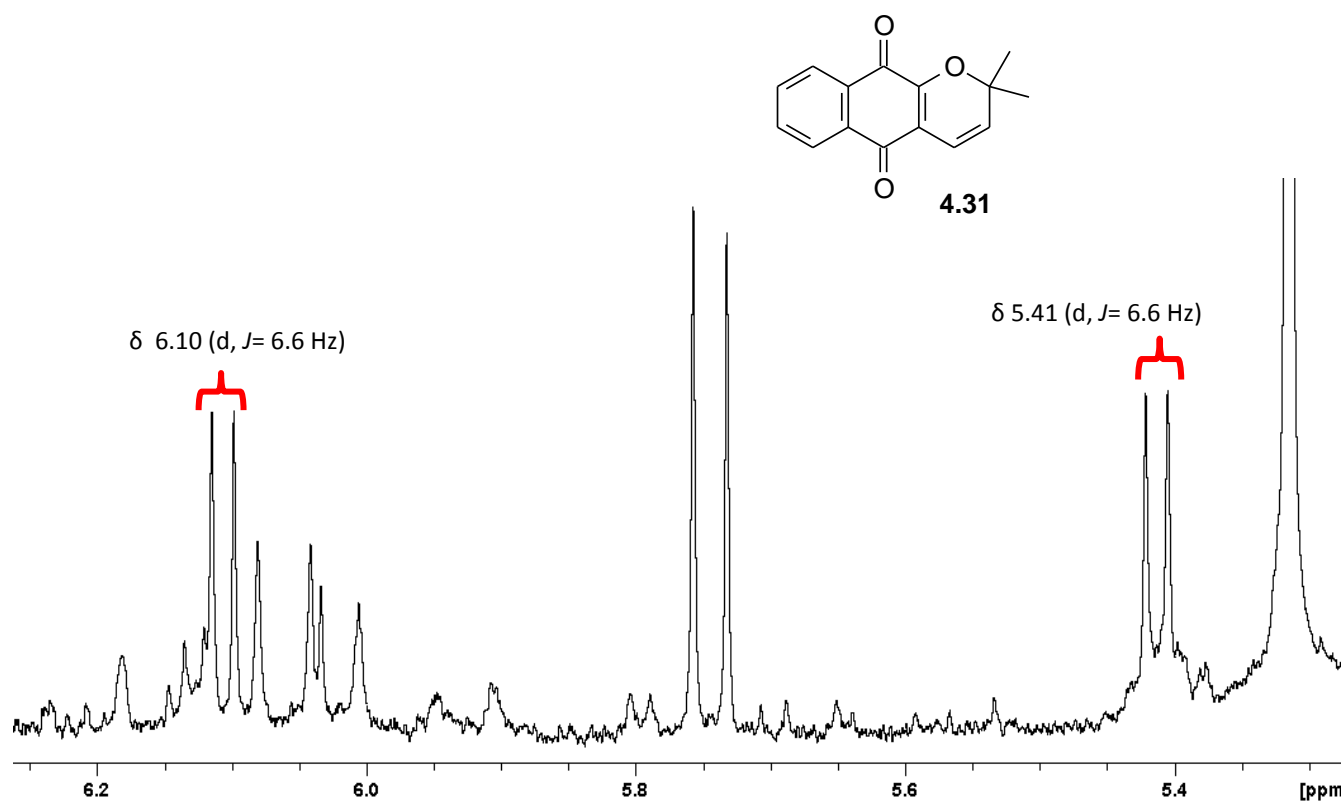


**Figure 4.14** <sup>1</sup>H-NMR (400 MHz, CDCl<sub>3</sub>) region  $\delta$  5.25- 7.50 with signals for **4.31**

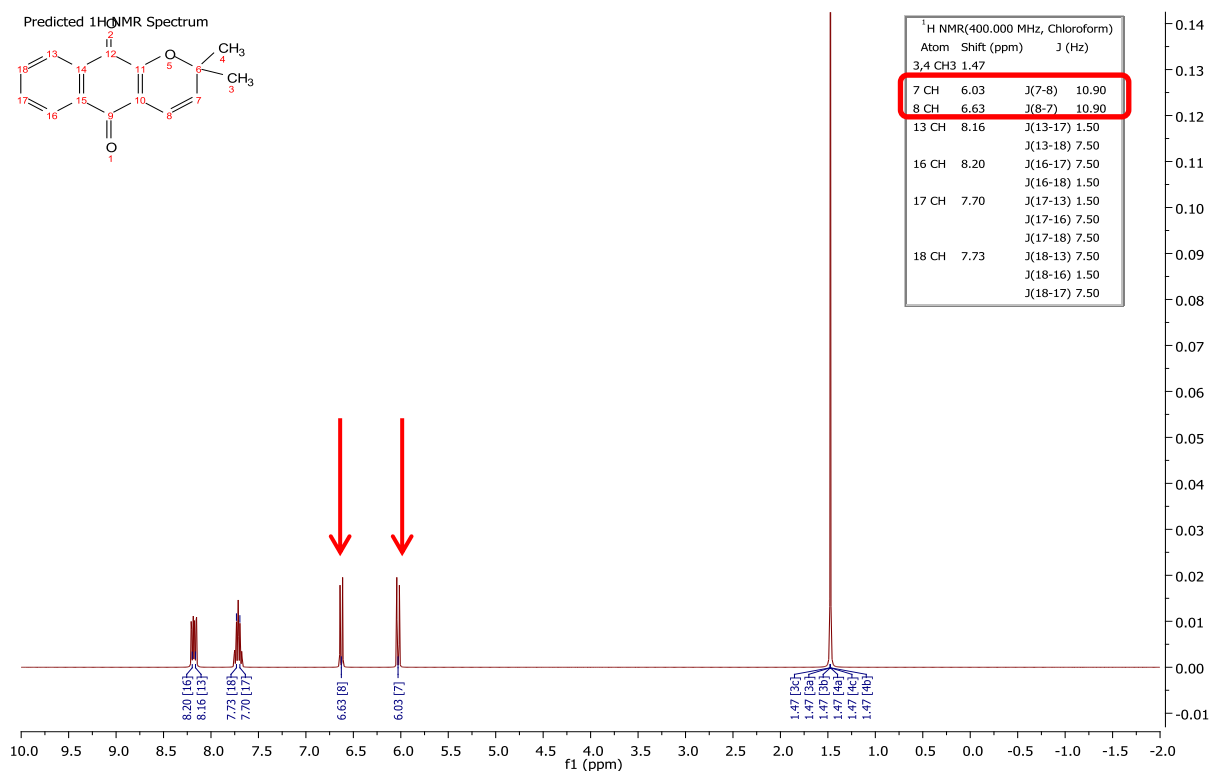


**Figure 4.15** Mestrenova<sup>®</sup>  $^1\text{H-NMR}$  (400.00 MHz,  $\text{CDCl}_3$ ) spectrum prediction of compound **4.31** highlighting the distinguishing doublet signals

The second  $^1\text{H-NMR}$  spectral region analyzed was the  $\delta$  2.90-5.10 region (Figure 4.16) which was characterized by a doublet at  $\delta$  3.17 (d,  $J= 10.0$  Hz) and a triplet at  $\delta$  4.85 (t,  $J= 10.0$  Hz). The doublet at  $\delta$  3.17 corresponds to the methylene protons, while the triplet at  $\delta$  4.85 is due to the methine proton all within the furanolactone ring. These values were compared to literature values to again assist with the assignment of a furanonaphthoquinone, 2-(1-Hydroxy-1-methylethyl)-2,3-dihydronaphtho[2,3-b]furan-4,9-dione (**4.32**). Compound **4.32** has also been previously isolated in biomimetic oxidation reactions of lapachol by Pires *et al.*, (2011).

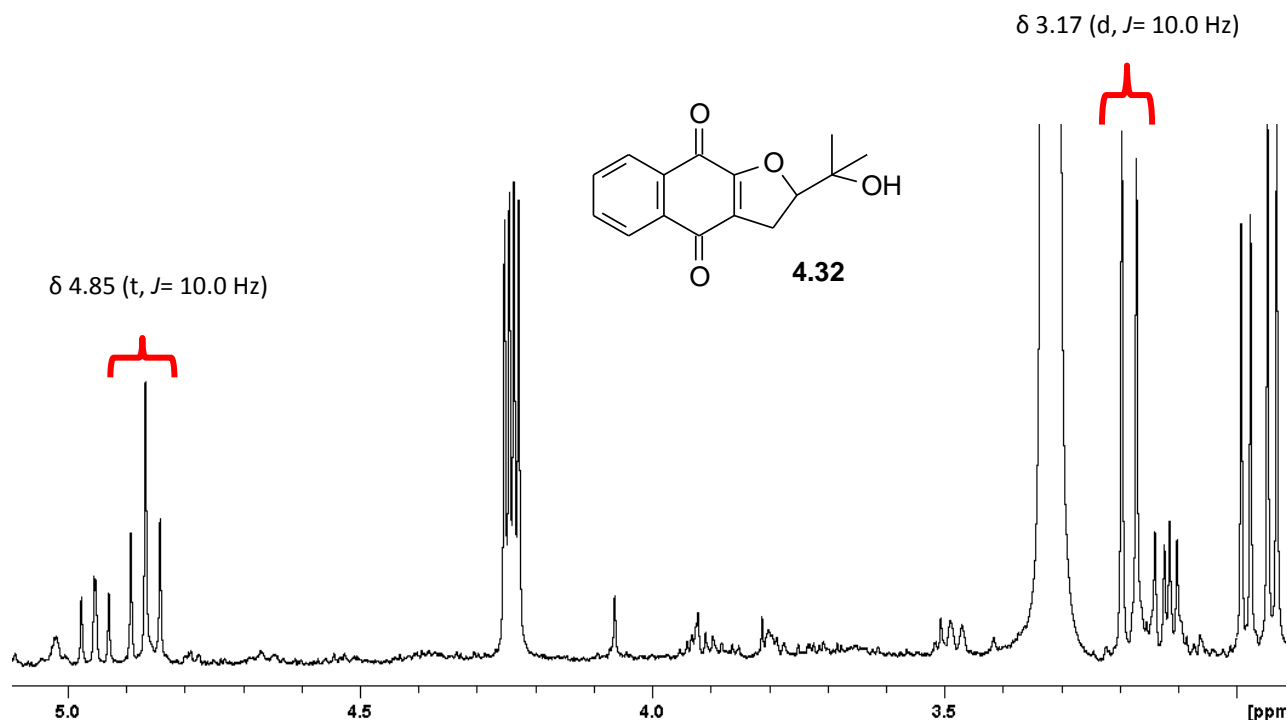


**Figure 4.16** <sup>1</sup>H-NMR (400 MHz, CDCl<sub>3</sub>) region  $\delta$  2.90- 5.10 with signals for **4.32**

The <sup>1</sup>H-NMR spectral regions between 2.50-4.50 ppm (Figure 4.17) provided three key spectral features in the elucidation of metabolite **4.33**. A doublet of doublets at  $\delta$  2.56 (dd,  $J = 3.3, 18.0$  Hz), a doublet of doublets at  $\delta$  2.95 (dd,  $J = 6.7, 18.0$  Hz) and a double doublet at  $\delta$  4.24 (dd,  $J = 3.3, 6.4$  Hz) were observed. The <sup>13</sup>C-NMR (100 MHz, CDCl<sub>3</sub>) and 2D NMR data were instrumental in providing insight into the structure of compound **4.33** and suggested that it could be a furanolactone. Firstly, an HSQC correlation (Figure 4.18) was observed between the main key protons at  $\delta$  2.56 and 2.95 to the methylene carbon signal at  $\delta$  38.2 while the multiplet at  $\delta$  4.20 was found to be attached to the oxymethine carbon at  $\delta$  74.3. These values were compared to literature values (Pires *et al.*, 2011) which assisted with the assignment of a furanolactone, 4-Hydroxy-5,5-dimethyldihydrofuran-2(3H)-one (**4.33**).

Lapachol H2O2 crude  
 PROTON CDCl3 (C:\Bruker\TopSpin3.2) EA 17

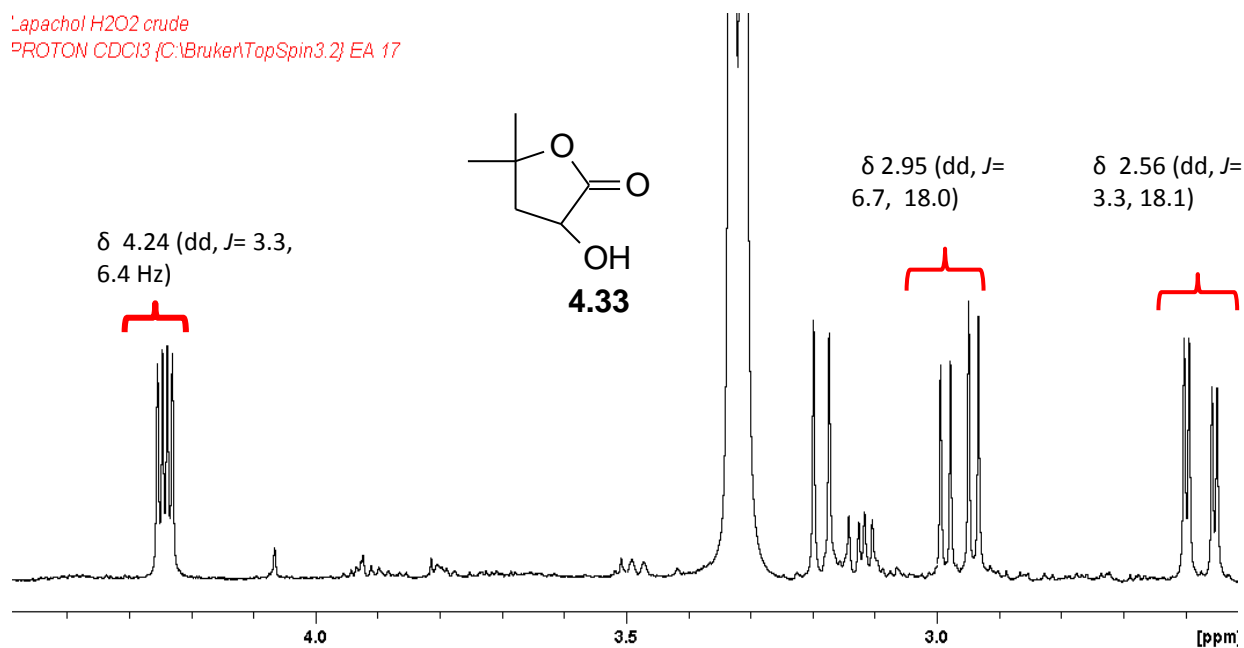


**Figure 4.17**  $^1\text{H-NMR}$  (400 MHz,  $\text{CDCl}_3$ ) region  $\delta$  2.50- 4.50 with signals for **4.33**

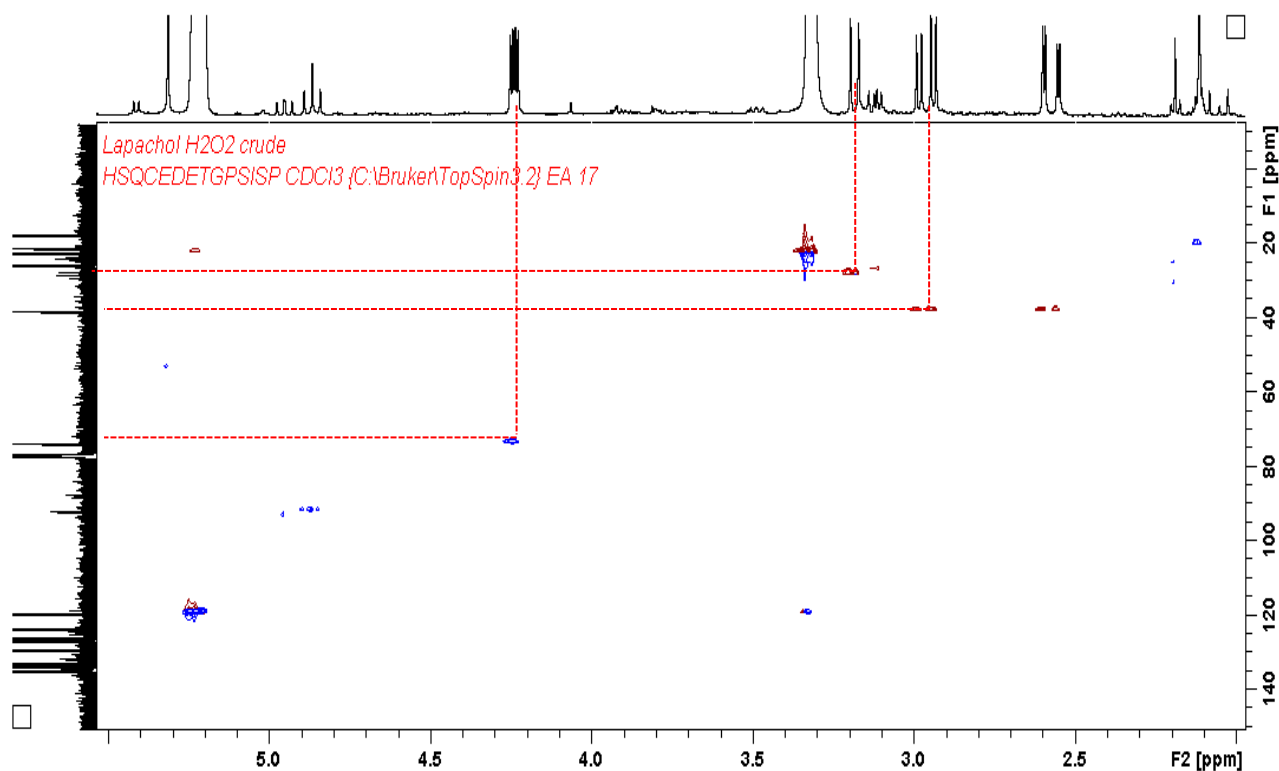
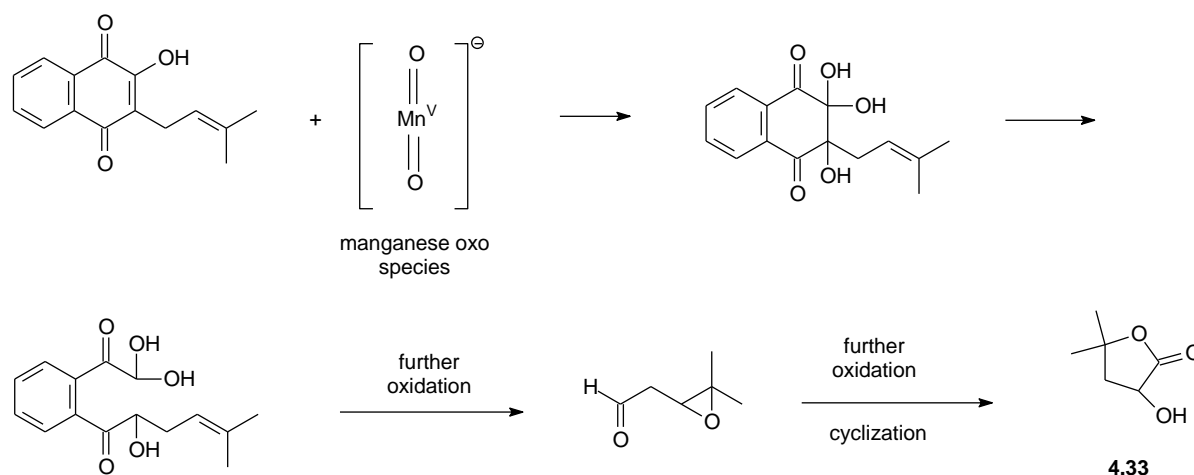


**Figure 4.18** Edited HSQC spectrum of crude reaction mixture of lapachol biomimetic oxidation illustrating key correlations in compound **4.33**

This metabolite (**4.33**) has been proposed to form as a result of a series of oxidation, ring opening and cleavage reactions of the prenyl moiety of lapachol illustrated in Scheme 4.9 below. An initial epoxidation of the alkene in the quinone ring is presumed to be the initial step of lapachol oxidation, followed by cleavage of the quinone ring and further oxidation and cleavage of the prenyl side chain (Niehues *et al.*, 2012). Cyclization of the cleaved prenyl chain occurs after another oxidation step to form the furanolactone metabolite (**4.33**).



**Scheme 4.9** Proposed reaction mechanism for the formation of **4.33** in a biomimetic oxidation model (Pires *et al.*, 2011)

Dehydro- $\alpha$ -lapachone (**4.31**) has previously been isolated in the *in vivo* metabolism studies of lapachol conducted on female wistar rats. It has been suggested to be a metabolite formed as a result of cytochrome P450 catalyzed oxidation reactions of lapachol. Therefore, this confirms that biomimetic oxidation models are useful tools in predicting the possible metabolites that can be obtained from potential drug molecules.

Biomimetic oxidation reactions were also attempted on other natural products; however no success was achieved with these reactions. These have been summarised in the table below (Table 4.7).

**Table 4.7** Summary of natural product biomimetic oxidation reactions

Substrate	Biomimetic model I	Biomimetic model II
	(MnTPPs/H <sub>2</sub> O <sub>2</sub> )	(MnTPPs/PhIO(Ac) <sub>2</sub> )
Sargahydroquinoic acid	✓	✓
Sargaquinoic acid	X	X
Sargachromenol	X	X
Fucoxanthin	X	X
Lapachol	✓	✓
Cholesterol	X	X
Cinnamic acid	X	X
Sclareol	X	X

✓ = successful reaction;  
X = failed reaction



## 4.3 Experimental

### 4.3.1 General experimental

#### Solvents

All solvents used for extraction and chromatography were HPLC grade (LiChrosolv<sup>®</sup>; Merck<sup>®</sup>, Darmstadt, Germany).

#### Reagents

All reagents used for the two biomimetic models which are hydrogen peroxide (30% v/v) solution, imidazole, iodobenzene diacetate, cinnamic acid and the metalloporphyrins: MnTPPs, MnPYP were purchased from Sigma-Aldrich<sup>®</sup>, South Africa. Formic acid, acetanilide and cholesterol were obtained from Saarchem (Pty) Limited, South Africa. Phenylbutazone, lapachol, ibuprofen and indomethacin, were obtained from the library of compounds in the Faculty of Pharmacy at Rhodes University. Sclareol and crude *Sargassum incisifolium* extract was obtained from the library of compounds from the Faculty of Pharmacy at University of Western Cape. The purity of all natural products and NSAIDs was determined by <sup>1</sup>H-NMR spectroscopy prior to starting the oxidation reactions.

#### Chromatographic procedures

Column chromatographic purification procedures were achieved using Merck<sup>®</sup> silica gel 60 (0.040-0.063mm) 230-400 mesh ASTM products. All thin layer chromatography experiments were run on Merck<sup>®</sup> silica gel 60F<sub>254</sub> 20x20 aluminium sheets and visualization was done using Syngene UV lamp, with dual wavelengths 254nm and 365nm.

#### Nuclear magnetic resonance

NMR studies were conducted using a Bruker<sup>®</sup> Avance 400 MHz spectrometer with deuterated chloroform (CDCl<sub>3</sub>) as the NMR solvent. All chemical shifts were recorded in part per million ( $\delta$ ) and coupling constants  $J$  given in hertz (Hz). All spectra were referenced to residual solvent ( $\delta_{\text{H}}$  7.28,  $\delta_{\text{C}}$  77.0) for CDCl<sub>3</sub>.

### 4.3.2 Isolation of sargahydroquinonic acid

The crude product (2.34g) obtained from the initial extraction of *Sargassum incisifolium* was fractionated via step gradient chromatography and eluted using Hexane-EtOAc (ethyl acetate) in increasing polarity. The 6:4 Hexane-EtOAc fraction (0.95g) was of importance containing since it contained the sargahydroquinonic acid component. The fraction was analyzed using  $^1\text{H-NMR}$  and  $^{13}\text{C-NMR}$ .

### 4.3.3 Determination of the hydrogen peroxide content

The exogenous oxygen donor for biomimetic oxidation model catalyst- $\text{H}_2\text{O}_2$  was hydrogen peroxide. There was therefore a need to determine its peroxide content prior to conducting any metabolism studies. The content of hydrogen peroxide was determined by titration with  $\text{KMnO}_4$  (0.025M) in the presence of  $\text{H}_2\text{SO}_4$  (3M). The content of peroxide was found to be 29.68%.

### 4.3.4 Biomimetic oxidation model (Catalyst- $\text{H}_2\text{O}_2$ )

#### General procedure

Hydrogen peroxide ( $\text{H}_2\text{O}_2$ ) (30% v/v) (5 mmol) in acetonitrile (1:9 v/v) was slowly added to a solution of catalyst (0.025 mol equiv.), imidazole (0.6 mmol), substrate (1 mmol), and formic acid (168 mmol) in DCM/acetonitrile (1:1 v/v) over 2h at room temperature. The reaction mixture was then stirred for a further 2h. Total reaction time was 4h. Reaction progress was assessed via TLC every 1h. The solvent from the successful reaction mixture (as determined by TLC) was then evaporated under reduced pressure and subjected to column chromatography and analysed by NMR. For natural product biomimetic reactions, crude reaction product was extracted by DCM.

### 4.3.5 Biomimetic oxidation model (Catalyst-PhIO(Ac)<sub>2</sub>)

#### General procedure

Iodosobenzene diacetate (PhIO(Ac)<sub>2</sub>) (1.5 mmol) for the olefin epoxidations was added to a reaction mixture with catalyst (0.005 mol equiv.), H<sub>2</sub>O (5 μL), and substrate (1 mmol) in solution of DCM/acetonitrile (1:1 v/v). The reaction mixture was then stirred at room temperature for 30 min (NSAID oxidations) 1h 30min (natural product oxidations). Reaction progress was assessed every 30 min via TLC. Successful reaction mixtures were further purified via column chromatography to isolate oxidized products and analysed via NMR techniques. For natural product biomimetic reactions, crude reaction product was extracted by DCM.

#### Control reactions

The control reactions were conducted one in the absence of metalloporphrin (control 1) catalyst and the other in the absence of oxidant (control 2).

#### Thin layer chromatography procedures

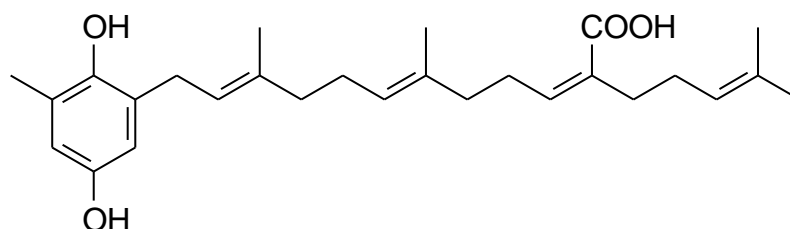
The TLC solvent used in analyzing each of the substrates used in the biomimetic models above have been tabulated below (Table 4.8). TLC staining with 10% methanolic sulphuric acid was employed in the analysis of cholesterol reaction products. All the other TLC visualizations were done under UV at 254 nm wavelength. TLC solvent systems were used in column chromatographic procedures.

**Table 4.8** TLC solvent systems used in the biomimetic oxidation models

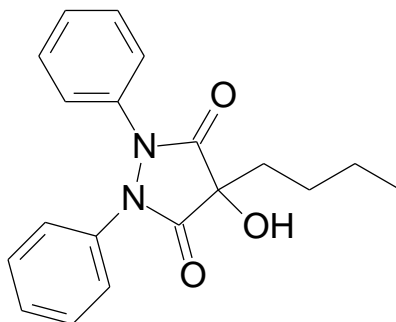
Substrate	TLC solvent system
Phenylbutazone	Hexane/DCM/Acetic acid (7:3:1)
Acetanilide	Acetonitrile/DCM (1:1)
Indomethacin	Chloroform/MeOH (5:1)
Ibuprofen	DCM/Diethyl ether
Sargahydroquinoic acid	Hexane/EtOAc(6:4)
Sargaquinoic acid	Hexane/EtOAc (6:4)
Sargachromenol	Hexane/EtOAc (6:4)
Fucoxanthin	Hexane/EtOAc (4:6)
Lapachol	Hexane/EtOAc (1:2)
Cholesterol	Hexane/EtOAc (8:2)
Cinnamic acid	DCM/EtOAc/Acetic acid (5:5:1)
Sclareol	Hexane/EtOAc (6:4)

### 4.3.6 Isolated oxidation products

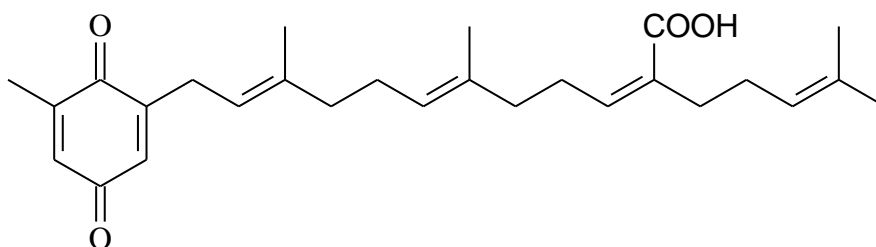
#### Compound 4.20



*Sargahydroquinoic acid* (**4.20**): Green paste- $^1\text{H-NMR}$  (400 MHz,  $\text{CDCl}_3$ ),  $^{13}\text{C-NMR}$  (100 MHz,  $\text{CDCl}_3$ ). See Table 4.6.

**Compound 4.28**

*4-hydroxy-4-n-butyl-1,2-diphenylpyrazolidine-3,5-dione* (**4.26**): White solid-  $^1\text{H-NMR}$  (400 MHz,  $\text{CDCl}_3$ ). See Table 4.3.

**Compound 4.30**

*Sargaquinoic acid* (**4.30**): Green paste-  $^1\text{H-NMR}$  (400 MHz,  $\text{CDCl}_3$ ),  $^{13}\text{C-NMR}$  (100 MHz,  $\text{CDCl}_3$ ). See Table 4.6.

#### 4.4 References

Afolayan A.F., Bolton J.J., Lategan C.A., Smith P.J., Beukes D.R. (2008). Fucoxanthin, tetraprenylated toluquinone and toluhydroquinone metabolites from *Sargassum heterophyllum* inhibit the *in vitro* growth of malaria parasite *Plasmodium falciparum*. *Zeitschrift für Naturforschung B* 63: 848-852

Alexander D.M., Mathew G.M., Wilson B.J. (1985). Metabolism of phenylbutazone in rats. *Xenobiotica* 15: 123-128

Artkinson A.J., Markey S.A. (2012). Chapter 16 Biochemical mechanisms of drug toxicity. *Principles of Clinical Pharmacology* 3<sup>rd</sup> Ed. (Atkinson A.J Ed.). Academic Press, USA: 259-280

Balogh G., Keserű G. (2004). Metalloporphyrin mediated biomimetic oxidations. A useful tool for the investigation of cytochrome P450 catalyzed oxidative metabolism. *Arkivoc* 7: 124-139

Bombarda I., Becerra V.O., Mela P., Gaydou E.M. (1997). Cyclization of sclareol epoxides catalyzed by boron trifluoride in methanol. *Journal of Essential Oil Research* 9:551-554

Bussy U., Giraudeau P., Tea I., Boujtita M. Understanding the degradation of electrochemically-generated reactive drug metabolites by quantitative NMR. *Talanta* 116: 554-558

Chauhan S.M.S., Srinivas K.A., Mohapatra P.P. (1999). Oxidation of phenylbutazone with hydrogen peroxide catalyzed by 5, 10, 15,20-tetraaryl-porphyrinatoiron (III) chlorides in dichloromethane. *Indian Journal of Chemistry* 38B: 724-725

Chorgade M.S., Hill D.R., Lee E.C., Pariza R.J., Dolphin D.H., Hino F., Zhang L. (1996). Metalloporphyrins as chemical mimics of cytochrome P-450 systems. *Pure and Applied Chemistry* 68: 753-756

Chorgade M.S., Dolphin D.H., Hill D.R., Hino F., Lee E.C. (1998). Use of synthetic metalloporphyrins for preparation and prediction of drug metabolites. US Patent 5760216

De Almeida E.R. (2009). Preclinical and clinical studies of lapachol and beta-lapachone. *The Open Natural Products Journal* 2: 42-47

De Faria E.H., Ricci G.P., Lemos F.M., e Silva M.L.A., Filho A.A.D., Calefi P.S., Nassar E.J., Ciuffi K.J. (2011). Chapter 7 Green oxidation reactions of drugs catalyzed by bio-inspired complexes as an efficient methodology to obtain new active molecules. *Biomimetic Based Applications*. (Prof. Marko Cavrak Ed.) 163-182. ISBN: 978-953-307-195-4. InTech, Available from: <http://www.intechopen.com/books/biomimetic-based-applications/green-oxidationreactions-of-drugs-catalyzed-by-bio-inspired-complexes-as-an-efficient-methodology-t>

Dieterle W., Faigle J.W., Früh F., Mory H., Theoblad W., Alt K.O., Richter W.J. (1976). Metabolism of phenylbutazone in man. *Arzneimittel-Forschung* 26: 572-577.

Duggan D.E., Hogans A.F., Kwan K.C., McMahon F.G. (1972). The metabolism of indomethacin in man. *The Journal of Pharmacology and Experimental Therapeutics* 181: 563-575

Fox M.A., Whitesell J.K. (2004). Chapter 11 Electrophilic Aromatic Substitution . *Organic Chemistry* 3<sup>rd</sup> Ed. (Bruno L.C Ed). Jones and Bartlett, Canada: 524-569

Goh Y.M., Nam W. (1999). Significant electronic effect of porphyrin ligand on the reactivities of high valent iron (IV) oxo porphyrin cation radical complexes. *Inorganic Chemistry* 38: 914-920

Gotardo M.C.A.F., De Moraes L.A.B., Assis M.D. (2006). Metalloporphyrins as biomimetic models for cytochrome P-450 in the oxidation of atrazine. *Journal of Agricultural and Food Chemistry* 54: 10011-10018

Huguet M., Simon V., Gallard H. (2014). Transformation of paracetamol into 1,4-benzoquinone by a manganese oxide filter. *Journal of Hazardous Materials* 271:245-251

In J., Park S., Song R., Nam W. (2003). Iodobenzene diacetate as an efficient terminal oxidant in iron (III) porphyrin complex-catalyzed oxygenation reactions. *Inorganica Chimica Acta* 343: 373-376

Jeong Y.J., Kang Y., Han A., Lee Y., Kotani H., Fukuzumi S., Nam W. (2008). Hydroge atom abstraction and hydride transfer reactions by iron (IV)-oxo porphyrins. *Angewandte Chemie International Edition* 47: 7321-7324

Kanazawa A., Yoshioka M., Teshima S. (1972). Sterols in some red algae. *Memoirs of Faculty of Fisheries Kagoshima University* 21: 103-107

Kapetanović R., Sladić D., Popov S., Zlatović M., Kljajić Z., Gašić. (2005). Sterol composition of the Adriatic Sea algae *Ulva lactuca*, *Codium dichotomum*, *Cystoseira adriatica* and *Fucus virsoides*. *Journal of Serbian Chemical Society* 70: 1395-1400

Kepp D.R., Sidemann U.G., Hansen S.H. (1997). Isolation and characterization of major phase I and II metabolites of ibuprofen. *Pharmaceutical Research* 14: 676-680

Kim S., Choi H.Y., Lee W., Park G.M., Shin W.S., Kim Y.K. (2008). Sargaquinoic acid and sargahydroquinoic acid from *Sargassum yezoense* stimulate adipocyte differentiation through PPAR $\alpha/\gamma$  activation in 3T3-L1 cells. *FEBS Letters* 582: 3465-3472

Kim M.C., Kwon H.C., Kim S.N., Kim H.S., Um B.H. (2011). Plastoquinones from *Sargassum yezoense*; chemical structures and effects on the activation of peroxisome proliferator-activated receptor gamma. *Chemical and Pharmaceutical Bulletin* 59: 834-838

Kim S., Lee M., Lee B., Gwon W., Joung E., Yoon N., Kim H. (2014). Anti-inflammatory effects of sargachromenol-rich ethanolic extract of *Myagropis myagroides* on lipopolysaccharide-stimulated BV-2 cells. *BMC Complementary and Alternative Medicine* 14: 231-243

Lee J.Y., Lee Y., Kotani H., Nam W., Fukuzumi S. (2009). High-valent manganese (v)-oxo porphyrin complexes in hydride transfer reactions. *Chemical Communications* 6: 704-706

Lees P., Toutain P. (2013). Pharmacokinetics, pharmacodynamics, metabolism, toxicology and residues of phenylbutazone in humans and horses. *The Veterinary Journal* 196: 294-303

Liu L., Hudgins W.R., Shack S., Yin M.Q. (1995). Cinnamic acid: a natural product with potential use in cancer intervention. *International Journal of Cancer* 62: 345-350



Lohmann W., Karst U. (2008). Biomimetic modeling of oxidative drug metabolism. *Analytical and Bioanalytical Chemistry* 391: 79-96

MacLeod T.C.O., Faria A.L., Barros V.P., Queiroz M.E.C., Assis M.D. (2008). Primidone oxidation catalyzed by metalloporphyrins and Jacobsen catalyst. *Journal of Molecular Catalysis A: Chemical* 296: 54-60

Mansuy D., Battioni P., Battioni J. (1989). Chemical model systems for drug-metabolizing cytochrome-P-450-dependent monooxygenases. *European Journal of Biochemistry* 184: 267-285

Meunier B. (1992). Metalloporphyrins as versatile catalysts for oxidation reactions and oxidative DNA cleavage. *Chemical Reviews* 92: 1411-1456

Nakajima M., Inoue T., Shimada N., Tokudome S., Yamamoto T., Kuroiwa Y. (1998). Cytochrome P450 2C9 catalyzes indomethacin *o*-demethylation in human liver microsomes. *Drug Metabolism and Disposition* 26: 261-266

Neunzing I., Göhring A., Drăgan C., Zapp J., Peters F.T., Maurer H.H., Bureik M. (2012). Production and NMR analysis of the human ibuprofen metabolite 3-hydroxyibuprofen. *Journal of Biotechnology* 157: 717-420.

Niehues M., Barros V. P., Emery F. D., Dias-Baruffi M., Assis M.D., Lopes N.P. (2012). Biomimetic *in vitro* oxidation of lapachol: A model to predict and analyse the *in vivo* phase I metabolism of bioactive compounds. *European Journal of Medicinal Chemistry*: 804-812

Othman S., Mansuy-Mouries V., Bensoussan C., Battioni P., Mansuy D. (2000). Hydroxylation of diclofenac: an illustration of the complementary roles of biomimetic metalloporphyrin catalysts and yeasts expressing human cytochromes P450 in drug metabolism studies. *Bioorganic and Medicinal Chemistry* 3: 751-755

Peng J., Yuan J., Wu C., Wang J. (2011). Fucoxanthin, a marine carotenoid present in brown seaweeds and diatoms: metabolism and bioactivities relevant to human health. *Marine Drugs* 9: 1806-1828

Pires S.M.G., De Paula R., Simões M.M.Q., Silva A.M.S., Domingues M.R.M., Santos I.C.M.S., Vargas M.D., Ferreira V.F., Neves M.G.P.M.S., Cavaleiro J.A.S. (2011). Novel biomimetic oxidation of lapachol with H<sub>2</sub>O<sub>2</sub> catalysed by a manganese (III) porphyrin complex . RSC Advances 1: 1195-1199

Potter D.W., Hinson J.A. (1987). Mechanisms of acetaminophen oxidation to N-acetyl-P-benzoquinone imine by horseradish peroxidase and cytochrome P450. The Journal of Biological Chemistry 262: 966-973

Rommel R.P., Crews B.C., Kozak K.R., Kalgutkar A.S., Marnett L.J. (2004). Studies on the metabolism of novel, selective cyclooxygenase-2 inhibitor indomethacin phenethylamide in rat, mouse and human liver microsomes: identification of active metabolites. Drug Metabolism and Disposition 32: 113-122

Segrestaa J., Vérité P., Estour F., Ménager S., Lafont O. (2002). Improvements of a biomimetic porphyrin catalytic system by addition of acids. Chemical and Pharmaceutical Bulletin 50: 744-748

Stang P.J., Zhdankin V.V. (1996). Organic polyvalent iodine compounds. Chemical Reviews 96: 1123-1178

Tedeschi E., Rezende D.B. (2009). On the <sup>1</sup>H-NMR spectra of 2-substituted benzoquinones. Annals of Magnetic Resonance 8: 9-13

Valenzuela A., Sanhueza J., Nieto S. (2003). Cholesterol oxidation: Health hazard and the role of antioxidants in prevention. Biological Research 36: 291-302

Vijayarahavan B., Chauhan S.M.S. (1990). Chloroiron(III)-5,10,15,20-tetraarylporphyrinate/N-methylimidazole catalyzed oxidation of androst-4-en-3,17-dione by cumene hydroperoxide. Tetrahedron Letters 31: 6223-6226

Zhang D., Luo G., Ding X., Lu C. (2012). Preclinical experimental models of drug metabolism and disposition in drug discovery and development. Acta Pharmaceutica Sinica B 2: 549-561

Zivanovic A. (2012). Marine natural products isolation, screening and analogue synthesis. PhD thesis. University of Wollongong

# Chapter 5

## Conclusions

With the ever increasing need for new drug molecules, it is important to facilitate the drug discovery and development process to increase the turnover of new drug molecules on the market. Implementing early drug metabolism studies in the drug development process is important in selecting appropriate potential drug molecules with suitable pharmacokinetic and metabolic profiles. Biomimetic oxidation models provide a simple chemical model which allows the isolation and characterization of possible drug metabolites from potential drug molecules.

In this study, two biomimetic model systems catalyzed by water-soluble metalloporphyrins were successfully developed in assessing possible metabolites from natural products with therapeutic importance. Lapachol derivatives were determined which were isolated in a previous biomimetic oxidation model study with dehydro- $\alpha$ -lapachone also isolated from an *in vivo* metabolism model with female wistar rats. This therefore illustrates the potential of biomimetic oxidation models as a useful *in vitro* system to predict *in vivo* drug metabolism. The most efficient biomimetic oxidation model was in the presence of PhIO(Ac)<sub>2</sub> but this is associated with unfavourable by-products such iodobenzene resulting in complex NMR signals. However, the biomimetic oxidation model in the presence of hydrogen peroxide was the most favourable as it closely resembles molecular oxygen, produces water as the only by-product and is environmentally friendly.

The phytochemical analysis of *Brassicophycus brassicaeformis* resulted in the isolation of four compounds: fucosterol (**3.9**), fucoxanthin (**3.16**), two Monogalactosyldiacylglycerols; 1-*O*-(5Z,8Z,11Z,14Z-eicosatetraenoyl)-2-*O*-(9Z,12Z,15Z-octadecatrienoyl)-3-*O*- $\beta$ -D-galactopyranosyl-*sn*-glycerol (**3.17**) and 1-*O*-(9Z-octadecenoyl)-2-*O*-(hexadecanoyl)-3-*O*- $\beta$ -

D-galactopyranosyl-*sn*-glycerol (**3.18**). This study represents the first phytochemical analysis of *Brassicophycus brassicaeformis*.

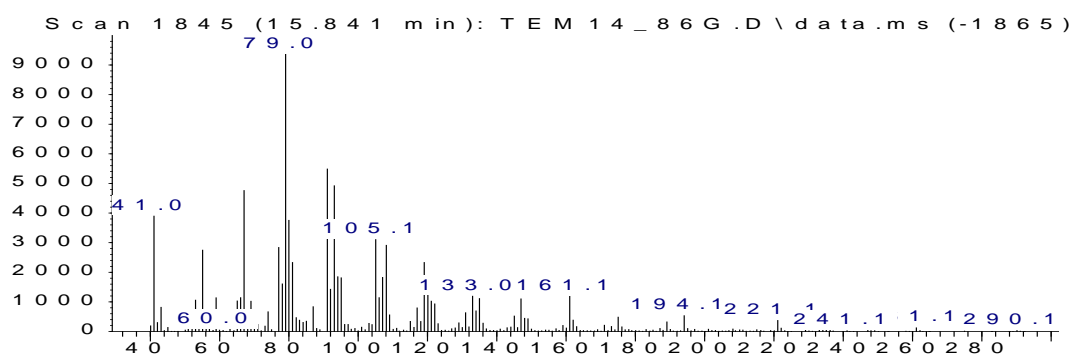
#### **Future work and considerations**

The biomimetic oxidation model can be modified by controlling the pH of the reaction medium to pH 7.4 as well as providing an aqueous environment for oxidation reactions to occur. This provides a better environment mimicking the physiological environment at the cytochrome P450 active site. Furthermore, it is essential to determine the biological activity or lack thereof of all metabolites derived from the biomimetic oxidation models of natural products including toxicological tests. A major consideration should therefore be the scale-up and isolation of all biomimetic products.

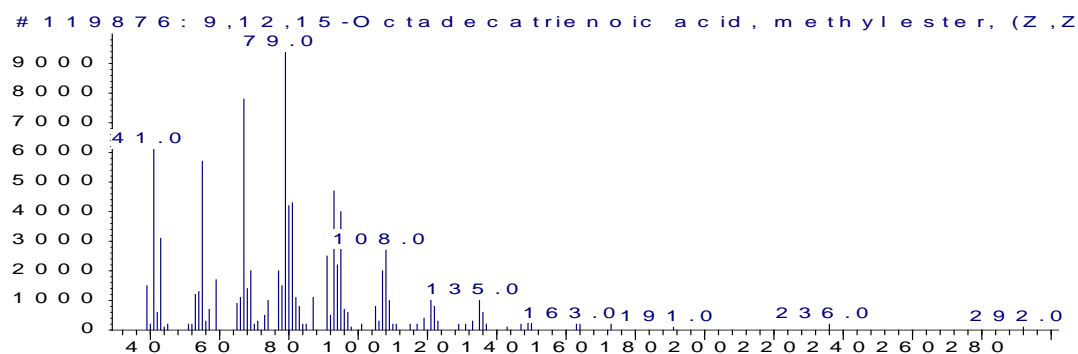
## Appendix 1

### Identification of fatty acids fatty acids from monogalactosyldiacylglycerol **3.17** and **3.18**<sup>7</sup>

Abundance



Abundance



Name 9,12,15-Octadecatrienoic acid, methyl ester, (Z,Z,Z)-

CAS Number 000301-00-8

Entry Number 119876

Molecular Formula C<sub>19</sub>H<sub>32</sub>O<sub>2</sub>

Misc Information NIST MS# 27738, Seq# R9583

Match Quality 38

Company ID NIST 2005

Retention Index 0

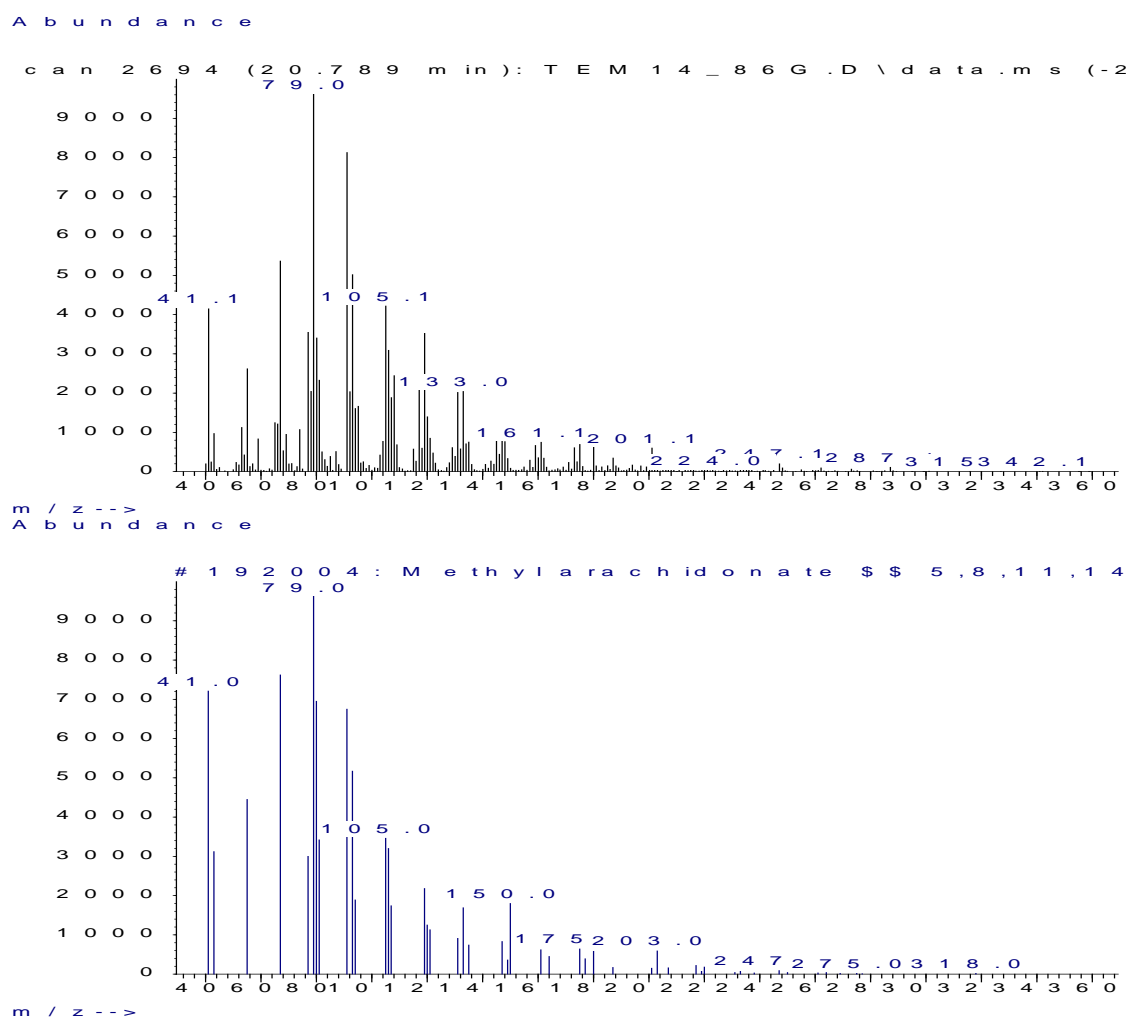
Melting Point

Boiling Point

Molecular Weight 292.24

**Figure A:** Identification of FAME ester **3.17**<sup>1</sup>

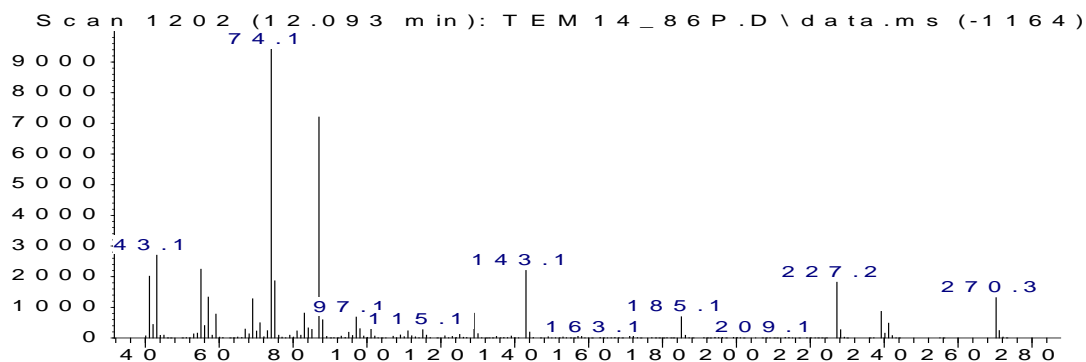
<sup>7</sup>All FAME esters compared to library of FAME esters at the Central Analytical Facilities, University of Stellenbosch



Name Methyl arachidonate \$\$ 5,8,11,14-Eicosatetraenoic acid, methyl ester, (all-Z)- (CAS) \$\$ METHYL 5,8,11,14-EICOSATETRAENOATE  
 \$\$ Arachidonic acid methyl ester \$\$ Methyl all-cis-5,8,11,14-eicosatetraenoate \$\$ 5,8,11,14-Eicosatetraenoic acid, methyl ester  
 CAS Number 002566-89-4  
 Entry Number 192004  
 Molecular Formula C<sub>21</sub>H<sub>34</sub>O<sub>2</sub>  
 Misc Information QI=563, Source=NS-0-0-0  
 Match Quality 52  
 Company ID 330326  
 Retention Index 0  
 Melting Point  
 Boiling Point  
 Molecular Weight 318.26

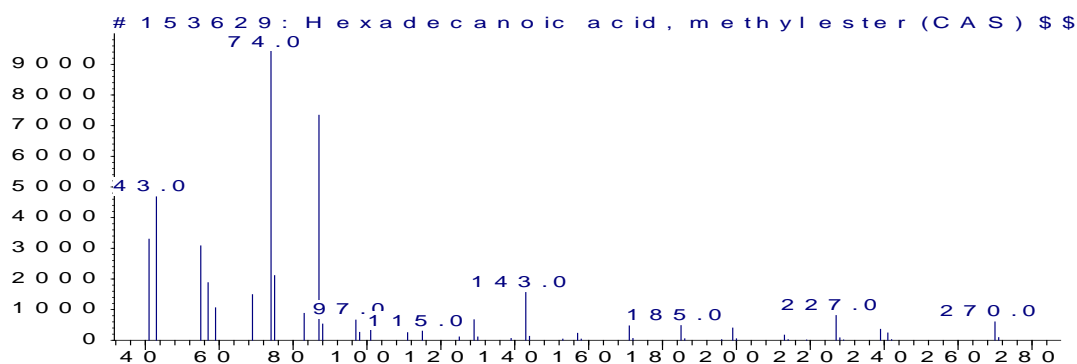
**Figure B:** Identification of FAME ester **3.17<sup>2</sup>**

Abundance



m / z-->

Abundance

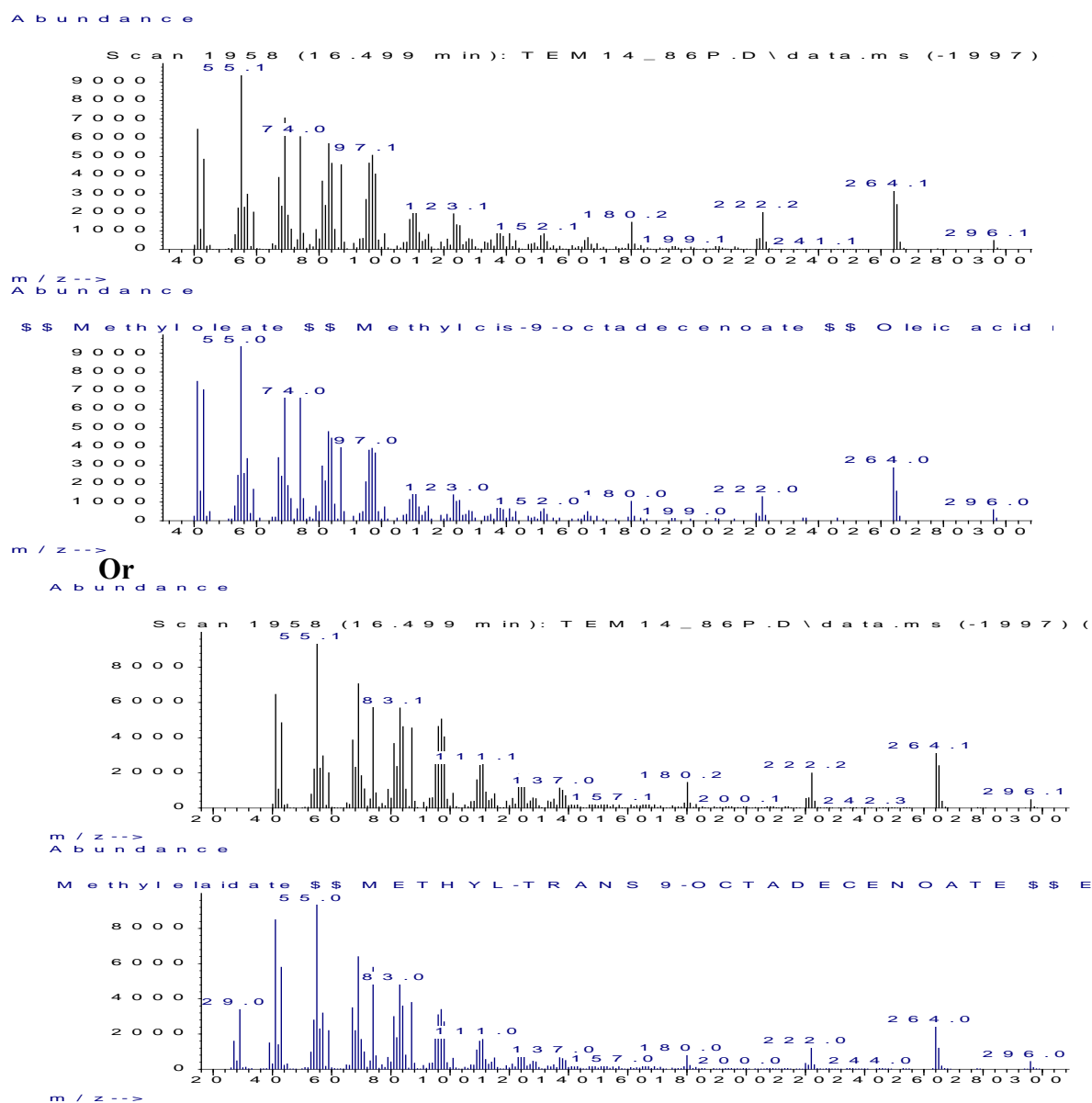


m / z-->

Name Hexadecanoic acid, methyl ester (CAS) \$\$ Methyl palmitate \$\$  
Methyl hexadecanoate \$\$ Methyl n-hexadecanoate \$\$ Uniphat A60 \$\$  
Metholene 2216 \$\$ Palmitic acid methyl ester \$\$ Palmitic acid, methyl  
ester \$\$ n-Hexadecanoic acid methyl ester \$\$ PALMITIC ACID-  
CAS Number 000112-39-0  
Entry Number 153629  
Molecular Formula C17H34O2  
Misc Information QI=553, Source=NS-0-0-0  
Match Quality 99  
Company ID 329104  
Retention Index 0  
Melting Point  
Boiling Point  
Molecular Weight 270.26

Figure C: Identification of FAME ester 3.18<sup>1</sup>





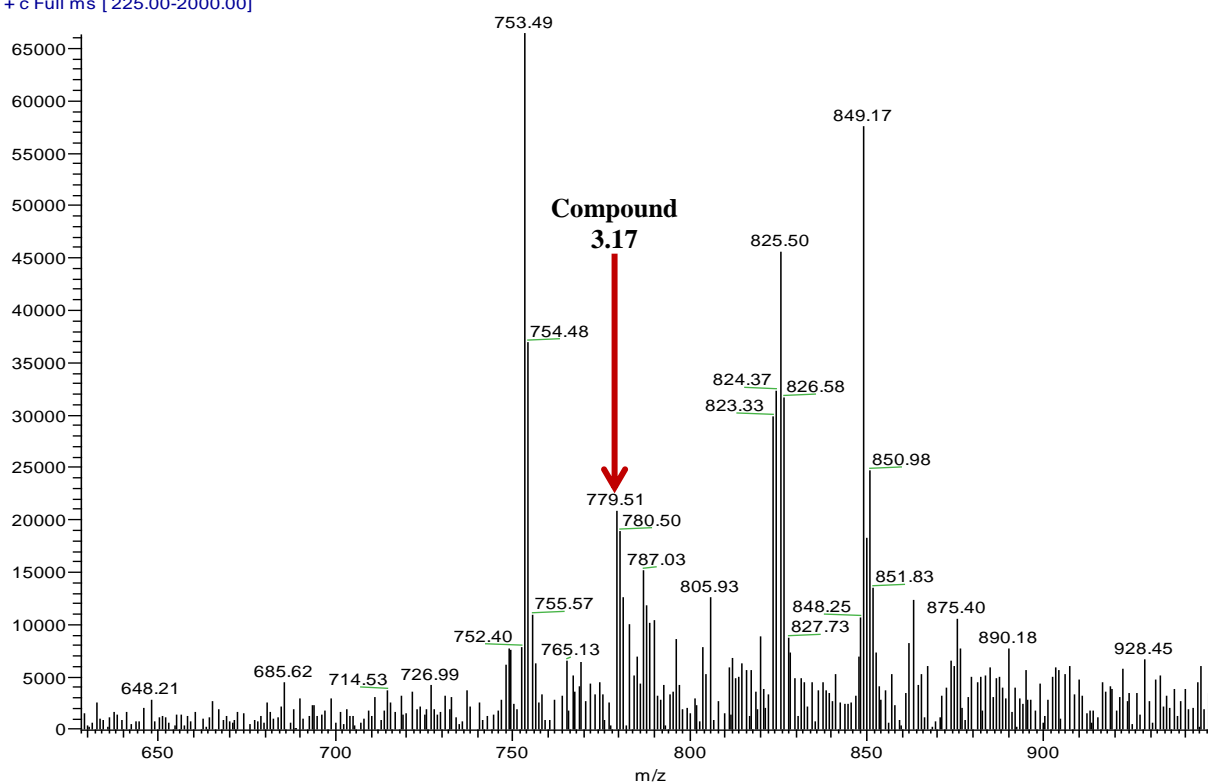
Name 9-Octadecenoic acid, methyl ester, (E)- (CAS) \$\$ Methyl elaidate \$\$ METHYL-TRANS 9-OCTADECENOATE \$\$ Elaidic acid methyl ester \$\$ Elaidic acid, methyl ester \$\$ Methyl trans-9-octadecenoate \$\$ (E)-9-Octadecenoic acid methyl ester  
 CAS Number 001937-62-8  
 Entry Number 175241  
 Molecular Formula C19H36O2  
 Misc Information QI=883, Source=NS-0-0-0  
 Match Quality 99  
 Company ID 299237  
 Retention Index 0  
 Melting Point  
 Boiling Point  
 Molecular Weight 296.27

Figure D: Identification of FAME ester 3.18<sup>2</sup>

## Appendix 2

### LC-MS Data for crude fraction G containing Monogalactosyldiacylglycerols **3.17** and **3.18**

TEM13-32G pos #2-5 RT: 0.05-0.14 AV: 4 NL: 6.63E4  
T: + c Full ms [ 225.00-2000.00]



**Figure A:** LC-MS spectrum of crude fraction G identifying monogalactosyldiacylglycerol **3.17**

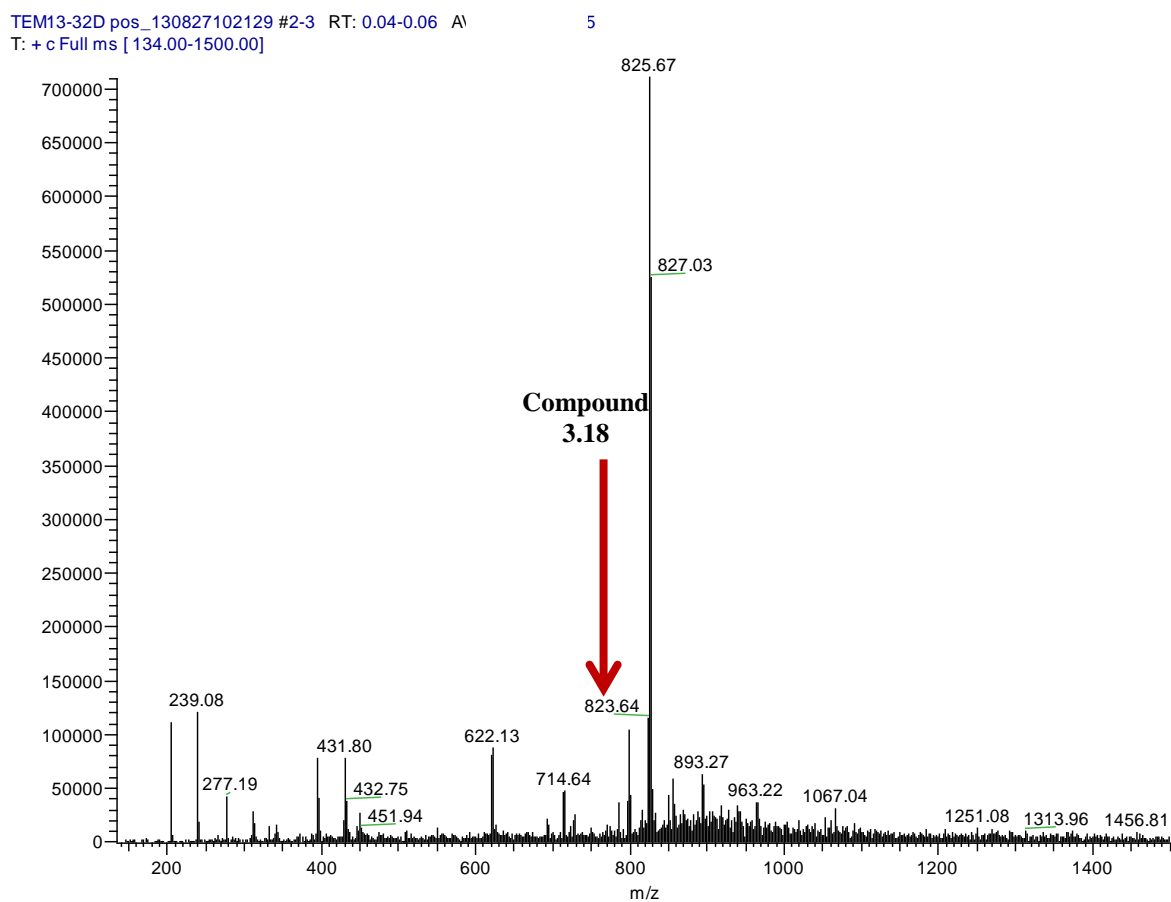


**Figure B:** LC-MS spectrum of crude fraction G identifying monogalactosyldiacylglycerol **3.18**

## Appendix 3

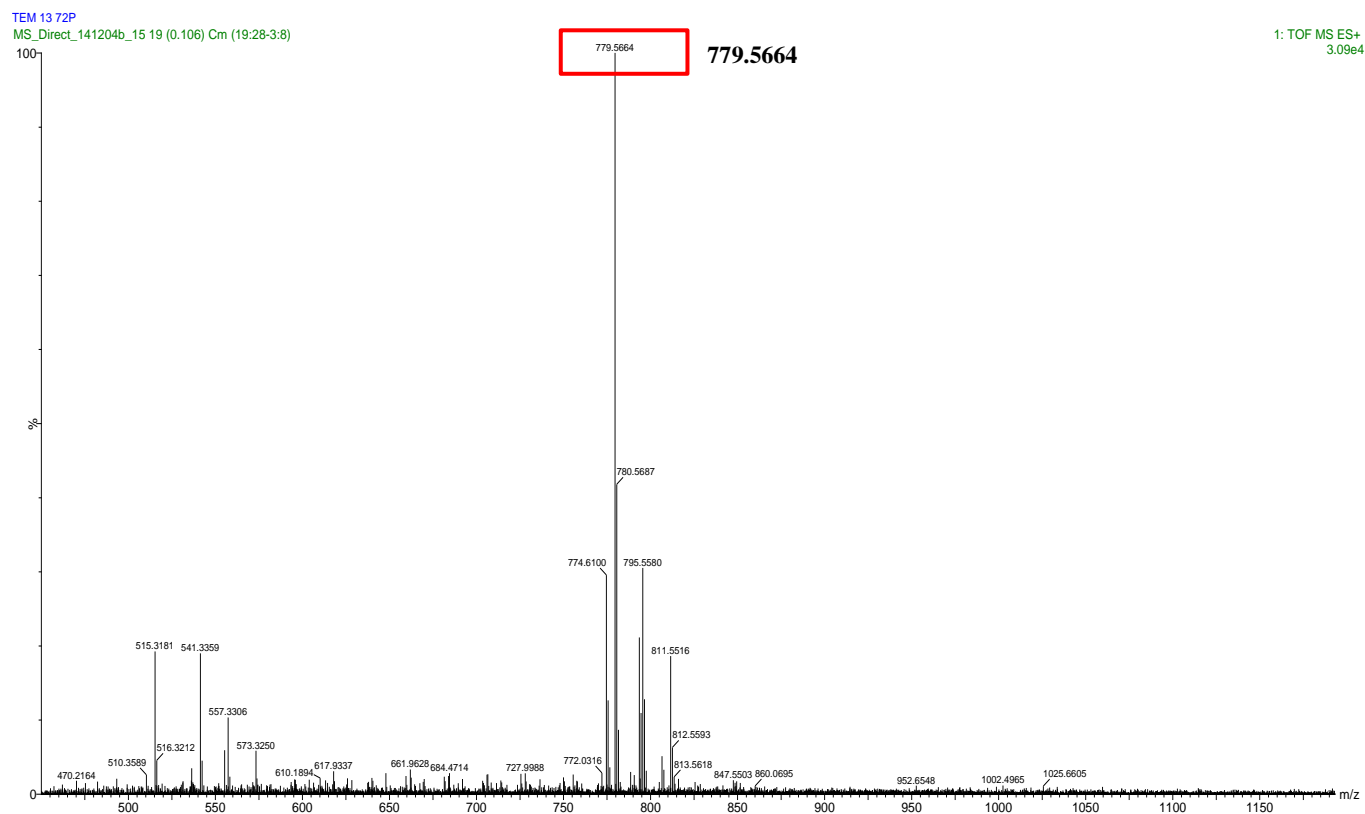
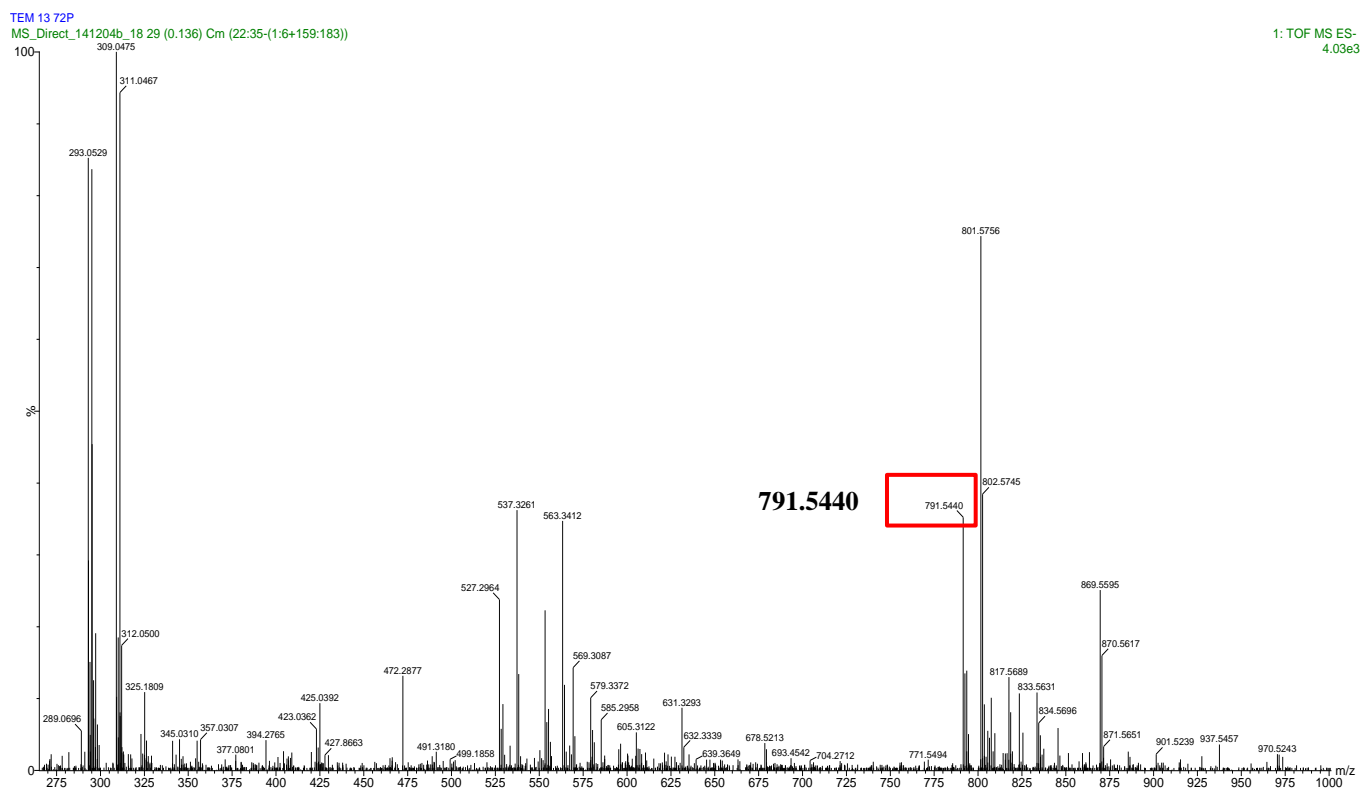
High resolution mass spectrometry (HRESIMS) of monogalactosyldiacylglycerol **3.17**

Figure A: HRESIMS of monogalactosyldiacylglycerol **3.18** (ESI+ mode)



**Figure B:** HRESIMS of monogalactosyldiacylglycerol **3.18** (ESI- mode)

## Appendix 4

Antimicrobial assays<sup>8</sup> were conducted on fucosterol (**3.9**), monogalactosyldiacylglycerol **3.17** and monogalactosyldiacylglycerol **3.18** against *Acinetobacter baumannii* (ATCC BAA-1605), *Enterococcus faecalis* (ATCC 51299), *Escherichia coli* (ATCC 25922), *Staphylococcus aureus* (ATCC 33591) and *Candida albicans* (ATCC 90028D-5). The results have been tabulated below.

**Table 1:** Antimicrobial assays of the natural products **3.9**, **3.17** and **3.18**

Compound code	Disk-diffusion assay	Bioautography	MIC (µg/ml)
TEM13-72P <b>3.18</b>	-	-	<i>Candida albicans</i> – 50 <i>Escherichia coli</i> – 100 <i>Enterococcus faecalis</i> – 100
TEM13-72 g <b>3.17</b>	-	+ Ef	<i>Escherichia faecalis</i> – 100 <i>Acinetobacter baumannii</i> – 1
TEM13-16 <b>3.9</b>	-	-	

The results above illustrate positive antimicrobial activity of 1-*O*-(5Z,8Z,11Z,14Z-eicosatetraenoyl)-2-*O*-(9Z,12Z,15Z-octadecatrienoyl)-3-*O*-β-D-galactopyranosyl-*sn*-glycerol (**3.17**) against *Acinetobacter baumannii* with monogalactosyldiacylglycerol 3.18 showing less antimicrobial activity. This supports the fact that biological activity in Monogalactosyldiacylglycerols is linked to the degree of unsaturation of the fatty acids with more unsaturated fatty acids resulting in more biological activity (Bruno *et al.*, 2005; Imbs *et al.*, 2013).

No antimicrobial activity was determined for fucosterol.

<sup>8</sup> Assays were conducted at University of Kwazulu Natal by Roes-Hill M.L and Durrell K.A.

## References

- Bruno A., Rossi C., Marcolongo G., Di Lena A., Venzo A., Berrie C.P., Corda D. (2005). Selective in vivo anti-inflammatory action of the galactolipid monogalactosyldiacylglycerol. *European Journal of Pharmacology* 524: 159-168
- Imbs T.I., Ermakova S.P., Fedoreyev S.A., Anastyuk S.D., Zvyagintseva T.N. (2013). Isolation of fucoxanthin and highly unsaturated monogalactosyldiacylglycerol from brown alga *Fucus evanescens* C Agardh and in vitro investigation of their antitumor activity. *Marine Biotechnology* 15: 606-612